

D2.1 Holistic modeling framework for multi-hazard events



D2.1: Holistic modeling framework for multi-hazard events

Summary

Deliverable 2.1 of project ICARIA is the main outcome of Task 2.1 (Hazards dynamics and multi-hazards interconnectivities analysis). Its main objective is to provide a conceptual and methodological basis of hazard risk assessment for later developments of multi-hazard risk assessments. Initially, the document provides a description of the main hazards that affect each case study of the project. Next, the physical interaction between individual hazards in multi-hazard scenarios are analyzed based on literature review. Additionally, examples of single and multi-hazard extreme events that have affected each case study in recent years are provided. Finally, methodologies for hazard assessment of single-hazard events are provided as a summary of tools and models developed in former research projects.

Deliverable number	Work package	
D2.1	WP2	
Deliverable lead beneficiary	Deliverable author(s)	Contributor(s)
Aquatec (AQUA)	Àlex de la Cruz (AQUA)	Barry Evans (UNEXE) Agnese Turchi (PLINIVS) Nicola Addabbo (PLINIVS) Marianne Bügelmayer-Blaschek (AIT) Ioannis Zarikos (DMKTS)
Internal reviewer(s)	External reviewer(s)	
Beniamino Russo (AQUA)	Fausto Guzzetti (PAB)	
Planned delivery date	Actual delivery date	
29/12/2023	29/12/2023	
Dissemination level	<input checked="" type="checkbox"/> PU = Public <input type="checkbox"/> PP = Restricted to other programme participants <input type="checkbox"/> RE = Restricted to a group specified by the consortium. Please specify: _____ <input type="checkbox"/> CO = Confidential, only for members of the consortium	

Document history

Date	Version	Author	Comments
01/12/2023	v1	Àlex de la Cruz (AQUA)	1st full draft of the document
12/12/2023	v2	Beniamino Russo (AQUA) Fausto Guzzetti (PAB)	Full review of the 1st full draft
29/12/2023	v3	Àlex de la Cruz (AQUA)	Final document incorporating improvements based on the reviewers inputs

DRAFT

Table of contents

List of Figures	5
List of Tables	9
List of Acronyms and Abbreviations	10
Executive summary	13
1 Introduction to project ICARIA	15
2 Objectives of the deliverable	17
3 Identification of single and multi hazard scenarios of interest	18
3.1 Àrea Metropolitana de Barcelona CS	19
3.2 Salzburg Region CS	22
3.3 South Aegean Region CS	25
4 Hazard physical interaction mechanisms	28
4.1 Modeling of risks/impacts from hazard events	28
4.2 Concept of multi-hazard events	29
4.2.1 Coincident hazards	30
4.2.2 Consecutive hazards	31
4.3 Modelling Multi-Hazard Interactions	32
4.3.1 Modeling from Single to Multi-Hazard Events	35
4.4 Specific multi-hazard events physical interactions	37
4.4.1 Pluvial flood and storm surge	37
4.4.1.1 Flooding and extreme wind	39
4.4.2 Drought and forest fire	40
4.4.3 Drought and heatwave	41
4.4.4 Heatwave and forest fire	41
4.4.5 Extreme Wind and forest fire	43
4.4.6 Heat Wave, drought and forest fire	45
5 Historic single and multi-hazard extreme events	46
5.1 Àrea Metropolitana de Barcelona CS	47
5.2 Salzburg Region CS	51
5.3 South Aegean Region CS	54
5.3.1 Syros	54
5.3.2 Rhodes	56
6 Single hazard models	62
6.1 Pluvial flooding in urban areas	63
6.1.1 Model setup, calibration and validation	63
6.1.2 Model conceptual design	65
6.1.3 Model results	66
6.1.4 Data requirements	68
6.2 Storm surge flooding	69

6.2.1 Model setup, calibration and validation	69
6.2.2 Model results	70
6.2.3 Data requirements	71
6.3 Fluvial flooding	71
6.3.1 Model setup, calibration and validation	72
6.3.2 Data requirements	73
6.4 Heat wave in urban areas	74
6.4.1 Model setup, calibration and validation	74
6.4.2 Model results	78
6.4.3 Data requirements	81
6.5 Forest fire	82
6.5.1 Model setup, calibration and validation	82
6.5.2 Model results	85
6.5.3 Data requirements	87
6.6 Drought	87
6.6.1 Model setup, calibration and validation	87
6.6.2 Model results	90
6.6.3 Data requirements	91
6.7 Extreme winds	91
6.7.1 Model explanation	92
6.7.2 Model calibration and validation	94
6.7.3 Data requirements	96
7 Conclusions	97
References	99
Annex A: Data Management Statement	111

List of Figures

Figure 1. Location of the three case study regions of project ICARIA.	19
Figure 2. Summary of the Trial and Mini-Trial of each Case Study in project ICARIA.	20
Figure 3. Map of the AMB representing main land uses (orange: urban land, yellow: agricultural land; green: natural areas) and its main water courses (AMB 2023).	21
Figure 4. Results of the AMB CoP survey concerning the risk perception of different climate-related hazards by the stakeholders involved.	23
Figure 5. Map of the Salzburg region.	23
Figure 6. Observed events: blue dots: avalanches; orange: river flooding; green: landslide; grey: mass movement; source.	24
Figure 7. Results of the 1st CoP meeting in the Salzburg Region.	25
Figure 8. South Aegean region case study area.	26
Figure 9. Results of the SAR CoP survey concerning the risk perception of different climate-related hazards by the stakeholders involved.	27
Figure 10. Results of the SAR CoP survey concerning the vulnerability perception of different climate-related hazards by the stakeholders involved.	28
Figure 11. Typical configuration of a Risk/Impact assessment model (UNDRR, 2015).	29
Figure 12. Dynamic changes in vulnerability of exposed assets as a result preceding hazard (Gill et al., 2021).	30
Figure 13. Dynamic Risk equation based on interactions between hazard, exposure, and vulnerability over time (Gill et al., 2021).	30
Figure 14. Example overlapping time frames of two hydrological hazards.	32
Figure 15. Difference between independent and dependent consecutive hazards (de Ruiter et al., 2020).	33
Figure 16. Multi-hazard interaction matrix modified from De Pippo et al., (2008).	34
Figure 17. Hazard interrelationship matrix for modeled hazards within ICARIA.	35
Figure 18. BN approach for assessing flood risks that consider variations in Hazard, Exposure and Vulnerability, where the hazard level Flood duration (FDU). Maximum flood depth (FDE), and Maximum flood velocity (FVE) are considered (Harris et al.,	36

2022).

Figure 19. Elementary brick model depicting the holistic modeling framework for risk/impact assessment in ICARIA (modified after Zuccaro et al., 2018 and Russo et al., 2023). 37

Figure 20. Timeline of events showing compound (coincident, causally or not causally correlated, and consecutive) events and cascading effects where “H” is Hazard, and “I” is Impact. The influence of key-variables (i.e., time, space, and human behaviour) in the risk/impact/resilience assessment process has been considered (modified after Zuccaro et al., 2018). 38

Figure 21. Conceptual model of the backflow phenomenon occurring during coincident storm surges and extreme rain events in coastal urban areas (figure from Qiang et al., 2021). 39

Figure 22. Hazard pairs related to extreme precipitation and temperatures (source: Ridder et al., 2020 - part of Fig. 3b). Hazard pairs related to extreme precipitation and temperatures, including combinations of high temperatures (T), low precipitation (lowP), heatwaves (HW), high probability of large hail (hail), low SPI (drought), and extreme McArthur forest fire index (FFDI) values 43

Figure 23. Total occurrence of single and compound hazards, calculated as the number of days per hazard (or compound hazard as, H=heatwave, D=Drought, DH=Drought-Heatwave, F=Fire, HF=Heatwave-Fire, DF=Drought-Fire, DHF=Drought-HeatWave-Fire) divided by the total number of JJA days (2668) over the period 1990–2018 across Europe (source: Sutanto et al., 2020) 44

Figure 24. Example of the temporal and spatial range in reported forward rate of spread and 10-m open wind speed for five recent wildfire disasters involving large numbers of human fatalities. (source: Cruz et al., 2020). 45

Figure 25. Map of historic flooding events at Rhodes island 62

Figure 26. Conceptual representations of the 1D and 2D domains interaction (a) (Henonin et al., 2013); (b) (Schmitt et al., 2004) 64

Figure 27. (a) Scheme of semi-distributed (SD), (b) fully-distributed (FD) and (c) and hybrid (H) 1D/2D coupled urban stormwater model approaches (adapted from Russo et al., 2020a). 66

Figure 28. Example of a 1D/2D drainage model results in the city of Barcelona. The blue areas represent the flooded parts of the 2D domain (city surface). The coloured lines represent the pressure conscious in the pipes of the sewer network (Ajuntament de Barcelona 2019). 68

Figure 29. Examples of coastal flood hazard maps for pedestrians (on the left) and vehicles (on the right). Red = high, orange = medium and green = low. T=100 for Baseline (current) scenario (Russo et al., 2020b).	71
Figure 30. Example of Mittersill, an area within the Salzburg region highly affected by flooding, displaying the elevation within the modeling area, rivers, settlements and road network.	74
Figure 31. Comparison of surface temperature values between HWLEM and ENVI-MET model results (left) and Tmrt values between HWLEM and SOLWEIG model results (right).	78
Figure 32. Calibration of surface temperature values within HWLEM: land surface temperature observed on July 19th, 2015 in the Municipality of Naples, corresponding to a 3-day heat wave with maximum temperatures of about 36-37°C (Landsat satellite data).	79
Figure 33. Calibration of surface temperature values within HWLEM: land surface temperature observed on July 30th, 2020 in the Municipality of Naples, corresponding to a 5-day heat wave with maximum temperatures of about 34-35°C (data collected during a drone campaign).	79
Figure 34. Example of the heat wave hazard simulation in the Paris metropolitan area . The simulation, developed with GIS tools, corresponds to a “rare” event characterized by a 38°C air temperature in the period 2011-2040, and RCP 8.5.	80
Figure 35. Example of the heat wave hazard simulation in the Paris metropolitan area. The simulation, developed with the Rhinoceros/Grasshopper tools, corresponds to a “rare” event characterized by a 38°C air temperature in the period 2011-2040, and RCP 8.5.	80
Figure 36. Example of application of the HWLEM model for performance evaluation of adaptation/mitigation measures applied to a neighborhood scale intervention.	81
Figure 37. Structure components on the left and flow diagram of the FWI calculation process of the Canadian Forest Fire Behaviour Prediction System on the right.	84
Figure 38. Structure and flow diagram of WRF-Fire.	84
Figure 39. Example with the spatial distribution in the categories of yearly number of days with extreme fire weather (FWI > 50) in period: 2006–2015. (Varela et al., 2019, Sfetsos et al., 2021)	86
Figure 40. Fire spreading overlaid by extreme 95% value of FWI under RCP8.5 period: 2036–2045 (Sfetsos et al., 2021).	87

Figure 41. The extreme percentile of FWI (left) and the mean initial spread index (right) for the period 1980-2004 in the Attica region (Politi et al., 2023c).	87
Figure 42. Schematic representation of the routines in HBV Light.	89
Figure 43. Representation of la Baells catchment and sub-catchment divisions	90
Figure 44. Graphic conceptualization of the approach to assess water volume storage in reservoirs based on the HBV model results.	91
Figure 45. Graphical representation of the estimate of water availability in a reservoir up to year 2100 considering a climate scenario corresponding to RCP 4.5 (results corresponding to project RESCCUE (RESCCUE, 2019)).	91
Figure 46. Workflow of the data processing to the WRF model.	94
Figure 47. The case study areas are simulated at a 2kmx2km resolution until 2100.	95
Figure 48. Topography of the greek region along with the height of the stations used for calibrating the model in the SAR case study.	95
Figure 49. Extreme wind speeds values for 50-y return period for (a) historic data and (b) RCP 4.5 and (c) RCP 8.5.	96
Figure 50. Mean wind extreme value over 40 m/s at 100 m for	96

List of Tables

Table 1. Recent single and multi-hazard events affecting the AMB.	48
Table 2. Recent single and multi-hazard events affecting the SBG region.	52
Table 3. Historical flooding events affecting Syros island.	55
Table 4. Historical events affecting Rhodes Island.	57
Table 5. Summary of characteristics of single hazard models	63
Table 6. Data required (model inputs) for the pluvial flooding hazard model	69
Table 7. Data required (model inputs) for the storm surge flooding hazard model	72
Table 8. Data required (model inputs) for the fluvial flooding hazard model	75
Table 9. Data required (model inputs) for the heat wave hazard model.	82
Table 10. The classification of values for the FWI and its sub-component the ISI. (Politi et al, 2023b)	86
Table 11. Data requirements (model inputs) for the forest fire hazard model.	88
Table 12. Data requirements (model inputs) for the drought hazard model.	92
Table 13. Data required (model inputs) for the extreme wind hazard model	97

List of Acronyms and Abbreviations

AMB	Àrea Metropolitana de Barcelona
AAD	Algorithm Aided Design
BN	Bayesian Networks
BUI	Buildup Index
CA	Consortium Agreement
CCLM	COSMO climate model
CoP	Community of Practice
CS	Case study
CSF	Case Study Facilitator
CSOs	Combined SystemOverflows
DC	Drought Codeisi
DoA	Description of Action
DR	Deliverable Responsible
DSR	Daily Severity Rating
DSS	Decision Support System
DTM	Digital Terrain Mode
E	Hydraulic Efficiency
EC	European Commission
EFFIS	European Forest Fire Information System
EU	European Union
ESL	Extreme Sea Level
FD	Fully-Distributed
FDU	Flood duration

FDE	Maximum flood depth
FFDI	Forest fire index
FFMC	Fine Fuel Moisture Code
FVE	Maximum flood velocity
FWI	Fire Weather Index
GA	Gran Agreement
GDP	Gross domestic product
GIS	Geographical Information System
GRIB	Gridded Binary
H	Hybrid
HBV	Hydrologiska Byråns Vattenbalansavdelning
HFI	Head Fire Intensity
HW	Heatwave
HWLEM	Heat Wave Local Effect Model
IPCC	International Panel of Climate Change
ISI	Initial Spread Index
LOWP	Low Precipitation
LST	Land Surface Temperature
NCAR	National Center for Atmospheric Research
PAB	Project Advisory Board
PC	Project Coordinator
PMM	Project Management Manual
PMT	Project Management Team
PSB	Project Steering Board
RCPs	Representative Concentration Pathway
ROS	Rate of Spread

RP	Reporting Period
SAR	South Aegean Region
SD	Semi-Distributed
SFINCS	Structure Functions In Catchments and Soils
SMC	Servei Meteorològic de Catalunya
SPI	Standardized Precipitation Index
SPEI	Standardized Precipitation and Evapotranspiration Index
SSO	Specific Subobjective
SSPs	shared socioeconomic pathways
T	Return period
TMRT	Mean Radiant Temperature
UNDRR	United Nation Disaster Risk Reduction
UNISDR	United Nations International Strategy for Disaster Reduction
UTCI	Universal Thermal Climate Index
WP	Work Package
WRF	Weather Research and Forecast

Executive summary

Deliverable 2.1 presents the main results of the activity developed in Task 2.1 of Work Package 2 of project ICARIA. The main objectives of this document can be summarized as follows: (1) identify the main climatic hazards that currently affect the three case study regions and how will this situation evolve in the expected climate change context, (2) analyze extreme multi-hazard events to identify the mechanisms of interaction between the individual climate hazards and (3) identify historic extreme climate events (both single and multi hazard) that have affected the case studies.

As a Mediterranean region, the Metropolitan Area of Barcelona is, and will be, affected by climate hazards related to an extreme behavior of the water cycle (e.g. floods and droughts). In addition, the raise in mean temperature will lead to more frequent and intense heat waves. As a consequence of the previous conditions, wildfires are also expected to become more usual and destructive.

The Central Europe mountain areas, represented by the Salzburg region, are especially affected by increasing global temperature due to melting of glaciers, changed precipitation pattern (from solid to liquid) and the change in intensity of convective events intensified by the prevailing orography. Further, lower areas within the Salzburg region are starting to be affected by heat and drought, experiencing it as an emerging climate risk.

The islands of the Mediterranean region, in this case South Aegean region, are affected by numerous climate hazards linked to their geographical location and geomorphology. Due to the Mediterranean climate, the islands suffer from prolonged heatwaves and drought events in the summer months, accompanied by an increasing number of forest fires. On the contrary, in the winter months the area suffers from extreme winds and increased chance of flash floods.

Risk assessment of multi-hazard extreme events is the core of ICARIA innovative work. This kind of event refers to scenarios where two or more hazards occur in the same region and/or time period where the resulting impact can be greater than the sum of the individual impacts. The dynamics between single hazards during multi-hazard events are complex and diverse. Hence, as a first step, it is necessary to differentiate their main typologies (coincident or consecutive) and identify the interrelationships established (between single hazards) during compound events (interdependence, triggering, change conditions, association of mutual exclusion). Such work has been done in alignment with the Holistic multi-hazard modeling framework developed in Deliverable 1.1.

According to the previous nomenclature, the specific multi-hazard events of interest for the ICARIA case studies have been identified. Following this, based on a thorough literature review, the dynamics and physical interaction between individual hazards have been established. The multi-hazard events considered in this document are:

- Pluvial flood and storm surge
- Drought and forest fire

- Drought and heatwave
- Heatwave and forest fire
- Extreme wind and forest fire
- Heatwave, drought and forest fire

Furthermore, in order to sustain the work that will be developed in subsequent tasks of the project, a review of hazard assessment methodologies for single hazard events is provided in the last chapter of the report. Specifically, it presents modeling approaches to assess the hazard associated with the following climate hazard drivers: pluvial floods, storm surges, fluvial floods, heat waves, hydrological droughts, forest fires and extreme winds. It is worth remarking that most of the methodologies presented correspond to the results of previous EU research projects related to climate change and natural hazards risk assessment. In this sense, these contents collect methodologies and tools description that will support later steps of the project and the development of novel multi-hazard assessment procedures.

1 Introduction to project ICARIA

The number of climate-related disasters has been progressively increasing in the last two decades and this trend could be drastically exacerbated in the medium- and long-term horizons according to climate change projections. It is estimated that, between 2000 and 2019, 7,348 natural hazard-related disasters have occurred worldwide, causing 2.97 trillion US\$ losses and affecting 4 billion people (UNDRR, 2020). These numbers represent a sharp increase of the number of recorded disaster events in comparison with the previous twenty years. Much of this increase is due to a significant rise in the number of climate-related disasters (heatwaves, droughts, flooding, etc.), including compound events, whose frequency is dramatically increasing because of the effects of climate change and the related global warming. In the future, by mid-century, the world stands to lose around 10% of total economic value from climate change if temperature increase stays on the current trajectory, and both the Paris Agreement and 2050 net-zero emissions targets are not met.

In this framework, **Project ICARIA** has the overall objective to promote the definition and the use of a comprehensive asset level modeling framework to achieve a better understanding about climate related impacts produced by complex, compound and cascading disasters and the possible risk reduction provided by suitable, sustainable and cost-effective adaptation solutions.

This project will be especially devoted to critical assets and infrastructures that are susceptible to climate change, in a sense that its local effects can result in significant increases in cost of potential losses for unplanned outages and failures, as well as maintenance – unless an effort is undertaken in making these assets more resilient. ICARIA aims to understand how future climate might affect life-cycle costs of these assets in the coming decades and to ensure that, where possible, investments in terms of adaptation measures are made up front to face these changes.

To achieve this aim, ICARIA has identified 7 Strategic Subobjectives (SSO), each one related to one or several work packages. They have been classified according to different categories: scientific, corresponding to research activities for advances beyond the state of the art (SSO1, SSO2, SSO3, SSO4, SSO5); technological, suggesting and/or developing novel solutions, integrating state-of-the art and digital advances (SSO6); societal, contributing to improved dialogue, awareness, cooperation and community engagement as highlighted by the European Climate Pact (SSO7); and related to dissemination and exploitation, aimed at sharing ICARIA results to a broader audience and number of regions and communities to maximize project impact (SSO7).

- SSO1.- Achievement of a comprehensive methodology to assess climate related risk produced by complex, cascading and compound disasters

- SS02.- Obtaining tailored scenarios for the case studies regions
- SS03.- Quantify uncertainty and manage data gaps through model input requirements and innovative methods
- SS04.- Increase the knowledge on climate related disasters (including interactions between compound events and cascading effects) by developing and implementing advanced modeling for multi-hazard assessment
- SS05.- Better assessment of holistic resilience and climate-related impacts for current and future scenarios
- SS06.- Better decision taking for cost-efficient adaptation solutions by developing a Decision Support System (DSS) to compare adaptation solutions
- SS07.- Ensure the use and impact of the ICARIA outputs

DRAFT

2 Objectives of the deliverable

Work Package 2 (WP2) is focused on the hazard assessment dimension of the asset-based risk assessment modeling framework developed in ICARIA (ICARIA 2023a). In general terms, this WP focuses on analyzing dynamics between individual hazards during compound events, evaluating their likelihood of occurrence, identifying triggering effects and quantifying the hazard associated with the extreme weather events of interest. These lines of work will help to achieve the following specific objectives.

- Establish a holistic framework for scalable multi-hazards assessment.
- Quantify the likelihoods of occurrence of extreme compound hazard events.
- Identify critical pathways through which one hazard triggers/cascades other hazards.
- Develop and test coupled modeling approaches to simulate the dynamics and cascading effects of multi-hazard events.

As a first step in this effort, Task 2.1 has the objective of defining the hazard scenarios of interest for the project and analyzing the dynamics and interconnectivities generated between single hazards during multi-hazard events. Furthermore, it aims at collecting information of historic compound events. The present deliverable (Deliverable 2.1) compiles the information gathered in this task. Firstly, this document provides a justification of the selection of climatic hazards for the three case studies based on reports and the assessment of future climate change impacts. Furthermore, the perspective of relevant stakeholders is taken into account (Section 2). Secondly, a conceptual definition of multi-hazard events is provided based on the risk assessment framework presented in the ICARIA Deliverable 1.1 (ICARIA 2023a). Special focus is put on the multi-hazard scenarios that will be assessed in the three case studies (CS) of the project (Section 3). Thirdly, based on historic events reports and a literature review, the interaction between single hazards during multi-hazard events are identified and analyzed in order to determine the main physical mechanisms of hazard interaction (Section 4). Fourthly, a historic record of extreme weather events, including single and multi-hazard events, is provided for each CS region (Section 5).

Furthermore, Deliverable 2.1 presents an extensive description of modeling approaches to develop quantitative hazard assessments of all the single hazards considered in the ICARIA CSs. These models correspond to the outputs of previous research projects focused on critical assets resilience and climate change risk assessment from a single hazard perspective (Section 6). This modeling knowledge, in combination with the multi-hazard interdependencies and mechanisms identified in the previously mentioned sections, sets the basis for the development of methodologies and modeling tools to quantify the hazard associated with extreme multi-hazard events in Task 2.3.

3 Identification of single and multi hazard scenarios of interest

The main objective of project ICARIA is to develop and promote a comprehensive asset-level modeling framework to achieve a better understanding about the climate-related impacts caused by complex, compound, and cascading disasters to improve the climate resilience of critical assets. Importantly, this project has been conceived with a regional scope, aiming to develop tools and methodologies that can serve European regions to improve the holistic climate resilience of their critical assets against multi-hazard extreme events.

This section presents hazard scenarios of interest of the three case study regions around which multi-hazard risk assessment tools will be developed. These regions are the Barcelona Metropolitan Area in Spain, the Salzburg Region in Austria, and the South Aegean Region in Greece (see Figure 1). All of them have profound differences regarding their geography, population characteristics, dependency and structure of critical infrastructures.

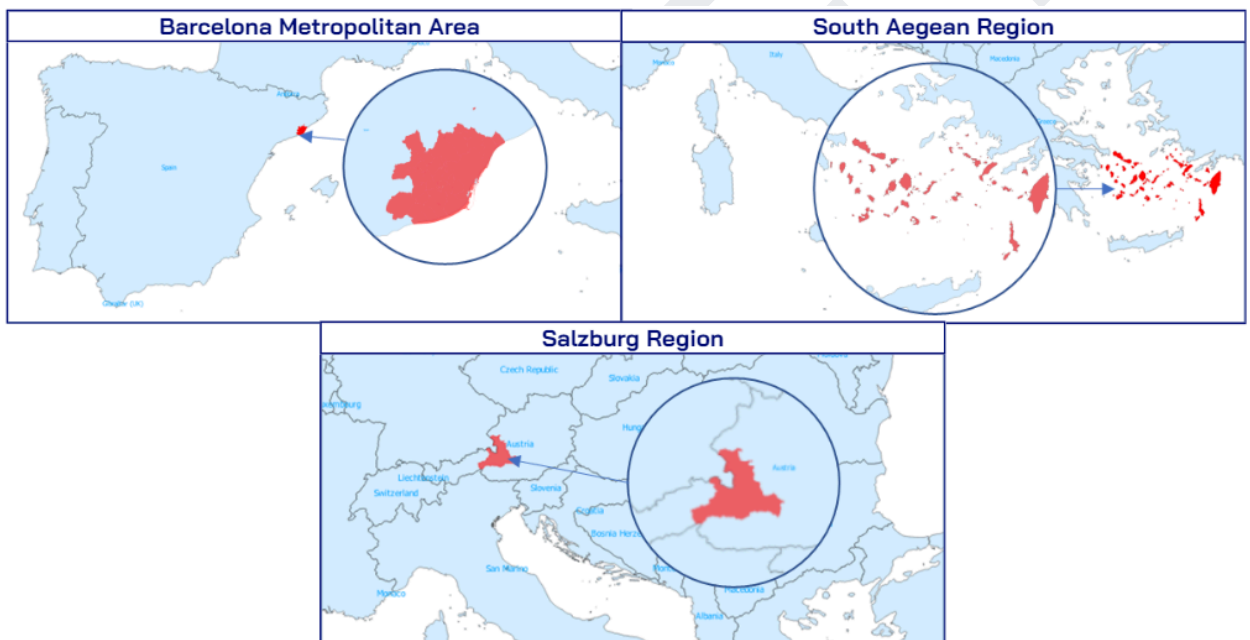


Figure 1. Location of the three case study regions of project ICARIA.

Despite the fact that (single and multi) hazard models will be implemented in these three regions, all methodologies and tools developed in ICARIA will ensure a maximum replicability for other regions to ultimately develop useful tools for end-users beyond the end of project ICARIA. To this end, the development of risk assessment methodologies in the project has been structured in a Trials and Mini-Trials organization. Trials aim at achieving the highest possible (or highest necessary) quality of predictions with highly detailed models so that results can be used “as they are” for operative decision making. Mini-Trials are focused on replicating in different regions the model originally developed in the Trials to evaluate the possibility to achieve similar results in

other contexts with potentially strong differences in terms of data availability and resources. The Deliverable 5.4 of ICARIA presents this organization in more detail (ICARIA 2023b).

The definition of the climatic hazards of main interest for the three case study regions is the result of three parallel processes:

- Partners knowledge of context and challenges of each CS.
- Review of reports and literature on effect of climate changes in each region.
- Validation of risks and scenarios with local stakeholders in the first community of practice (CoP) celebrated in M6 of the project (June 2023) according to the work plan defined in Deliverable 5.4 (ICARIA 2023b).

Figure 2 depicts the hazards, assets and tangible impacts defined for each CS of project ICARIA.

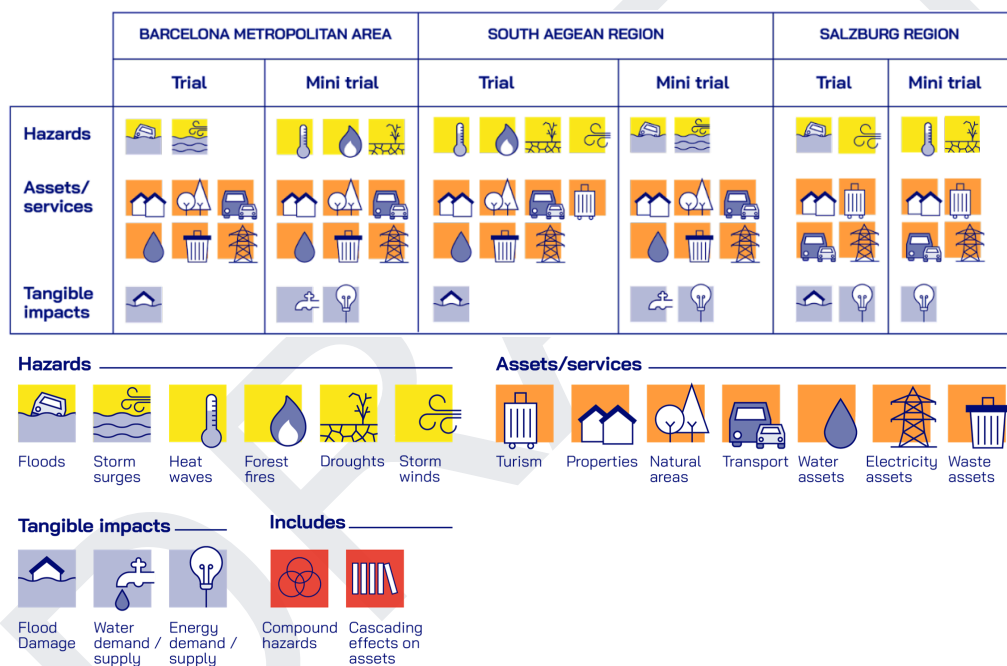


Figure 2. Summary of the Trial and Mini-Trial of each Case Study in project ICARIA.

The following subsections present the reasoning behind the selection of hazards of interest for the three case study regions of the project.

3.1 Àrea Metropolitana de Barcelona CS

The Barcelona Metropolitan Area (AMB, for its acronym in Catalan) is the largest conurbation of Catalonia (Spain). Encompassing 36 municipalities, it covers 636 km², has over 3.2 million inhabitants and is responsible for half of the region of Catalonia’s GDP (123,023 M€ in 2020). In terms of territorial organization, about 48% of the terrain is occupied by urban land, industry,

irrigation (Hoerling et al., 2012, Trambly et al., 2020, Forero-Ortiz et al., 2020). Drier and warmer conditions, especially in the summer season, are expected to contribute to more prone conditions for forest fire in the region (Ruffault et al., 2020).

As mentioned earlier, future climate projections indicate that droughts will become more severe in the Mediterranean basin. This trend is the result of a more extreme hydrological cycle, where floods and droughts are the two opposite extremes of the same cycle. Therefore, the severity of drought events in the Mediterranean basin will grow in parallel to the frequency and intensity of flooding events associated with extreme rain events in the same region (Ward et al., 2020). Many investigations coincide in the conclusion that flash floods will become one of the more harmful climate hazards considering their frequent occurrence and high economic impacts (Russo et al., 2020a, Monjo et al., 2016, Llasat et al., 2010 and 2016)

In addition to the mentioned hazards, extreme sea level events are a threat to low-lying Mediterranean coastal cities. Historically, storm surges have led to coastal flooding events associated with large damages in the affected areas. Several investigations have concluded that climate change projections do not seem to have a direct effect on the frequency and severity of storm surges in the western Mediterranean region. Despite this fact, even if the frequency of these events remains stable, storm surges still stand as a significant climate hazard for this case study region (Vousdoukas et al., 2016, Androulidakis et al., 2015, Lin-Ye et al., 2020)

One remarkable event that affected the AMB, and the whole Spanish Mediterranean coast, was the Gloria storm of January 2020 (a record-breaking combined event in which a coincident storm surge and extreme rainfall caused unprecedented damage in the region). Despite that there are not many precedents of similar events in the region, this storm is a clear example of their capacity of devastation. Furthermore, it is a good paradigm of the risk that compound events pose to coastal urban areas (Sanuy et al., 2021).

In parallel to academic research, the AMB authority and the Barcelona City council have developed their own assessment of future climate changes related risks for the region: the “Pla Clima i Energia 2030” (“Climate and Energy Plan 2023” in english) (AMB 2016) and the “Pla Clima” (“Climate Plan” in english) (Ajuntament de Barcelona 2018) respectively. Both documents reached similar conclusions regarding the main hazards to consider in adaptation plans as the above mentioned sources. Furthermore, both documents stress the importance of improving the climate resilience of the regional critical assets, among other measures, to cope with climate change. Importantly, the definition of ICARIA’s hazards and assets of interest has been defined in accordance with region-specific documents.

The identification of the hazards of main importance for the AMB Case Study has been further validated with the local Community of Practice according to the roadmap defined in Deliverable 5.4 of ICARIA project (ICARIA 2023b). The participant stakeholders were surveyed to understand their perception of risk about the different hazards in the AMB for the sectors and assets that they represented. Figure 4 shows that, on a scale from 0 to 10, floods, droughts and heat waves were ranked as the most critical climate hazards for the AMB.

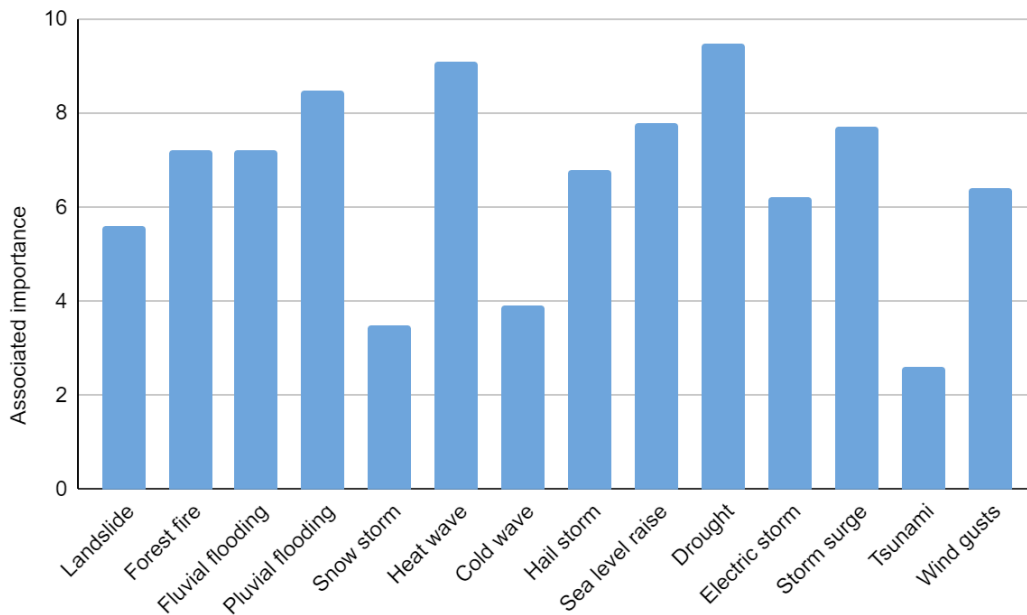


Figure 4. Results of the AMB CoP survey concerning the risk perception of different climate-related hazards by the stakeholders involved.

3.2 Salzburg Region CS

Salzburg is situated in the Eastern Alps region of Austria. It is home to 562.704 inhabitants, covers 7.154,56 km² and represents one of the major tourist areas in the country. It consists of 5 regions (see Figure 5) and its capital is the city of Salzburg. Within the Salzburg region there are multiple hydropower plants, making it a crucial area for renewable energy production in Austria.

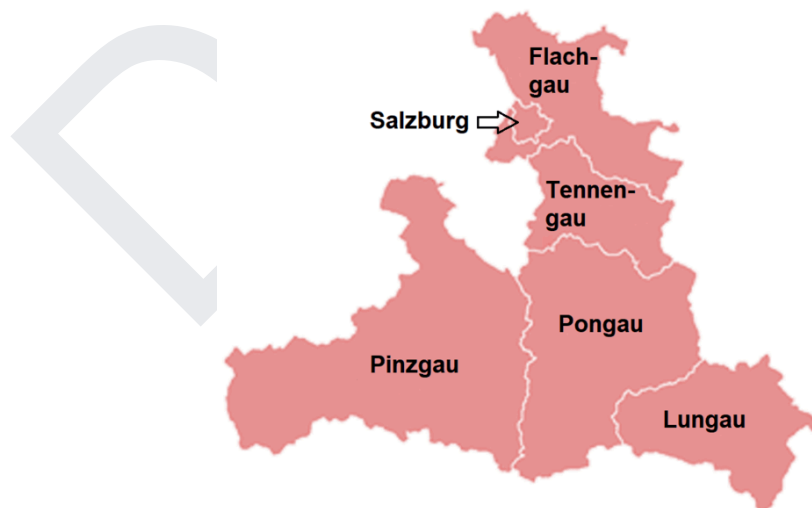


Figure 5. Map of the Salzburg region.

ICARIA focuses on the rural areas, especially the region of Pinzgau as a representative area. It is already highly affected by extreme events and covers 2.641 km² and has about 89,625 inhabitants.

The mountainous regions are already suffering from the effects of global warming and Salzburg has recognised the risk the whole region is facing by developing its climate adaptation strategy in 2017 (Land Salzburg 2017). Within this strategy 14 fields of action were defined based on the Austria climate adaptation strategy (Bundesministerium 2021). These 14 areas encompass the energy and electricity industry, health, agriculture, ecosystems and biodiversity, spatial planning, natural disasters etc. For each field of action, climate change impacts were gathered and qualitatively assessed by experts. This strategy was updated in 2022 (Land Salzburg 2022) where possible adaptation measures were stated and assessed according to their degree of implementation, time horizon and potential barriers.

All the occurred and documented extreme events with respect to avalanches, river flooding, landslides (fast event, related to extreme precipitation) and mass movements (slow, gravitational process) for the Salzburg region are depicted in Figure 6. Even though extreme events have always threatened the region, their occurrence and magnitude increased continuously over the past years, even though adaptation measures such as flooding barriers have been implemented, in total not only the magnitude and quantity of extreme events, but also their economic damage has increased over the past years.

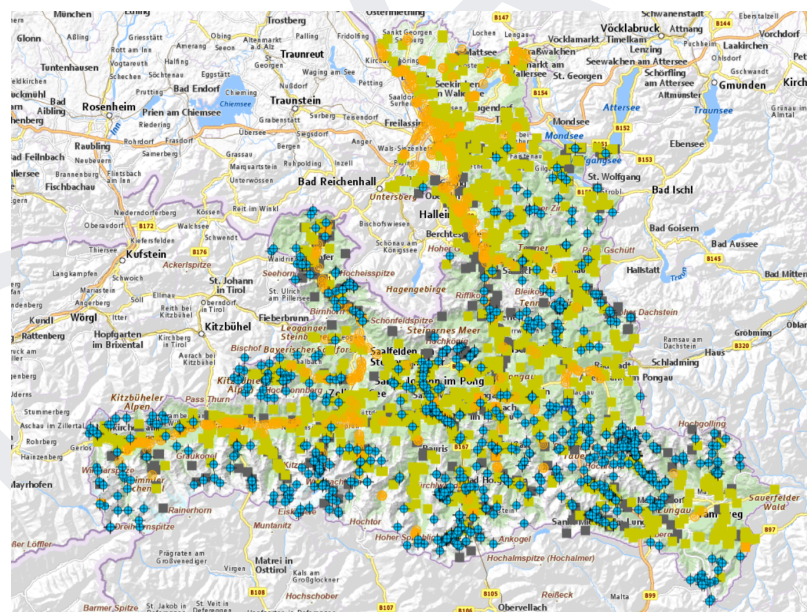


Figure 6. Observed events: blue dots: avalanches; orange: river flooding; green: landslide; grey: mass movement; source¹.

1

<https://www.salzburg.gv.at/sagismobile/sagisonline/map/Wasser/Naturgefahren-Gefahrenzonen>

Especially, events related to extreme precipitation threaten the Pinzgau Region as they cause flooding and landslides, thereby impacting private houses, the transport network and electricity-related assets. This was also reflected by the answers of the participants during the first CoP, where all precipitation related events were identified as extreme high or high risk. This risk is already perceived as extremely high and expected to further increase due to human made climate change. First, the increased air temperature leads to stronger convective precipitation events as up to 10% more water vapor can be stored (Stangl et al., 2022), second the increased occurrence of blocking weather patterns relates to higher precipitation amounts over a longer time period, third the melting of glaciers and the higher snow line relate to more and faster runoff. Furthermore, the impact of storms was identified as high as winter storms, foehn and high wind speed in relation to convective precipitation events have led to damage in the past.

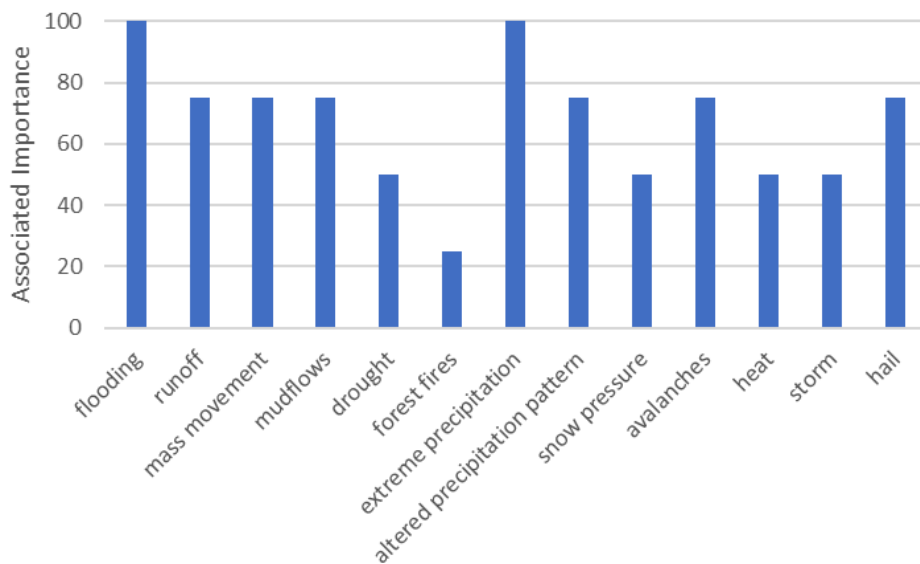


Figure 7. Results of the 1st CoP meeting in the Salzburg Region.

Within the stakeholders of the region there is a common understanding that the assets at risk are the electricity and transport infrastructure, telecommunication and private homes. Indirectly, the tourism sector is highly affected by interruptions in the aforementioned sectors, especially transport (e.g due to blocked roads).

The Salzburg region, due to its high altitude and loosely built settlement structure, is not yet strongly experiencing the impact of human made climate change with respect to increased temperatures, as can be seen as it being described as “emerging risk” by the stakeholders. However, it is expected to increasingly impact the prevailing conditions, as is the case for drought. Furthermore, Austria has seen a rise in wildfires, in Salzburg the risk of wildfires is expected to strongly grow over the next years and decades.

Based on the results of the CoP and the observations of the past years, the flooding and storm risk will be investigated as trials within Salzburg, focusing on longer-lasting rain events and also

on high intensity rainfalls (flash floods). Furthermore, the hazards of heat, drought and related wildfires will be investigated within the Mini-Trial, based on the findings of the other regions.

3.3 South Aegean Region CS

The South Aegean Region (SAR) is an archipelago region at the south-eastern edge of Greece that administratively includes the island clusters of the Cyclades and the Dodecanese. The Region has a total area of 5,286 square km and covers 4% of the total land area of the country.

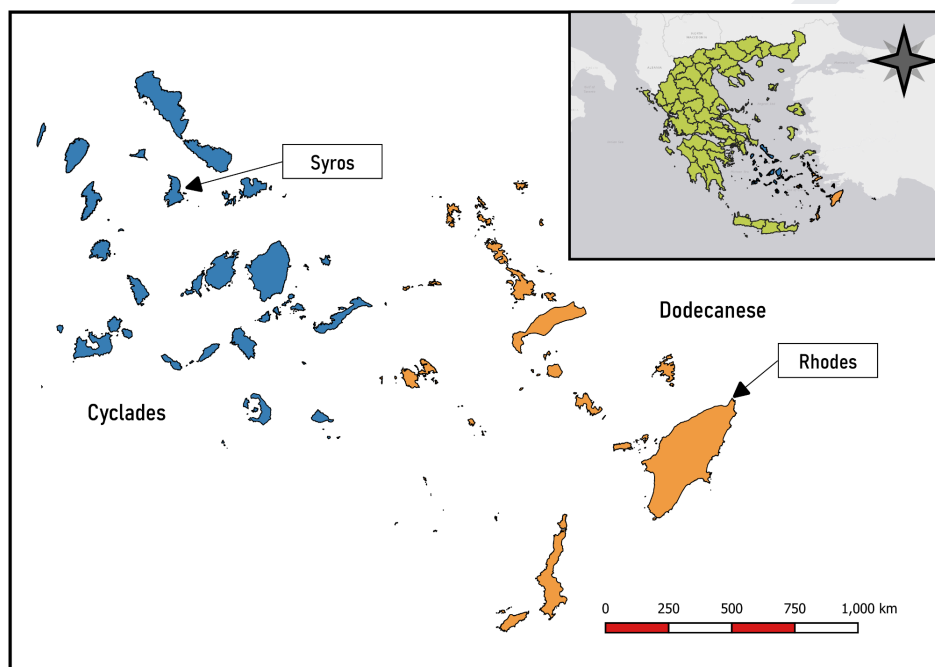


Figure 8. South Aegean region case study area.

With a total population of 308,957 inhabitants (2.9% of total population) and the distinct geographical characteristics of the region (52 inhabited islands), the GDP of the province accounts for 2.5% of the country’s total GDP, mainly due to tourism and primary products. The effect of climate change in this region is more pronounced than in continental Greece or Europe and historic data, especially from the past 30 years, confirm it (increase of extreme weather events such as heavy rain, floods, fires, sea level rise in combination with higher average temperatures with heat waves showing a yearly increase in duration) (Katopodis et al., 2021, Politi et al., 2020, Politi et al., 2023a).

All these islands, due to their geographical location and the local terrain morphology, encounter severe problems to meet local population basic needs (water, food supplies, electricity, healthcare, etc.). Moreover, the seasonal changes of the island’s population, due to tourism, puts additional stresses on infrastructures and resources. To overcome the problem of water shortages, the islands are supplied either by water tanker vessels or with the use of local

desalination facilities (Politi et al., 2022, Zarikos et al., 2023). The latter counts for nearly 70% of the consumed water, especially in summer.

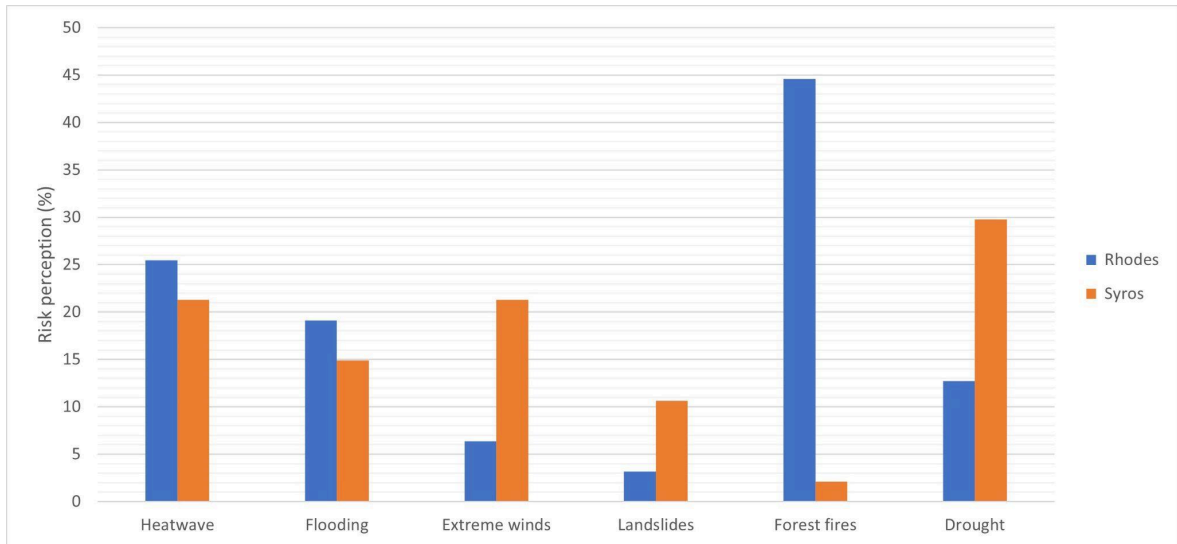


Figure 9. Results of the SAR CoP survey concerning the risk perception of different climate-related hazards by the stakeholders involved.

Ports and airports are also an important infrastructure, they are the main access points for food supplies, fuel, goods and also for tourists, since airports are only located in larger islands. These infrastructures are mainly affected by extreme winds and associated high sea level. The CoP input indicated, based on submitted data by the members, that on average the ports in the region are closed from 5 to 10 days a year. The main effect is on supplies availability, since they are transferred by ships. Another negative effect, uncommon to the other regions, is emergency airlifts and boat transfers of patients towards the main hospitals, located on the larger islands, as well as to continental Greece.

Electricity production and distribution is also a problem because the islands do not have an underwater connection with the continental network distribution, thus almost each island has its own power plant (fuel oil) (Tzanes et al. 2019). The effect of climate change in energy production and distribution, according to the input from the CoP meeting, is mainly linked to the negative effects of forest fires and flooding, in addition to a minor effect on high wind speeds. More specifically, Rhodes island, historically affected by forest fires, experienced power shortages due to extensive damages on the high and medium voltage distribution network. This is mainly due to the fact that the majority of the above ground distribution pillars are wooden. In addition, the high voltage distribution network, transferring power to the southern part of the island, runs through a densely forested area. In the case of Syros, electricity distribution disruption is caused by flooding of underground substations in the Hermoupolis urban area. Moreover, the island hosts a small wind farm with a potential of 2.4GWh, whose production is directly affected by extreme winds. The effect is mainly production disruption during high wind speed days, when they are

deactivated, or in the worst case scenario damaged in the rotor or braking system, putting them out of service for a notable time period.

It is evident this region’s infrastructures are vulnerable to the effects of climate change both in a direct and indirect manner. The limited infrastructure and the distance from mainland Greece, make the importance of strengthening disaster risk reduction and resilience even greater. Analyzing the occurrence and characteristics of climate related compounds and extreme events along the SAR region (with special focus on Syros, Rhodes, Kos and Naxos islands) and the cascading effects on the main services, are a paradigm of archipelago / coastal zones in the Mediterranean area.

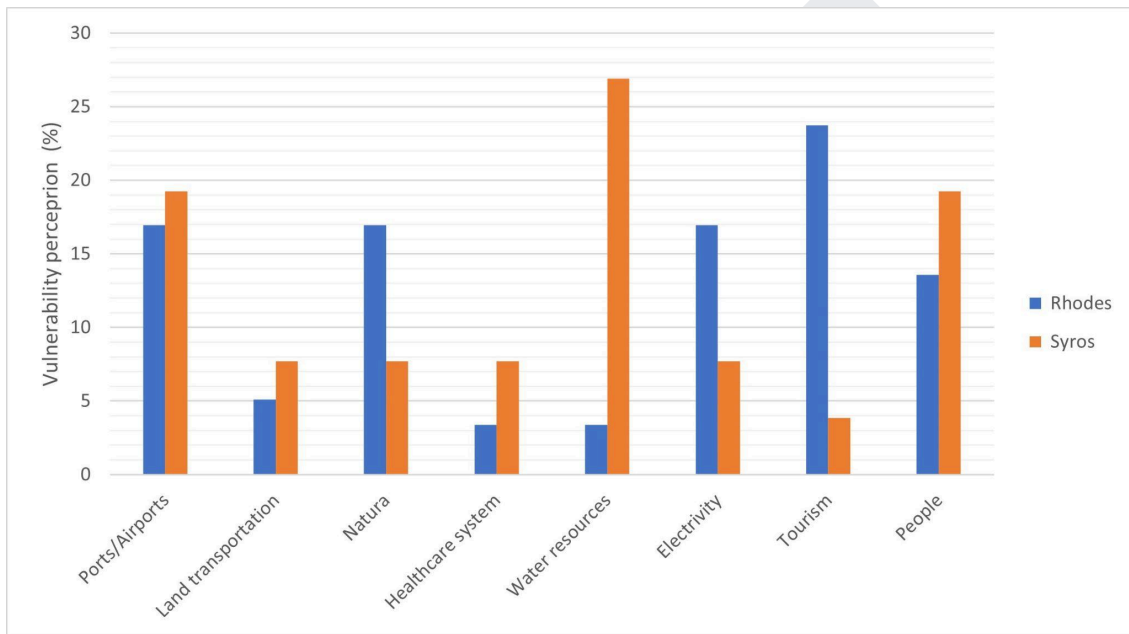


Figure 10. Results of the SAR CoP survey concerning the vulnerability perception of different climate-related hazards by the stakeholders involved.

4 Hazard physical interaction mechanisms

4.1 Modeling of risks/impacts from hazard events

The derivation of risks and/or estimated impacts to infrastructure, services, people, etc. are commonly expressed as the likelihood of loss of life, injury or destruction and damage resulting from a disaster in a given period of time and is derived as a product of Hazard, Exposure, and Vulnerability (UNDRR 2015) (see Figure 11), where:

1. **Hazard:** Time-space distribution of the magnitude/severity of an event characterized by an assigned probability of occurrence in a given location and timeframe.
2. **Exposure:** Distribution of risk receptors (e.g. buildings, infrastructure, services, people, etc.) occupying a specific region at a specific time i.e. and the probability of them being affected by the modeled hazard.
3. **Vulnerability:** The susceptibility of exposed risk receptors to modeled hazard types and their intensities. This is expressed in terms of vulnerability curves that define the probability of damage or disruption to a service based on the magnitude of the hazard the risk receptor is exposed to.
4. **Risk/Impact:** A function of hazard, exposure, and vulnerability that can be used to define the probability or likelihood that a hazard event will cause harm, damage or loss (Risk) or the expected tangible damage/losses (Impact) expected as a result of a hazard (Figure 11)

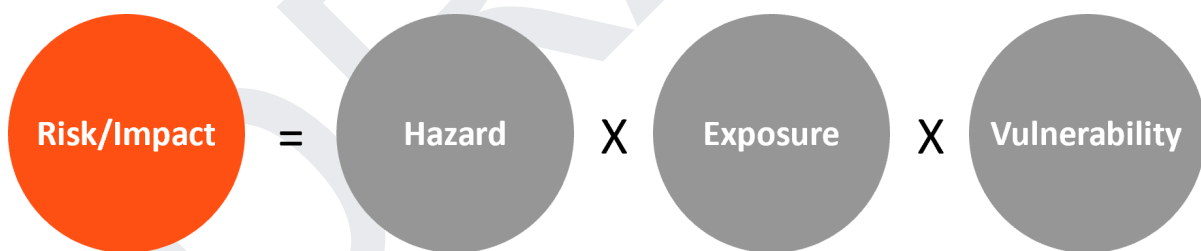


Figure 11. Typical configuration of a Risk/Impact assessment model (UNDRR, 2015).

Whilst this approach allows for assessment of a specified event, when examining risks/impacts a region is exposed to over long timeframes, it is important to consider that the components (hazard, exposure, and vulnerability) used to define risk can vary over time due to changes in land use, and population, implementation of adaptation measures, etc.

The derivation of risks/impacts is further complicated when the interdependent relationships between hazard, exposure and vulnerability are also considered (Gill et al., 2021), for example the vulnerability of assets within a region may change as a consequence of an initial hazard (Figure 12).

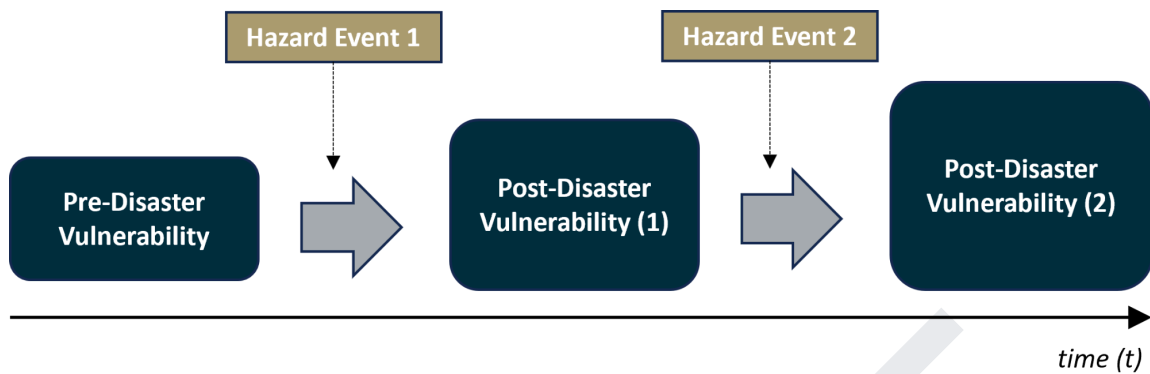


Figure 12. Dynamic changes in vulnerability of exposed assets as a result preceding hazard (Gill et al., 2021).

4.2 Concept of multi-hazard events

Multi-hazard events refers to scenarios where two or more hazards occur in the same region and/or time period where the resulting impact is either greater or lesser than the sum of their impacts if they were to occur independently (MYRIAD, 2022). The combined effects resulting from multi-hazard scenarios are therefore unlikely to be assessed through simple addition of losses, due to the independent effects, and instead require system approaches to understand risk (IPCC, 2022). When modeling the risks/impacts within a region we must consider that the hazard landscape is dynamic, where characteristics of a region that can influence the magnitude, duration, and likelihood of a hazard can change over time along with characteristics relating to the exposure and vulnerability of risk receptors. Furthermore, these aforementioned characteristics may also change as a response to a hazard event (Gill et al., 2021). Therefore, these dynamic interactions also need to be considered when assessing risks/impacts as a result of two or more hazards occurring in the same region either at the same time or sequentially. Gill et al., 2021 depicted the complexity of these interactions by expanding upon risk/impact equation outlined in Figure 11 to express it in terms of a time-dependent function that includes the potential interrelationships between hazard, exposure, and vulnerability (Figure 13).

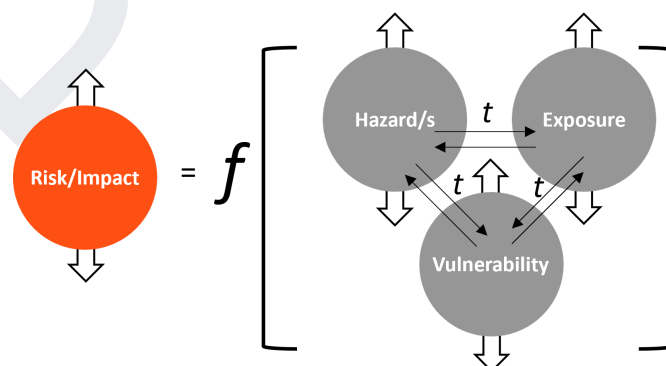


Figure 13. Dynamic Risk equation based on interactions between hazard, exposure, and vulnerability over time (Gill et al., 2021).

Analysis of the interrelationships between hazards, by Tilloy et al., 2019, showed five interrelation types between hazards that can be considered in multi-hazard events analysis:

1. **Independence:** Two or more hazards overlap in terms of space and time without any dependence or triggering relationship between them, such as the tropical storm that occurred 2 days after an earthquake in Haiti in 2021 (CDP 2021).
2. **Triggering (Cascading):** The effects of one hazard may cause a secondary hazard to occur e.g. flooding in a region that results in landslides within the same region.
3. **Change conditions:** The effects of one hazard change conditions within a region that result in changes to the magnitude of a secondary hazard, for example a drought within a region can change the characteristics of local vegetation making it more susceptible to combustion resulting in both increased likelihood and potential impacts of forest fires.
4. **Compound hazard (association):** In this example there is no “primary” or “secondary” hazard as they both occur simultaneously and occur as a result of the same triggering event. An example would be a storm surge coinciding with river flooding that has resulted from a tropical cyclone event. These two hazards are interdependent and result in an event referred to as “compound flooding”.
5. **Mutual exclusion:** Refers to scenarios where the occurrence of one hazard or event in a region reduces either the likelihood or risk of another specific hazard or event happening at the same time within that region, such as extreme rainfall event occurring during a forest fire event aiding in the extinguishing of the fire, reducing its capacity to propagate.

Within the ICARIA project, the multi-hazard combinations selected by the three case study regions fall within the four interrelation types, across six hazard classifications, **Floods** (Pluvial and Fluvial), **Storm Surge, Drought, Heatwave, Forest Fire** and **Storm winds**. From the temporal aspect, the modeled multi-hazard scenarios will consider overlapping time-frames of multiple hazards and/or sequential hazards where the timing of the secondary hazard begins prior to the region affected by the first hazard having fully recovered.

4.2.1 Coincident hazards

Within the scope of ICARIA, coincident hazard events refer to two or more hazard events occurring within the same geographical region, either simultaneously or with overlapping time frames, i.e. a secondary hazard is occurring whilst a primary hazard is still taking place. These hazards could be completely independent, such as an earthquake occurring during a wildfire, or be compound hazards with dependencies, for example a storm surge coinciding with pluvial flooding. As outlined in MYRIAD (2022), such scenarios can result in the cumulative risks/impacts being either greater or (in some combinations) lesser than if each of the risks/impacts were assessed independently.

From the hazard modeling perspective, the intensity/magnitude of a hazard varies over time along with the duration of the hazard itself. When considering coincident multi-hazard events

there can be a range of possible outcomes due to the variations in magnitudes of each event, their duration and their subsequent time of occurrence with respect to each other. For example, pluvial flooding triggered by extreme rainfall could occur towards the tail end of a storm surge event, a storm surge could occur during the middle of a pluvial flood event or at the tail end of the pluvial flood event (Figure 14). These variations in timings of both events could result in variances in compounded flood depths within the affected flooded regions and subsequently result in a range of potential risk/impacts. Therefore to model and capture the potential impacts as a result of these hazard combinations, an ensemble of multi-hazard simulations should be considered.

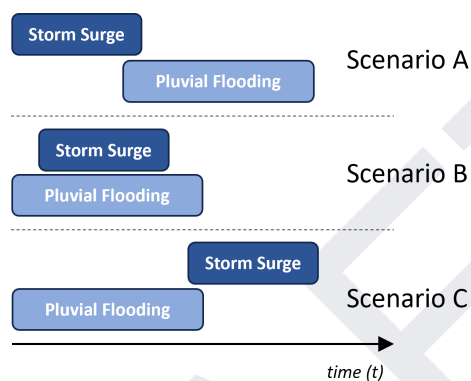


Figure 14. Example overlapping time frames of two hydrological hazards.

4.2.2 Consecutive hazards

In contrast to coincident hazards, consecutive hazards do not occur simultaneously but instead occur sequentially. These hazard scenarios can be either independent or dependent (where one hazard triggers the other) (de Ruiter et al. 2020) (Figure 15).

In the case of the “independent” hazards, although they may spatially and/or temporally overlap, neither hazard triggers the other or influences the others probability of occurrence. For the dependent hazards however, the effects of the first one (referred to as the triggering hazard) either directly results in occurrence of a secondary one, or increases its probability of occurrence, and potentially changes the conditions in the region that can influence the severity of the proceeding hazard.

When considering the time-frame of consecutive hazards, a secondary hazard is considered as “consecutive” if the hazard (independent or dependent) has occurred prior to the system fully recovering from the previous hazard. Defining such time-frames between events is not done without its challenges as, depending upon the type and severity of a given event, its effects within a region can span long timeframes. For example, the flood risk within a region previously affected by a wildfire, remains significantly higher until vegetation is restored, which can take up to 5 years. Therefore when modeling the potential implications of consecutive hazards we need to consider the uncertainty associated with the range of recovery times for the region as a result of the preceding hazard.

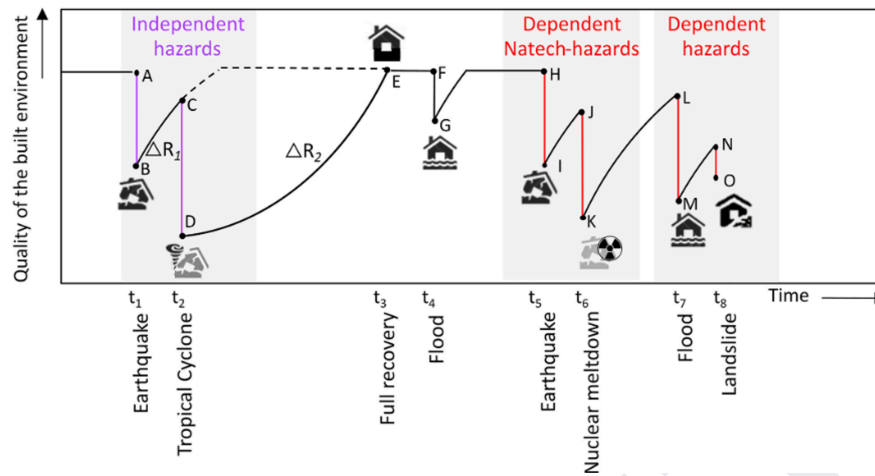


Figure 15. Difference between independent and dependent consecutive hazards (de Ruiter et al., 2020).

In defining the recovery time for a region following a catastrophic event, the relationship between shock/disruption and recovery can be defined as the resilience of the system, where, the term resilience (from the SENDAI framework definition) refers to “*the ability of a system, community or society exposed to hazards to resist, absorb, accommodate to and recover from the effects of a hazard in a timely and efficient manner, including through the preservation and restoration of its essential basic structures and functions.*” (UNISDR, 2012).

4.3 Modelling Multi-Hazard Interactions

Previous works by De Pippo et al., (2008) and Kappes et al., (2012) derived descriptive matrices for defining interactions between hazards via one hazard triggering another hazard or/and one hazard changing the local conditions that affects the magnitude of a proceeding hazard within that region. Figure 16 outlines a descriptive multi-hazard interaction matrix for the six hazard types being analyzed in ICARIA with the yellow boxes highlighting multi-combinations to be modeled.

		Influences →				
Influences ↑	Flooding (Pluvial and Fluvial)	Additional volume of water leads to increased flood depths and flood extent in coastal areas	May alleviate some of the effects of heatwave for short-term through cooling effect of evaporation	May alleviate some of the effects of drought in short-term. Reservoir recharge, soil moisture recharge	May reduce the severity of the forest fire through extinguishing of current fires and reducing its capacity of spread via moistening vegetation	No Interaction
	Changes in boundary conditions affecting the sewer networks' ability to discharge water	Storm Surge	No Interaction	Increased risk of seawater/saltwater intrusion	Potential increased movement of debris that can block channels, culverts etc. and results in greater flooding.	No Interaction
	Greater likelihood of more severe thunderstorms (lightning, hail) and intensity short duration rainfall.	No Interaction	Heatwave	Heatwave occurring during a drought can put increased pressure on water resources due to augmented consumption and evaporation.	Increase in forest fire severity due to higher temperatures and low humidity, easing combustion and propagation of fire, and making it more difficult to extinguish the fire.	Increased likelihood of "dry thunderstorms", leading to dry downbursts with extreme wind gusts.
	Increased surface runoff due to changes in surface conditions/infiltration rates	Increased surface water flooding due to changes in surface conditions/infiltration	Heatwave during drought puts increased pressure on already strained water resources. Reduction in surface moisture content results in higher surface temperatures during heatwave	Drought	Increase in forest fire risk and severity due to dry vegetation available for combustion. Further strain on water resources to deal with forest fire.	No Interaction
	Increase of runoff due to soil loss, leading to greater movement of debris that can block channels, culverts etc. and results in greater flooding. Potential mud flooding and increased erosion.	No Interaction	Higher temperatures in affected areas due to land albedo changes	Further strain on water resources (extinction, consumption and pollution due to ashes). Changes in land properties affecting soil moisture absorption.	Forest Fire	Under specific scenarios, a severe forest fire can alter weather dynamics, creating local erratic and strong wind gusts.
	Potential of increased movement of debris that can block channels, culverts, drainage networks etc. resulting in greater flooding. Movement of surface water by wind may change pattern of flooding. For fluvial flooding there is a connection to storms as they impact the barriers preventing settlements from torrents	Strong wind is one the main drivers of storm surges therefore wind gusts could increase the severity of storm surge	May alleviate some effects of heatwave though the cooling effect of moving air	High wind gusts or sustained winds increases evapotranspiration, worsening drought effects on vegetation	Increased ferocity of forest fire development/spreading due to wind	Storm Winds

Figure 16. Multi-hazard interaction matrix modified from De Pippo et al., (2008).

In addition to one hazard changing the regional conditions and/or triggering a hazard, the occurrence of one hazard may increase the probability of a secondary hazard occurring. A review of multiple hazards by Tsoutsos et al., 2023 compiled a comprehensive list of hazard interactions including geophysical, hydrological and atmospheric types, defining whether one hazard triggers the other, and/or one hazard increases the probability of another occurring. Utilizing this

information along with the interaction matrix defined in Figure 16, a hazard interrelation matrix (see Figure 17) has been derived. This figure summarizes the modeled hazards and combinations that should be modeled within ICARIA where three interactions between Primary and Secondary Hazards are considered:

1. **Primary Hazard Increases Magnitude of Secondary Hazard:** The effects of a primary hazard have changed characteristics of the region in such a manner that the magnitude of a secondary hazard will be larger. For example, as a result of drought within a region, the top soil has become hard with reduced porosity/infiltration rate. As such there would be increased surface runoff during an extreme rainfall event leading to increased flood depth.
2. **Primary Hazard Triggers Secondary Hazard:** The effects of the primary hazard result in a secondary hazard occurring. Such as an earthquake triggering a tsunami, or flooding triggering a landslide through erosion processes and ground saturation.
3. **Primary Hazard Increases the Probability of Secondary Hazard:** Changes to the environment as a result of a primary hazard increase the likelihood of occurrence for a secondary hazard. For example, a region experiencing periods of drought may be more susceptible to forest fires due to drying/degradation of local vegetation.

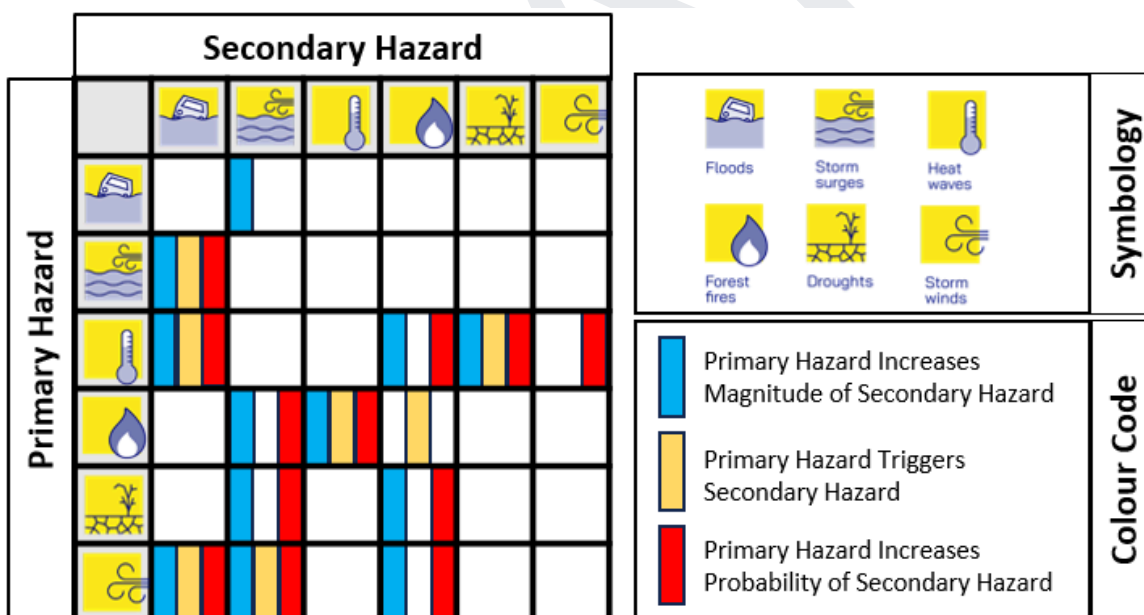


Figure 17. Hazard interrelationship matrix for modeled hazards within ICARIA.

Within the scope of ICARIA, when modeling multi-hazard events these interactions will be considered for both Compound Coincident and Compound Consecutive hazard events.

4.3.1 Modeling from Single to Multi-Hazard Events

As highlighted in Section 4.2, when modeling multi-hazard events, it is important to take into account the influence of one hazard on the magnitude and/or likelihood of subsequent hazards, along with the additional interrelationships between exposure and vulnerability for risk/impact assessments. The complex interactions result in a range of plausible scenarios that can play out over time during a multi-hazard event. From a modeling perspective, for scenarios where there are probabilistic interactions between variables, Bayesian Networks (BNs) can be applied where it is possible to define the probability of an event (in this instance a Hazard A) occurring given new information, for example that another event (Hazard B) is or has occurred. In Harris et al., (2022), a GIS-based Bayesian Network was developed to evaluate flood damages across multiple sectors that considered variations and uncertainty in hazard, exposure and vulnerability. This example demonstrated a range of possible scenarios at the hazard level for the single hazard type of flooding that considered flood duration, maximum depth and maximum flow velocity.

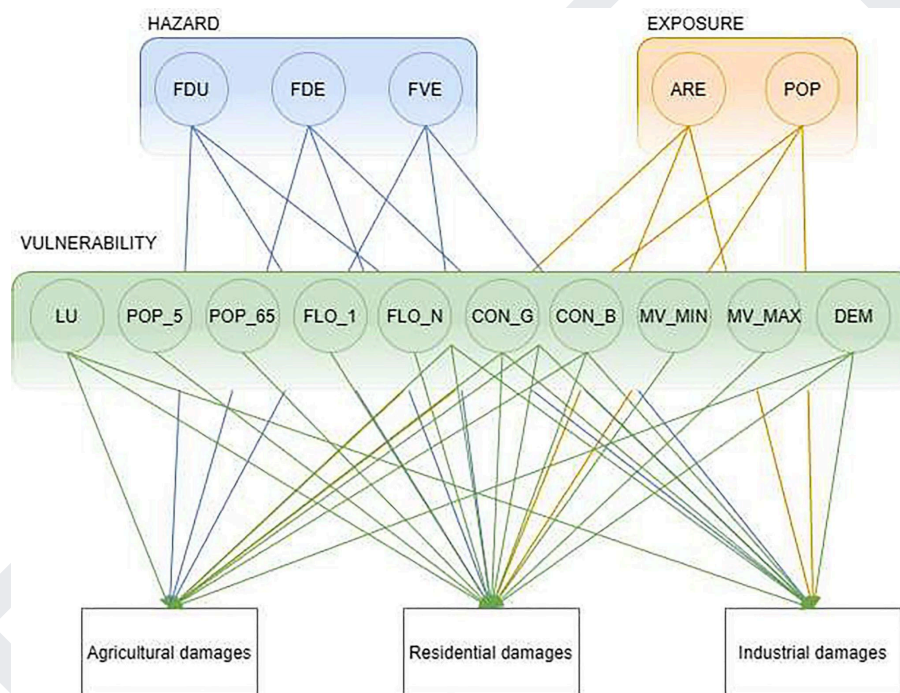


Figure 18. BN approach for assessing flood risks that consider variations in Hazard, Exposure and Vulnerability, where the hazard level Flood duration (FDU). Maximum flood depth (FDE), and Maximum flood velocity (FVE) are considered (Harris et al., 2022).

In the holistic modeling framework of ICARIA an elementary brick model (see Figure 19) is used to derive the risk/impact assessment for compound and cascading multi-hazard events. The term “elementary bricks” refers to model components such as “Hazard”, “Exposure”, “Vulnerability” etc. Within this approach, the interactions between modeled hazards are captured along with changes in exposure and vulnerability over time and due to prior events via the “Dynamic Vulnerability” functions based on prior work from EU-FP6 EXPLORIS project (EXPLORIS 2002; Zuccaro et al.,

2008; Zuccaro & De Gregorio, 2013) and EU-FP7 CRISMA project (CRISMA 2012; Garcia-Aristizabal et al., 2014; Aubrecht et al., 2013).

Climate Change context

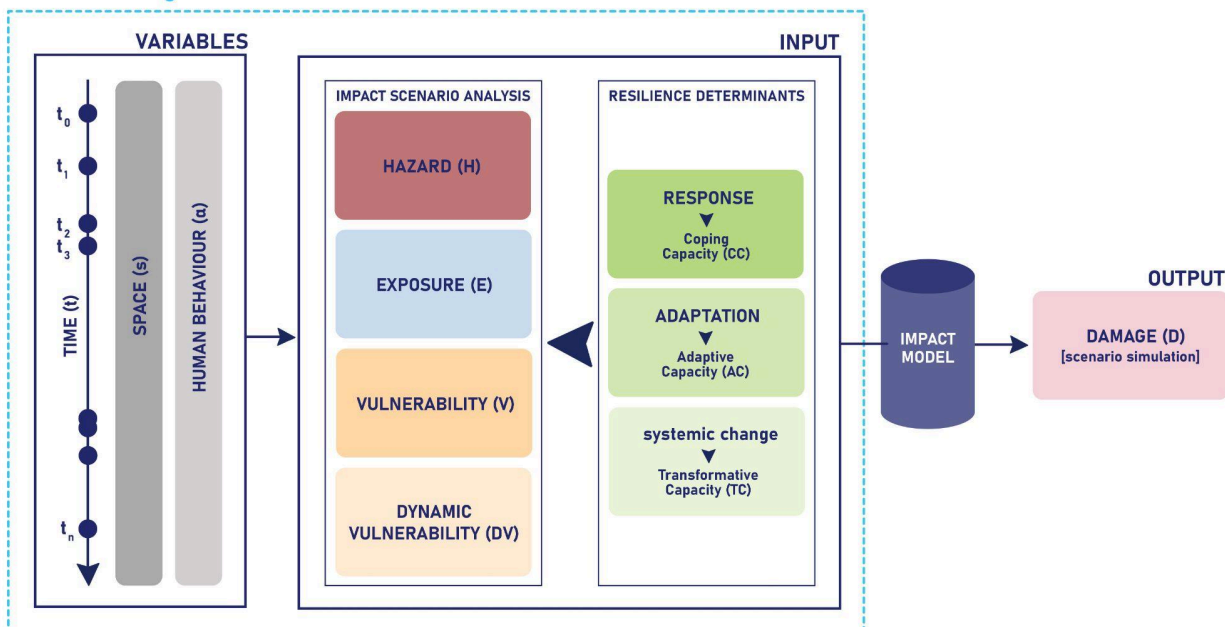


Figure 19. Elementary brick model depicting the holistic modeling framework for risk/impact assessment in ICARIA (modified after Zuccaro et al., 2018 and Russo et al., 2023).

Within this elementary brick model, in addition to the dynamic vulnerability, the modeled hazard scenarios will also take into consideration the interdependencies/physical interactions between hazards during compound events along with how the occurrence of one event may lead to the changes in the probability of occurrence of subsequent events through the use of BNs.

Whilst this elementary brick model outlines how hazard combinations are to be modeled within ICARIA, when examining the cumulative effects that natural hazards have over longer time-frames that consider climate change and shared socioeconomic pathways (SSPs) we need to expand the model to consider a range of potential future scenarios. Building on work from the EU-FP7 SNOWBALL project (Zuccaro et al., 2018), each case study will develop specific timelines depicting causal chains for their modeled hazards. These causal chain timelines (like that shown in Figure 20) show the modeled triggering events and hazards that will be used to highlight the potential impacts multi-hazard events can have over time.

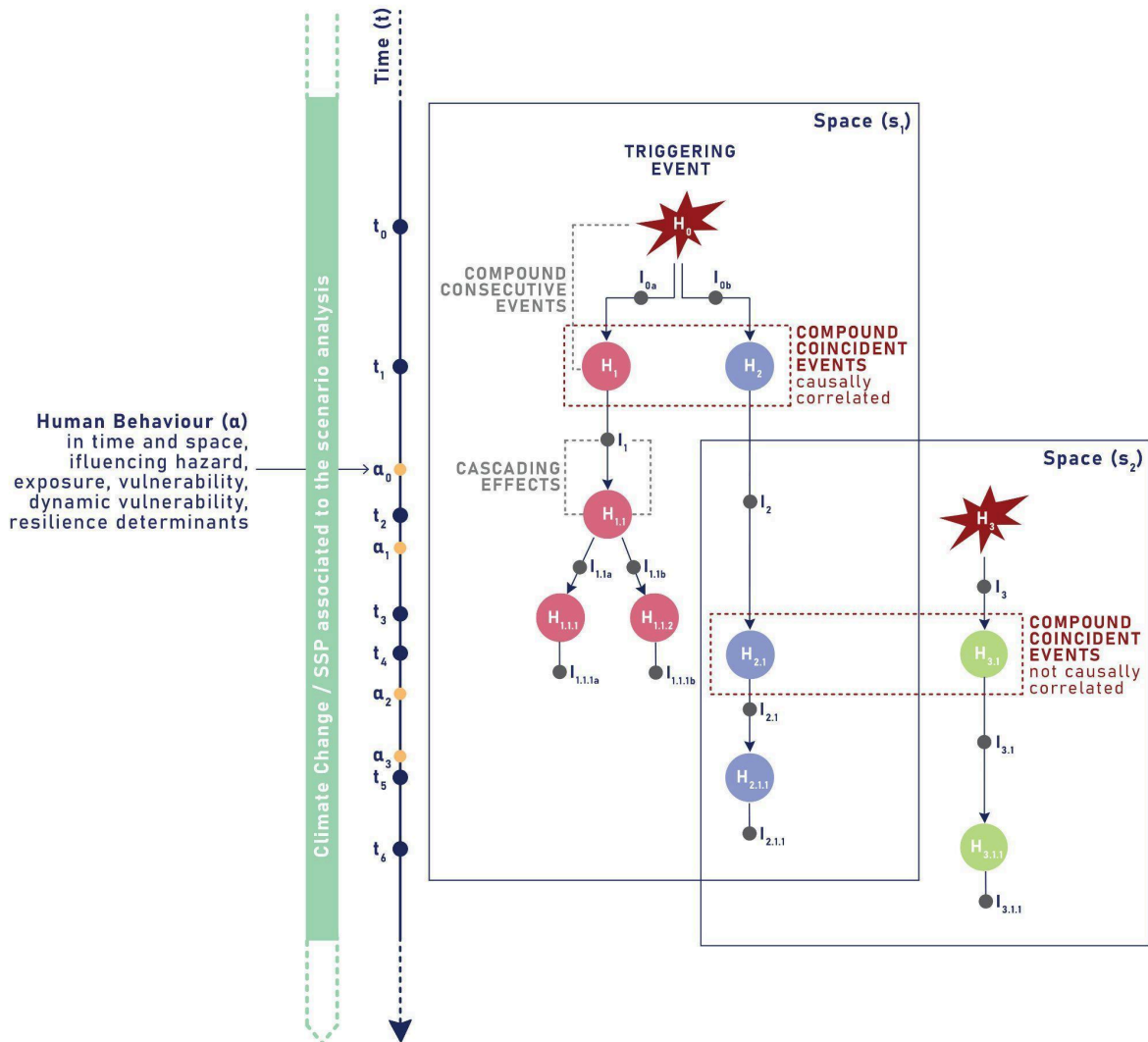


Figure 20. Timeline of events showing compound (coincident, causally or not causally correlated, and consecutive) events and cascading effects where “H” is Hazard, and “I” is Impact. The influence of key-variables (i.e., time, space, and human behaviour) in the risk/impact/resilience assessment process has been considered (modified after Zuccaro et al., 2018).

4.4 Specific multi-hazard events physical interactions

4.4.1 Pluvial flood and storm surge

The occurrence of a compound event involving a coincident storm surge and a pluvial flooding generates challenging flood management scenarios in coastal urban areas due to the interactions established between both hazards (Qiang et al., 2021, Ming et al., 2022).

On the one hand, a storm surge entails a temporary rise of the mean sea level and maximum wave height. On the other hand, in an urban area, an extreme rain event increases the amount of water

running through the sewer network and surface runoff. This rain water is meant to be discharged through the main sewer pipes of the urban drainage network to receiving water bodies. In coastal urban areas, often this body is the sea (Russo et al., 2015).

Typically, the drainage network outfalls that discharge water on the sea during combined system overflow (CSOs) episodes are built considering a safety height above the mean sea level. However, during storm surge events, the mean sea level can rise to the point where this safety height is exceeded by a transitory extreme sea level. If this occurs, sea water is able to intrude the outlet of the urban drainage systems through the lowermost point of the outfall pipes. As a result, the drainage capacity of the whole network is reduced according to the seawater intrusion level. This situation, which is known as “backflow” or “backwater” phenomenon, can lead to upstream saturation of the drainage network leading to flooding in upstream parts of the network drainage area. Extensive literature and research has demonstrated the relevance of this situation (Ming et al., 2022, Laster Grip et al., 2021, Bevacqua et al., 2019, Qiang et al., 2021, Domingo et al., 2010). The conceptual model proposed in Qiang et al., 2021 depicts this phenomenon.

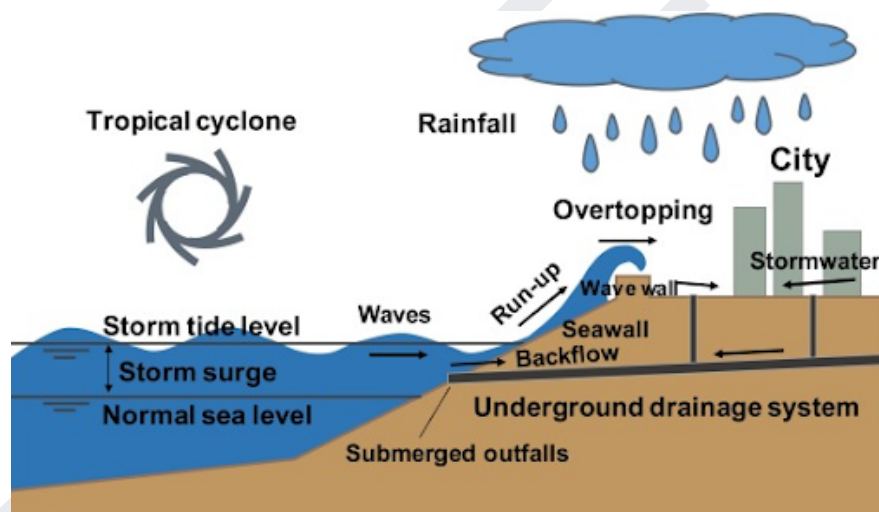


Figure 21. Conceptual model of the backflow phenomenon occurring during coincident storm surges and extreme rain events in coastal urban areas (figure from Qiang et al., 2021).

At the level of physical interaction between hazards during coincident compound events, extreme rain events (in urban coastal areas) and storm surges do interact in the following ways:

- The sea level rise during storm surges can increase the possibility of occurrence and severity of pluvial floods during extreme rain events due to the reduction of drainage efficiency of the urban drainage network caused by the backflow effect and/or overtopping of coastal defenses.
- Pluvial floods can generate additional flood volume in coastal areas leading to a quicker surcharge of the sewer network in coastal low-lying areas.

Based on the previous explanation, it is considered that neither extreme rain events have triggering effects on storm surges nor viceversa.

Typically, both extreme events have a short to mid duration. Extreme rain events don't usually last more than a few hours in the study areas, and in general, the highest rain intensity is recorded during an even shorter time span of a few minutes (Bulti et al., 2020). On the other hand, storm surge durations (in the Mediterranean sea) do not typically exceed a duration of 24 hours (Cid et al., 2016, Martzikos et al., 2021).

In Europe, such events are less frequent and intense compared to other regions. However, some precedent exists in the Mediterranean basin, for instance the Gloria storm, which affected the Spanish eastern coast in January 2020 causing major human and material losses (Sanuy et al., 2021).

Multiple sources agree upon the fact that the effect of climate change will lead to more frequent and intense extreme rain events (Russo et al., 2020a, Monjo et al., 2016, Llasat et al., 2010, AMB 2016). On the other hand, research on future storm surges in the Mediterranean indicate that intensity and duration of these events are likely to remain stable or even increase in some coastal regions of this sea (Androulidakis et al., 2015, Cid et al., 2016, Martzikos et al., 2021, Russo et al., 2020a). As a result of that, it seems evident that this kind of combined multi-hazard event will pose a growing threat to Mediterranean coastal regions.

Another fact that can exacerbate flooding in urban areas (either caused by single or multi-hazard events) is the reality that the urban drainage infrastructure of most urban areas were designed to cope with high return period events (e.g. T10 to T20). However, these design return periods did not account for the effect of climate change. As a result of this, it is expected that in the coming dates such sewer systems might become under-dimensioned for events with lower return periods than their design criteria (Russo et al., 2015, Russo et al., 2020a).

4.4.11 Flooding and extreme wind

Compound events of flooding and extreme wind pose a risk to various types of natural and settlement areas. There are mainly two types of synoptic situations resulting in compound precipitation and storm events in Europe: (i) events that are caused by extratropical cyclones (Owen et al., 2021); (ii) summertime convective events.

The recurrence time and magnitude of compound precipitation and wind extremes is predicted to increase under future conditions due to anthropogenic climate change (Ridder et al., 2022) and especially, convective events will gain importance since warmer air can store more water, thereby causing increased precipitation intensities. At the level of physical interaction between hazards during coincident compound events, extreme rain events and wind storm do interact in the following ways (as also depicted in Figure 17).

- Storms can increase the magnitude of flooding, trigger them through blocking the outflow of rivers and increase the probability of occurrence as storms alter the vulnerability of the surroundings towards extreme precipitation intensities.

- In mountainous regions for instance, storms might lead to increased tree swamp, which causes increased inflow to the streams and decreased stability of the slopes. Both aspects affect flooding, the first one through blocked torrent barriers and therefore prevents the streams from flowing, the second increases the severity of extreme precipitation as destabilized slopes store less water, therefore increasing the runoff (Sebald et al., 2019).

It is important to note that we consider flooding as a hazard, not precipitation because extreme wind can trigger flooding, but can't trigger increased precipitation events.

4.4.2 Drought and forest fire

Meteorological drought, which is generally defined as a period of unusual precipitation deficit, is not a necessary or sufficient condition for forest fire occurrence as fires also happen during conditions of normal seasonal aridity. However, when a drought occurs, both live and dead fuels can dry out and become more flammable and the probability of ignition increases along with rate of fire spread (Andrews et al., 2003; Scott & Burgan, 2005). As indicated by Littell et al. (2016), drought influences fire both directly via fuel moisture and indirectly through biological effects on vegetation. Therefore, drought indices and fire behavior metrics have been used in the literature to model fire occurrence, spread and area burned. Interpretation of these metrics is complicated by the fact that fuel availability and flammability in different vegetation types respond differently to the same meteorological conditions, but the probability of ignition increases in most fuels when fuel moisture is low. However, even short-term drought generally increases wildfire occurrence through effects on fuel moisture.

The World Meteorological Organization has recommended the Standardized Precipitation Index (SPI) as the most commonly used indicator to be used by all National Meteorological and Hydrological Services around the world for detecting and characterizing meteorological droughts (Svoboda et al., 2012). The SPI indicator, which was developed by McKee et al., (1993) and was described in detail by Edwards and McKee (1997), measures precipitation anomalies at a given location. It is based on a comparison of observed total precipitation amounts for an accumulation period of interest (e.g. 1, 3, 12, 48 months) with the long-term historic rainfall record for that period. The historic record is fitted to a probability distribution (the "gamma" distribution), which is then transformed into a normal distribution such that the mean SPI value for that location and period is zero. For any given region, increasingly severe rainfall deficits (i.e. meteorological droughts) are indicated as SPI decreases below -1.0 . Riley et al., (2013) found that 3-month SPI explained 70% of the variability in area burned and 83% of the variability in the number of large fires in the western United States.

Because SPI is based only on precipitation, it does not address the effects of high temperatures on drought conditions, such as by damaging cultivated and natural ecosystems, and increasing evapotranspiration and water stress. A new variation of SPI - the Standardized Precipitation and Evapotranspiration Index (SPEI) - has been developed (Vicente-Serrano et al., 2010), which

includes precipitation and temperature, in order to identify increases in drought severity linked with higher water demand by evapotranspiration.

4.4.3 Drought and heatwave

The effects of climate change are resulting in periods of higher extremes in relation to weather patterns. These extremes are reflected in the increasing occurrences of heatwaves and periods of drought. Over the last decades a large number of regions across the planet have been affected by both hazards in a coincident and/or consecutive way (Sheffield et al., 2012, Miralles et al., 2018). These events have demonstrated a great damage potential on water resources among other important assets (Hao et al., 2022).

It is important to remark that multiple sources show a consensus on the fact that the land–atmosphere feedbacks between heat waves and droughts are not yet fully understood and remain as an open debate (Sheffield et al., 2012, Miralles et al., 2018). In this sense, novel metrics and/or criteria to evaluate the ability of climate models in simulating this kind of compound events are needed (Zscheischler et al., 2021). Nevertheless, certainty exists on the fact that combined precipitation deficits and warm periods cause reduced surface runoff that lead to hydrological drought conditions that pose a challenge to the management of water resources with negative impacts in water supply (Hao et al., 2022, Russo et al., 2019, Osman et al., 2022).

In the context of ICARIA, drought will be assessed from the point of view of hydrological drought, focussing on water resources and examining the implications these droughts have over long timeframes on water resources availability. Hao et al., 2022 concludes that the co-occurrence of precipitation deficit and warm periods lead to reduction of surface runoff that contribute to generate or exacerbate hydrological drought. From a meteorological point of view, other sources indicate that there is an existing negative relationship between high temperature periods and precipitation rates. Hence, atmospheric blockings and persistent anticyclonic systems, which can generate heatwave episodes, have a direct effect on reduction of water resources availability, especially in regions with a high dependency on surface water reservoirs (Dong et al., 2018, Russo et al., 2019, Osman et al., 2022).

Within the hydrological drought assessment, the derivation of available water resources is dependent in part upon evaporation and evapotranspiration rates that are derived from temperature projections provided by climate models. The proposal of modeling the effects of heatwaves on droughts is a probabilistic approach whereby data relating temperature extremes from heatwave climate predictions will be used to uplift the average temperatures used within the drought models for calculating evaporation and evapotranspiration rates. Based on the interactions between these two models, the proposed approach aims to capture the potential variances in water resources availability over time due to the compound effects of heatwaves occurring during the drought periods.

4.4.4 Heatwave and forest fire

According to the World Meteorological Organization, a heatwave can be defined as a period where local excess heat accumulates over a sequence of unusually hot days and nights. Heatwaves

amplify many risks, such as health-related or economic risks, including increased human mortality, drought and water quality, wildfire and smoke, power shortages and agricultural losses.

Heatwaves and forest fires are hazards that are associated with each other, with their cooccurrence to have been increased the past decades, constituting in multi-hazard events. These events are mainly controlled by the duration and severity of the heatwaves. Prolonged high temperatures and dry conditions makes vegetation more susceptible to the ignition of forest fires. Variations in weather and climate influence wildfire activity by modulating vegetation production and fuel aridity (Bradstock et., al 2010).

The mechanism that favors forest fire risk is based on hot and dry conditions that enhance evapotranspiration and reduce fuel moisture, leading to an increase in available fuel combustion. Therefore, hot and dry conditions are usually precursors to mega-wildfires. As arises from recent studies (Squire et al., 2021; White et al., 2023) recent global extreme events have also demonstrated that the wildfire risk readily escalates to an extreme level when subjected to combined hot and drought conditions. Thus, the risk of wildfires increases quickly, under combined circumstances and so finally the conditions conducive to wildfires can rapidly intensify. In the study of Sutanto et al., (2020), the compound heatwave-fire hazard appeared 2 times higher than concurrent drought-heat waves and affected regions mainly in Spain, Portugal, Sicily, Greece and in the Scandinavian countries (Figure 23).

The following figure depicts the relative importance of compound events in European territory here, as indicated by Ridder et al., 2020 who provided the first spatial estimates of the occurrences of compound events (see extreme McArthur forest fire index FFDI which represents fire danger and HW as Heatwave) on the global scale.

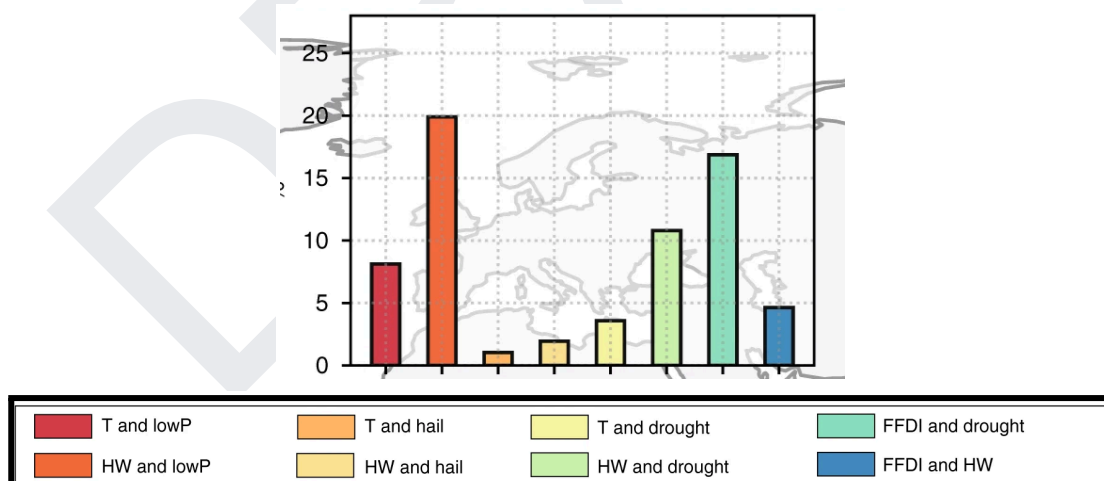


Figure 22. Hazard pairs related to extreme precipitation and temperatures (source: Ridder et al., 2020 - part of Fig. 3b). Hazard pairs related to extreme precipitation and temperatures, including combinations of high temperatures (T), low precipitation (lowP), heatwaves (HW), high probability of large hail (hail), low SPI (drought), and extreme McArthur forest fire index (FFDI) values

However, according to a recent study that aimed to investigate spatio-temporal patterns of compound and cascading hazards in Europe, dry hazards are expected to occur predominantly in isolation (19.8%) than in compound (5.1%). The total occurrence of single and compound hazards in the period 1990–2018 across Europe calculated, as the number of days per hazard (or compound hazard) divided by the total number of summer days as June, July and August (JJA) (2668), is presented in the following figure.

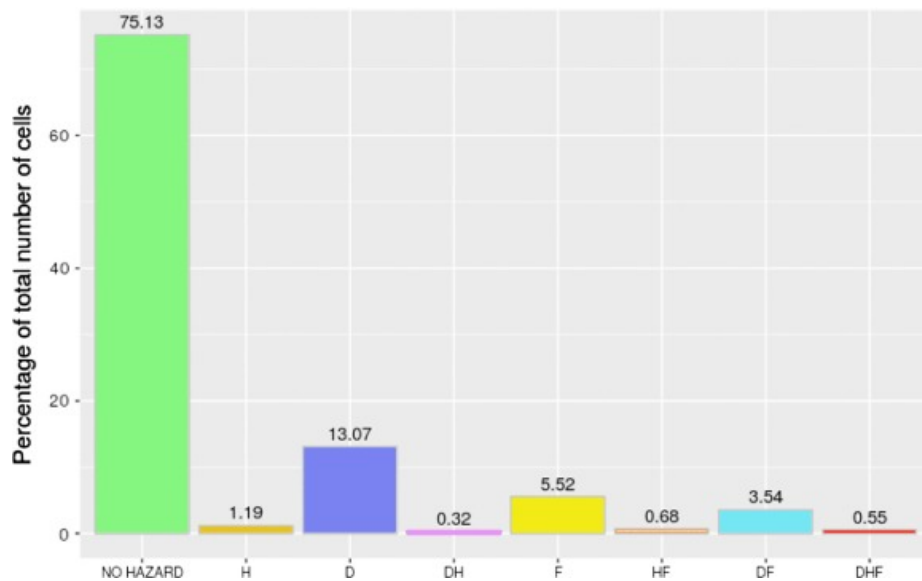


Figure 23. Total occurrence of single and compound hazards, calculated as the number of days per hazard (or compound hazard as, H=heatwave, D=Drought, DH=Drought-Heatwave, F=Fire, HF=Heatwave-Fire, DF=Drought-Fire, DHF= Drought-HeatWave-Fire) divided by the total number of JJA days (2668) over the period 1990–2018 across Europe (source: Sutanto et al., 2020)

It should be pointed out that as a product of multiple processes, fire weather is a form of compound event, which consists of wind, temperature, precipitation and relative humidity that can exacerbate flammability by warming and drying fuels.

4.4.5 Extreme Wind and forest fire

A notable association exists between high fire risk and the presence of strong winds. The coupling between high fire risk and extreme winds are distinguished by their frequent occurrence and substantial impact. The presence of strong winds play a crucial role in determining wildfire behavior by affecting their rapid spread (leading to the enlargement of burned areas), their intensity and by increasing the likelihood of surface fires evolving into more severe crown fires with extreme fire behavior (Zong et al., 2023, Richardson et al., 2022). Previous studies (Cruz et al., 2012, Bianchi et al., 2014) indicated that wildfires driven by extreme winds can rapidly grow to a large size after their ignition and quickly impact communities, where little or no official warning might be issued, and cause multiple fatalities.

The study of Cruz and Alexander (2019) aimed to provide first approximations of wildfire propagation for situations where there is little or no time to apply more comprehensive and accepted fire behavior prediction methods, known as rule of thumb, in conifer forests, eucalypt forests, and shrublands but not in grasslands. The rule of thumb states that a wildfire rate of forward spread is approximately 10% of the average 10-m open wind speed. For example, the figure below illustrates that the wind speed bar can be read as the 10% rule of thumb rate of fire spread prediction in the rate of fire spread axis label. More specifically, this rule yielded estimates that approximate the observed rates of spread of known wildfire disasters. Moreover, the results of the evaluation study of Cruz et al., (2020) in respect to the rule of thumb, have substantiated the dominant and strong control that wind speed exerts on the forward spread rate of wildfires when fuels are critically dry (i.e. both fine dead fuel moisture and overall long-term landscape dryness) and winds are strong. These burning conditions produce the type of fires that typically surprise emergency response agencies and communities as a result of their fast spread rates and corresponding high fireline intensities. Despite the high energy release rates associated with wildfires burning during these conditions, the convective plume tilt associated with the strong winds leads to a decoupling between the advancing flame front at the surface and the plume downwind that seems to reduce fire-plume interactions and the associated uncertainty with respect to weather conditions at the surface.

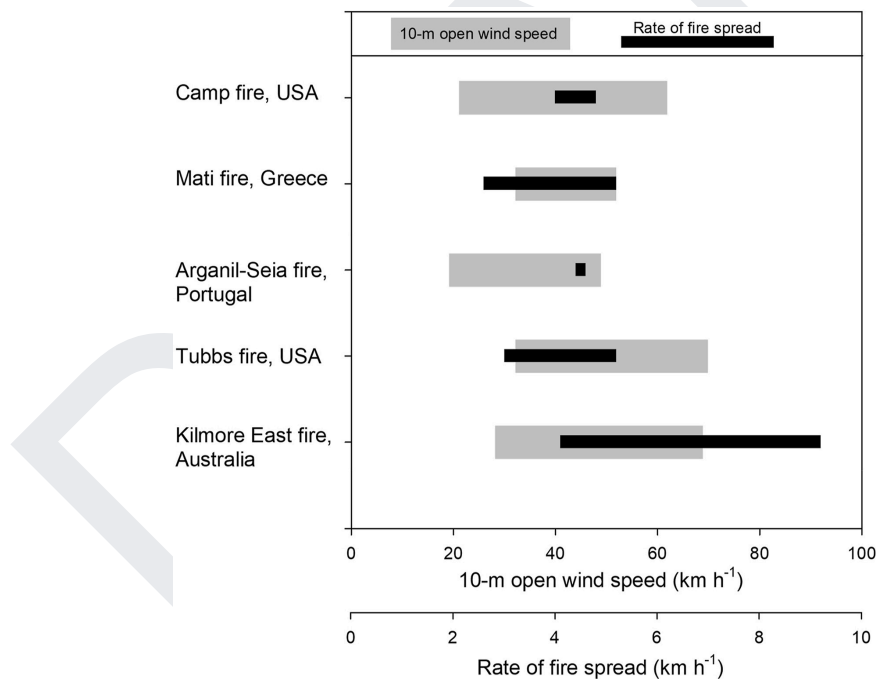


Figure 24. Example of the temporal and spatial range in reported forward rate of spread and 10-m open wind speed for five recent wildfire disasters involving large numbers of human fatalities. (source: Cruz et al., 2020).

4.4.6 Heat Wave, drought and forest fire

Heatwave, drought, and forest fire, as presented in sections 4.4.2, 4.4.3, and 4.4.4, are linked bilaterally with each other. A multi-hazard event which combines the negative effects of each hazard combination presented above can be seen as the “worst case scenario”.

The prolonged high temperature and low precipitation periods increase the risk for forest fire events. Despite the increased risk, such conditions are catalytic factors for the duration and severity of forest fires. As described in section 4.4.4, heatwaves enhance evapotranspiration and reduce fuel moisture and consequently increase the available fuel for combustion. This effect of heatwave can be enhanced by drought events (see section 4.4.2), which also lead to decreased fuel moisture before the occurrence of the heatwave. Thus, the probability of a forest fire or even a mega fire is increased. Such multi-hazard events took place in Spain and Rhodes Island in 2023 (Copernicus 2023). Heatwaves and forest fires can also be catalytic for increasing the severity of drought. Burned areas have decreased water retention capabilities (Ebel et al., 2012), causing not only flood events, but also decrease infiltration into the groundwater table. This can increase hydrological drought, by reducing water availability and water quality. Moreover, heat waves with large durations are associated with increased evapotranspiration and evaporation, which leads to decreasing soil moisture and decreasing water availability. Finally, heatwaves add an additional stress on decreased water resources as a result of the increased water consumption by the people during the heat waves period. In the same context, drought and forest fire also affect the severity of heat waves. The increased area of burned areas is associated with high local temperatures and the generation of heat island effect, in certain cases. This is enhanced by the dry areas' decreased cooling capacity due to moisture evaporation.

5 Historic single and multi-hazard extreme events

The present section presents examples of extreme single and multi-hazard events that have affected the case study regions historically. It is important to note that this list does not intend to provide an exhaustive documentation of all events that have affected these regions, but to illustrate their scale and damage capacity in different perspectives. Furthermore, this list of events provide examples that can be used by the case study leaders to test, calibrate and validate their hazard and impact assessment models in later steps of the project.

Another fact worth mentioning in this section is the difficulty that the authors of this document have encountered to find sources of information (e.g. official reports, databases...) focused on historic multi-hazard events. As it is highlighted in the methodological deliverable of project ICARIA (ICARIA, 2023a), the multi-hazard perspective in extreme events risk assessment is a rather new approach that goes beyond the classic “silo” framework. As a result of this, historic events involving more than one hazard often have not been studied nor classified as such. Consequently, it becomes challenging to identify a large number of specific events of this nature that have occurred in the case study regions.

5.1 Àrea Metropolitana de Barcelona CS

Table 1 provides a summary of single and multi-hazard extreme events that have affected the AMB in recent years.

Table 1. Recent single and multi-hazard extreme events affecting the AMB.

Date	Kind of event	Characteristics of the event	Impacts
1988 to 1989	Drought (Single hazard event)	In this period water reservoirs fell to the lowest level ever in Catalunya after 48 months with no significant precipitation.	Reduction of surface water reservoirs to the minimum values ever registered.
2 to 14/8/2003	Heatwave and forest fire (Compound multi-hazard event)	Persistent heat wave with 13 days of duration and daily maximum temperature above 35 °c (mean temperature of the period 26,7°C). Over the same period of time, several forest fires affected the region.	-
2005 to 2008	Drought (Single hazard event)	Major drought period with 16 straight months with no significant precipitation in the whole region.	Reduction of surface water reservoirs to values around 20%.
13/9/2006	Extreme rainfall (Single hazard event)	Most affected municipalities: Barcelona, Sant Cugat del Vallès and Cerdanyola del Vallès	Extensive floodings in urban areas Economic damage of 7.6M€
23 to 26/7/2006	Heat wave (Single hazard event)	4 days in a row with a daily maximum temperature above 35°C and night temperature above 26°C	-
26/12/2008	Storm surge (Single hazard event)	Flooding in coastal areas Significant wave height up to 3,5m	Economic damage of 3.7M€
28/12/2008	Storm surge	Flooding in coastal areas	Economic damage of 2.3M€

Date	Kind of event	Characteristics of the event	Impacts
	(Single hazard event)	Significant wave height up to 2,5m	
17 to 20/8/2009	Heat wave (Single hazard event)	4 days in a row with a daily maximum temperature above 35°C (maximum value of 36,1°C) and night temperature above 26°C	-
30/7/2011	Extreme rainfall (Single hazard event)	Observed precipitation of 60mm in 2h in the city of Barcelona	Flooding of urban areas, disruption of train service and electricity supply Economic damage of 3.3M€
19 to 23/8/2012	Heat wave (Single hazard event)	4 straight days with maximum temperature above 35°C	-
4 to 7/7/2013	Heat wave (Single hazard event)	3 straight days with maximum temperature above 35°C	-
21 and 22/1/2017	Storm surge (Single hazard event)	Flooding in coastal areas Significant wave height up to 4m	Economic damage of 6.3M€
17/8/2018	Extreme rainfall (Single hazard event)	Observed precipitation of 60 mm in 2.5 h Most affected municipalities: Barcelona, Sant Cugat and L'Hospitalet de Llobregat	Flooding of urban areas and partial inundation of highways and secondary roads Economic damage of 2.1M€
6/9/2018	Extreme rainfall (Single hazard event)	Observed precipitation of 20mm in 30 min and up to 86 mm in 12 h Most affected municipalities: Barcelona and L'Hospitalet de Llobregat	Flooding of several areas in Barcelona and flooding of underground metro stations Economic damage of 3.8M€
15/11/2018	Extreme rainfall	Observed precipitation of >100mm in 18 h	Flooding of several areas in Barcelona,

Date	Kind of event	Characteristics of the event	Impacts
	(Single hazard event)	Most affected municipalities: Barcelona, Castellbisbal, El Papiol and Sant Cugat del Vallès	electricity disruption in some areas and flooding of underground metro stations Economic damage of 4.1M€
28 to 29/6/2019	Heatwave (Single hazard event)	2 days with maximum temperature above 34°C	-
23 to 24/7/2019	Heatwave (Single hazard event)	2 days with maximum temperature above 34°C	-
27/7/2019	Extreme rainfall (Single hazard event)	Observed precipitation of 43 mm in 30 min Flooding observed in several municipalities: Barcelona, Sant Feliu de Llobregat, Sant Just Desvern and Viladecans	Flooding of several areas in Barcelona, flooding of underground metro stations Economic damage of 2.9M€
12/8/2019	Extreme rainfall (Single hazard event)	Observed precipitation of 40 mm in 30 minutes Foodings observed in the municipality of Castelldefels	Flooding of some low points in roads and interruption of train circulation Economic damage of 1.9M€
19 to 22/1/2020	Extreme rain and storm surge (Combined multi-hazard event)	Observed precipitation of 121 mm in 24 h and storm surge with significant wave height up to 6m	Flooding of coastal areas, impact on multiple assets in the coastline including important railway infrastructure. Economic damage of 19.4M€

Date	Kind of event	Characteristics of the event	Impacts
18/12/2020	Extreme rainfall (Single hazard event)	Observed precipitation of 290 mm in 12h Flooding observed in several municipalities: Montcada i Reixac, Molins de Rei, Sant Cugat del Vallès and Cerdanyola del Vallès	Flooding of major highways, urban areas and disruption of train service Economic damage of 9.4M€
13-15/8/2021	Heatwave (Single hazard event)	Two straight days with maximum temperature above 34°C	-
15-18/6/2022	Heatwave (Single hazard event)	Three straight days with maximum temperature above 35°C	-
July 2020 to December 2023 (current date)	Drought (Single hazard event)	Three consecutive years with mean precipitation far below the average. The Standard Precipitation Index of the last 36 months in the AMB and the catchment areas of its water reservoirs indicate extreme drought conditions.	Reduction of surface water reservoirs to values below 18%, leading to the deployment of emergency measures (according to local authorities drought management plan) and limitation of water consumption for several economic sectors and municipalities
18 to 24/08/2023	Heatwave (Single hazard event)	Five days in a row with maximum temperatures around 36°C Two straight nights with minimum temperature between 29 and 30°C	-

5.2 Salzburg Region CS

Flooding and extreme wind has impacted the rural areas of Salzburg increasingly over the past, resulting in flooded and damaged settlements and impacting the prevailing infrastructure. A few events are depicted in Table 2.

Table 2. Recent single and multi-hazard extreme events affecting the Salzburg region.

Date	Kind of event	Characteristics of the event	Impacts
08/2002	Extreme Precipitation (consecutive hazard event)	Two consecutive low pressure systems over Italy caused extreme precipitation amounts and flooding; precipitation of 150 – 180 mm in two days	> 13.5M€
31/7/2014	Extreme Precipitation (single hazard event)	low pressure system from Adria: 100 mm over large areas increasing the already high Salzach levels and resulting in flooding	Settlements: damage dependent on available flooding protection energy production: reduced supply in hydro power plants
12/07/2016	Extreme Wind (single hazard event)	Strong squall Wind up to 100 km/h	Uprooted trees, unroofed houses, streets closures, damaged houses and vehicles, power outages because of damaged power-supply lines
29-30/10/2018	Extreme Precipitation (single hazard event)	High water due to heavy precipitation in „Muhr“	Community of Muhr cut off from the outside world, river Mur overflowed its banks, numerous houses and streets were flooded

Date	Kind of event	Characteristics of the event	Impacts
03-15/01/2019	Extreme Precipitation and Wind (compound hazard event)	Persistent “Nordstau” weather pattern that brought strong winds and extreme amounts of snow	Closed off settlements, closed streets and railways, 1 casualty, 44 injured, damaged infrastructure, broken trees
01/07/2019	Extreme Precipitation (single hazard event)	High water in the region of „Pinzgau“	Several streams burst their banks, bridges, torrent barriers dredged up damaged/carried away, severe damage to 70 houses, ten businesses, twelve farms and several municipal roads
28-29/07/2019	Extreme Precipitation (single hazard event)	Heavy rainfalls in the night and high water in the whole federal state of Salzburg, especially in “Tennengau”	Flooding, traffic obstructions, road and train closures, flooded cellars, graves and garages as well as landslides and rockfalls, demolished bridges
11/2019	Extreme Precipitation (single hazard event)	Persistent inflow of warm and humid air causes in total extreme precipitation amounts; 3-day precipitation: 186 mm	Due to prevailing snow not that strong, small flooding and landslides
28/06/2020	Extreme Precipitation and Wind (compound hazard event)	Stormfront with heavy rainfall 1h = 35mm precipitation (measured in “Mattsee”)	Flooded cellars and streets, uprooted tree
22/06/2021	Extreme Precipitation and Wind (compound hazard event)	Hot and unstable air masses resulted in longlasting convective events with extreme precipitation and gusts	Damages in agriculture, buildings and vehicles

Date	Kind of event	Characteristics of the event	Impacts
			total damage Salzburg and lower Austria: 25M €
12-13/07/2023	Extreme Precipitation and Wind (compound hazard event)	Thunderstorm with heavy rainfall, storm and hail especially in "Zell am See" and "St. Johann im Pongau"	Flooding of roads, tracks, cellars and underground garages, uprooted trees, broken branches, damage to fields
18/07/2023	Extreme Wind (single hazard event)	Thunderstorm with heavy rainfall, squall and hail	Uprooted trees, power outages, unroofed houses, 157 people were evacuated from cable car gondolas, damage to fields
05/08/2023	Extreme Precipitation (single hazard event)	Heavy rainfall leads to high water 50 mm precipitation	Flooding, contamination of drinking water, as fertilizer and manure were washed into a spring in "Mittersill"
20/10/2023	Extreme Wind (single hazard event)	Wind storm due to foehn; >117 km/h	Multiple fallen trees affecting electricity cable, roofs were destroyed, electricity supply disrupted

5.3 South Aegean Region CS

5.3.1 Syros

The island of Syros has historically been affected mainly by the combination of extreme wind and precipitation events. These events are accompanied by extensive flash flooding of local torrents, located in various locations of the island, but most importantly in the city of Hermoupolis. The flooding events in the city of Hermoupolis have the highest impact on the populations (most densely populated area of the island), but also on critical infrastructure, since all of them are located in this area.

Table 3. Historical flooding events affecting Syros island.

Date	Kind of event	Characteristics of the event	Impacts
22/10/1976	Flooding associated with extreme precipitation (single hazard event)	Wind 7-8 Beaufort Yearly accumulated rainfall data indicated increase from 370mm to 720mm	<ol style="list-style-type: none"> Damages on road network and all critical infrastructures Lalakia torrent (main torrent flowing through Hermoupolis) destroyed houses and vehicles
13/1/1997	Flooding associated with extreme precipitation (single hazard event)	Yearly accumulated rainfall data indicated increase from 370mm to 620mm	Torrent flush flooding, with no damages to infrastructure

Date	Kind of event	Characteristics of the event	Impacts
17/2/2003	Flooding associated with extreme precipitation (single hazard event)	Total 149 mm rainfall at that date Yearly accumulated rainfall data indicated increase from 370 mm to 650 mm	<ol style="list-style-type: none"> 1. Emergency status declared 2. Torrent flush flooding 3. Road network (northern island) damaged 4. Road network blocked due to landslides and falled drystone walls 5. Abandoned houses destroyed 6. Schools not operational 7. Cost of damage for all Cyclades 74M € 8. 1 casualty at Foinikas village 9. 3 people rescued from flooded torrent 10. Water and Sewerage network damaged at Kini village
3/2/2011	Flooding associated with extreme precipitation (single hazard event)	Wind 7 Beaufort High waves (Eastern winds) 99 mm rainfall in 24 hours Yearly accumulated rainfall data indicated increase from 370mm to 480mm	<ol style="list-style-type: none"> 1. Landslide under airport runway 2. Vehicles damaged in Hermoupolis 3. Port flooded due to high waves from eastern winds, in combination with torrent flush floods 4. Port wave breakers damaged

5.3.2 Rhodes



The island of Rhodes, in comparison with Syros island, given its size, geographic location, and geomorphology is prone to: wildfires and floods. Wildfires are caused mainly by the extensive duration of heatwaves, with characteristic low humidity, and the unmanaged forests (with fire prone vegetation like pine trees). Flooding events in Rhodes are caused by the geomorphology of the island and the relatively high yearly accumulated precipitation, averaging 700 mm annually.

Table 4. Historical events affecting Rhodes Island.

Date	Kind of event	Characteristics of the event	Impacts
09/08/1987	Wildfire (single hazard event)	<ol style="list-style-type: none"> 1. Duration: 4 days 2. Total burned area: 12.865 acres 3. Damages: <ol style="list-style-type: none"> a. 47 agricultural facilities b. 935 animals c. 33 agricultural equipment 	
22/11/1989	Flooding associated with extreme precipitation (single hazard event)	Total precipitation: <ul style="list-style-type: none"> • 202 mm/day • Average wind speed: 12 km/h 	Damages: <ul style="list-style-type: none"> • 1 bridge collapsed • 60% of Archaggelos village flooded

Date	Kind of event	Characteristics of the event	Impacts
24/09/1992	Wildfire (single hazard event)	<ol style="list-style-type: none"> 1. Duration: 9 days 2. Total burned area: 7.200 acres 3. Human casualties: 1 4. Damages: <ol style="list-style-type: none"> a. 1 House b. 5 agricultural facilities c. 400 animals d. 4 agricultural equipment 	
20/11/1994	Flooding associated with extreme precipitation (single hazard event)	<p>Total precipitation: 163 mm in 15 hours</p> <p>Average wind speed: 13.9km/h</p>	Casualties: 2 people
26-28/11/1998	Flooding associated with extreme precipitation (single hazard event)	Total precipitation: 1135mm in 72 hours	Casualties: 3 people

Date	Kind of event	Characteristics of the event	Impacts
9/11/2004	Flooding associated with extreme precipitation (single hazard event)	Total precipitation: 532 mm in 24 hours	Extensive damages at Archaggelos village
22/07/2008	Wildfire (single hazard event)	1. Duration: 6 days 2. Total burned area: 13.300 acres 3. Damages: a. 4.164 animals	
28/01/2011	Flooding associated with extreme precipitation (single hazard event)	Total precipitation: • 150 mm in 16 hours	Damages at: Faliraki, Afantos, Archaggelos, Massari, and Lardos villages

Date	Kind of event	Characteristics of the event	Impacts
			
22/11/2013 - 23/11/2013	Flooding associated with extreme precipitation (single hazard event)	Total precipitation: <ul style="list-style-type: none"> • 164 mm in 24 hours 	<ul style="list-style-type: none"> • Casualties: 4 people • Damages at Ialysos, Kremmasti, and Pastida villages • Damages at Kalithies, Afantos, and Archaggelos villages • Houses and vehicles damaged 

Date	Kind of event	Characteristics of the event	Impacts
17/07/2023	Wildfire (single hazard event)	<ol style="list-style-type: none"> 1. Duration: 10 days 2. Total burned area: 17.630 acres 3. Damages: <ol style="list-style-type: none"> a. 45 houses b. 2.500 animals 	

DRAFT

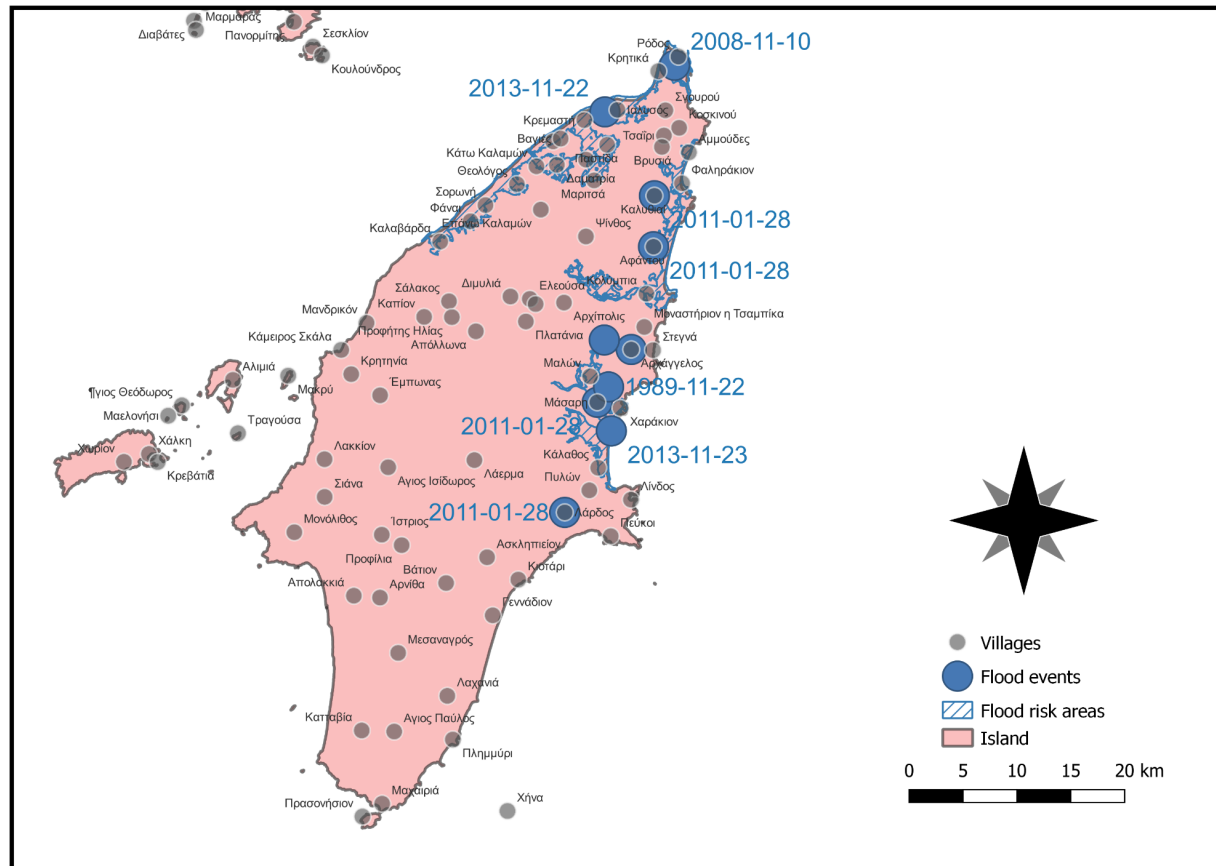


Figure 25. Map of historic flooding events at Rhodes island

6 Single hazard models

As it has been acknowledged in previous sections, historically climate risk management has been addressed from a single-hazard perspective. The “single-hazard models” developed in this context stand as a starting point to develop “multi-hazard models” to build holistic risk assessment methodologies. In this sense, project ICARIA integrates the efforts and results of previous research projects dedicated to the development of hazard models for risk assessment of extreme weather events.

The following subsections present the single-hazard models that will be implemented in the ICARIA case studies and that will support the development of multi-hazard models in later steps of the project. For each one, a general description and the source reference are provided together with a comprehensive list of the software and data requirements of the method.

The table below presents a short summary of the single hazard models presented in the following sections:

Table 5. Summary of characteristics of single hazard models

Hazard modeled	Data requirements	Model setup complexity	Modeling tool/method	Previous implementations
Pluvial flooding	High	High	Infoworks ICM	Project RESCCUE (Russo et al., 2020a) Project CORFU (Russo et al., 2012)
Storm surge	Low	Low	ArcGIS (or similar)	Project CRISIS ADAPT II (Russo et al., 2020b)
Fluvial flooding	Medium	Medium	HydrMT-SFINCS	-
Heat wave	Medium	Medium	QGIS and/or Rhinoceros (Grasshopper)	Project CLARITY (Zuccaro & Leone, 2021)
Forest fire	High	High	Canadian Fire Weather	Project EU-CIRCLE (Sfetsos et al., 2021)
Drought (hydrologic)	Medium	Medium	HBL Light	Project RESCCUE (Forero-Ortiz et al., 2020)
Extreme wind	High	High	WRF Model	CLIMPACT (Katopodis et al., 2021)

6.1 Pluvial flooding in urban areas

6.1.1 Model setup, calibration and validation

The aim of an urban pluvial flooding hazard model is to identify the areas of the model domain that will be affected by pluvial flooding during extreme rain events of a given return period and to determine the water depth and velocity in the affected areas. This information is essential to quantify the risk associated with simulated events (Russo et al., 2013).

However, the complex nature of urban areas, with small-scale elements such as gullies and sidewalks, makes modeling flooding scenarios in these environments a complex process. In order to obtain reliable results, it is necessary to employ high resolution models that represent all city-scale relevant features of an urban drainage network along with the terrain elevations, urbanistic elements, buildings and terrain land-uses. According to the current state-of-the-art, hydrodynamic 1D/2D models are the most reliable tool for this purpose, despite having a higher computational cost compared to alternative methods. Importantly, this kind of hydrodynamic (1D/2D) models are based on solving the free complete flow equations (mass and momentum equations) in a dynamic approach in 1D and 2D domains. (Henonin et al., 2013).

In 1D/2D models, the 1D domain simulates water behavior in the sewer network while the surface flow is computed using a 2D model (see Figure 26). This second domain is essential to generate realistic simulations of the flow spreading across complex urban surfaces, computing the flow depths and velocities anywhere in the urban model area for the whole simulation period. These parameters are essential to later quantify the risk and impacts generated by a specific flooding event (Pina et al., 2016).

For this hazard assessment, the modeling tool that will be used in project ICARIA is the software Infoworks ICM ultimate by Autodesk (www.innovyze.com).

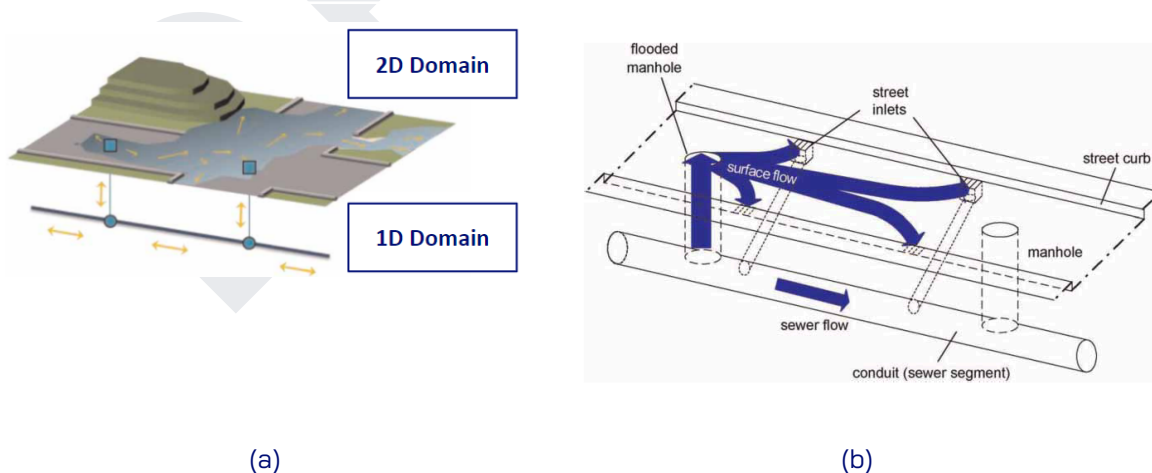


Figure 26. Conceptual representations of the 1D and 2D domains interaction (a) (Henonin et al., 2013); (b) (Schmitt et al., 2004)

The setup of 1D/2D urban drainage models involves a complex process and a significant amount of data and parameters (see Table 6). In summary, the main general tasks to setup a model of this characteristics are:

1. Data collection (see Table 6)
2. Import the network data in GIS format to Infoworks ICM
3. Implement singular infrastructures to the model
4. Definition, in case of semi-distributed models, of the subcatchments and their related features (hydrological losses and rainfall-runoff transformation methods)
5. Definition of 2D overland flow domain
6. Create the 1D/2D coupled model with special focus on the flow interaction between the 1D and the 2D domains
7. Dry weather flow model configuration
8. Boundary conditions definition

After the setup, the model has to be calibrated and validated. These are two essential steps to ensure realistic simulation results (Mark et al., 2014).

Calibration consists of simulating extreme rain events and comparing the model results with real observations (in terms of flow parameters like discharge, water depth, velocity, flood extension) of the same event. The hydraulic and hydrological parameters are generally adjusted to improve the agreement between the real (measured) and simulated flow or level time series both in the 1D and the 2D domains of the model. This is an iterative process and terminates when the model can reproduce the flow measurement and the flooding effects accurately for any simulated event. Flow measurement time series in automatic limnimeters or rain gauges are good data sources for calibrating the 1D modules. Such data is usually recorded by the sewer network operators. However, calibrating the 2D domain results becomes more difficult due to the lack of exact measurement of the flooding depths. Resources such as emergency teams reports and citizen recording of the events (often uploaded to social media) are often used for this purpose (Russo et al., 2022, Henonin et al., 2013). Validation follows the same principle as calibration and serves to ensure that, after being calibrated, the model is capable of adequately simulating other rain events that were not used in its calibration process.

As a good practice, it is recommended to consider 3 to 4 separate events for the model calibration and 2 to 3 for the validation. Importantly, both processes must be based on different historic flooding events that have affected the model domain for which there is a good and detailed data availability. Such data should include a record of precipitation with a high time resolution (1 to 5 minutes), records of water levels at different points of the sewer network (for

instance limnimeter measurements dataset) and information about surface areas affected by flooding during the events.

6.1.2 Model conceptual design

When developing a 1D/2D urban drainage model, it is essential to consider how the routing of rainfall to the sewer network and the interaction between the 1D and the 2D domains are modeled. Different approaches exist for this (Pina et al., 2016):

- Semi-Distributed (SD): in this approach, runoff is transformed by the rainfall–runoff module and is directly applied into the sewer flow module domain. Hence, the presence of water overflow in the city surface is only represented and computed when the drainage network is surcharged and floods occur.
- Fully-Distributed (FD): the result of the rainfall-runoff transformation is applied to the 2D superficial domain, previously discretized according to a terrain land use analysis, and computes its routing to the sewer system inlets where water enters the 1D model. This approach enables a more realistic representation of the overland flow of rainwater in pervious and impervious areas.
- Hybrid (H): in this case, the runoff generated in building areas (e.g. roofs, terraces, courtyards) is directly conveyed into the sewer systems similarity to a SD model. Nowadays, built areas in cities are directly connected to the sewer system. Hence, all the runoff generated in these spaces is directly conveyed to this network without reaching non-built urban areas such as streets. On the other hand, these non-built areas, including pervious (e.g. parks and natural areas) and impervious areas (e.g. streets, sidewalks, squares, etc.), generate 2D overland flow that is computed by the model and routed within the 2D domain until it enters the 1D domain through a surface inlet (FD approach).

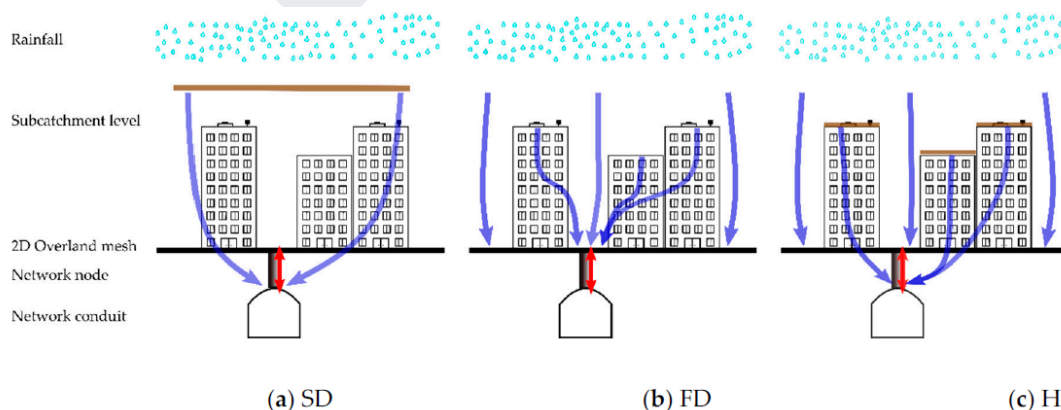


Figure 27. (a) Scheme of semi-distributed (SD), (b) fully-distributed (FD) and (c) and hybrid (H) 1D/2D coupled urban stormwater model approaches (adapted from Russo et al., 2020a).

Given its more realistic representation of the process of conveying runoff to the sewer system, the 1D/2D urban drainage models of project ICARIA will follow a Hybrid approach to define the interactions between the two model domains.

Another key conceptual aspect to consider in the model setup is the representation of the surface drainage systems. These systems are composed of runoff collection elements (generally grated inlets) and have an essential role in urban drainage. They allow runoff to be introduced into the sewer systems according to the design assumption and ensure safety conditions for pedestrians and vehicles during wet weather conditions (Russo et al., 2020). Furthermore, they are not only the runoff entry points to the underground drainage infrastructure, but they are the point (together with manholes) through which sewers overflows occur in case of pressurized pipes. So, grated inlets are the key elements that regulate the flow transferring between the 1D and the 2D domains of the model and, for this reason, need a proper hydraulic characterization. Despite their major importance, the simulation of these critical elements in large scale urban drainage models is often overlooked. Lack of information about inlets hydraulics, its typology and location and a poor representation of the secondary drainage network are usual constraints faced by model developers.

In order to adequately characterize the hydraulic performance of grated inlets it is necessary to incorporate equations that estimate inlet Hydraulic Efficiency (E) and the intercepted flow, such as the overflow in case of pressurized sewer pipes. Several experimental equations have been developed to estimate these parameters. Some of them determine the hydraulic efficiency of the grates as the ratio between approaching and intercepted flow rates. Other ones allow the estimation of discharge coefficient for grates under free flow and pressurized sewer pipes conditions (Russo et al., 2021).

6.1.3 Model results

The main outcome of this modeling approach are hazard maps displaying the flooding depths and water velocities in the city surface. It is also possible to visualize the water level in the pipe networks and other elements of the urban drainage system (e.g. flooding tanks, pumps, outfalls) during the rain event. Figure 28 depicts these results for a simulation in the city of Barcelona. On the one hand, flooding in the 2D domain of the model is represented by the blue areas, reflecting water depth in the urban surface. On the other hand, the flow conditions in the sewer system (1D domain) is reflected by a colored system based on the pressure condition in the pipes.

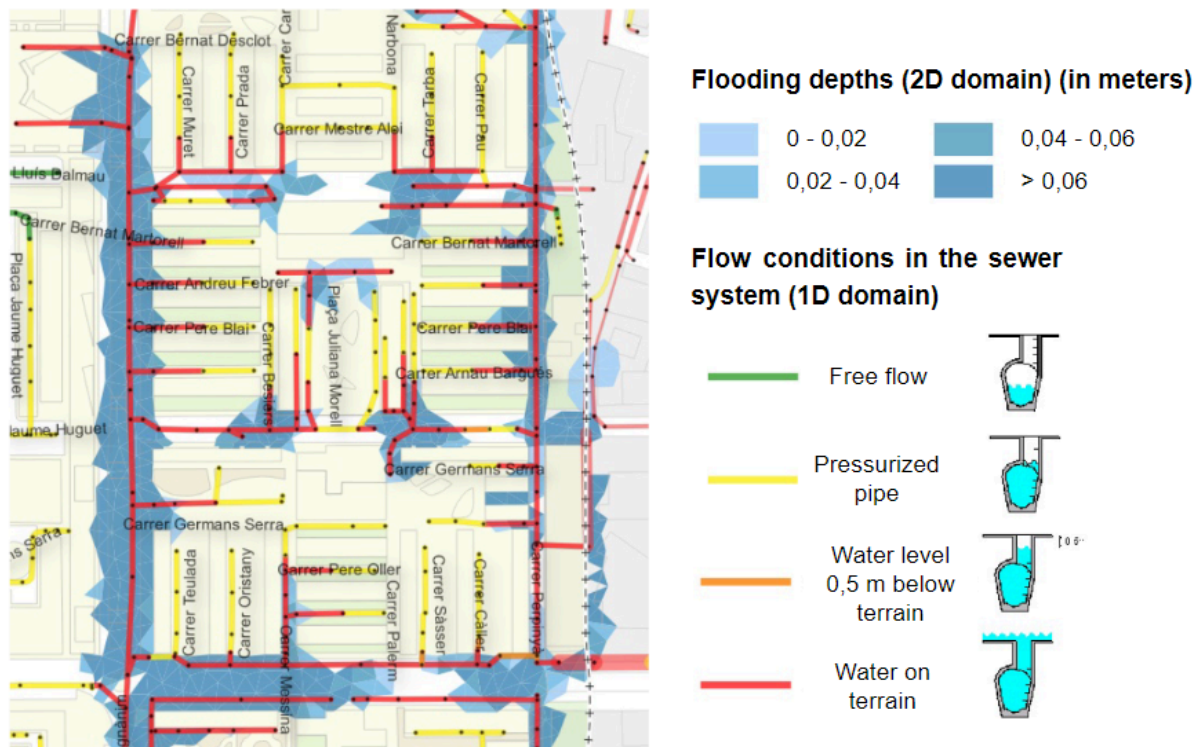


Figure 28. Example of a 1D/2D drainage model results in the city of Barcelona. The blue areas represent the flooded parts of the 2D domain (city surface). The coloured lines represent the pressure conscious in the pipes of the sewer network (Ajuntament de Barcelona 2019).

Based on these results it is possible to evaluate the following aspects in relation to a flooding event.

- 1) Risk associated with the flooding event
 - a) Identify hotspots more prone to be affected by flash floods
 - b) Determine the risk for pedestrians, vehicles and assets based on the water depth and flow velocity in the affected areas
- 2) Sewer system capacity to cope extreme rain events
 - a) Test the general capacity of a sewer system to drain stormwater during extreme rain events
 - b) Evaluate the performance of drainage single infrastructures (e.g. flooding tanks, pumps, outfalls)
 - c) Identify bottlenecks or under dimensioned points of drainage elements
 - d) Evaluate if the number of surface inlets to the sewer network is sufficient

- 3) Evaluate the capacity of specific improvements to the sewer network to reduce the severity of flooding events
 - a) Test the performance of potential new single infrastructures
 - b) Redimension old pipes to improve their drainage capacity
 - c) Assess the performance on sustainable urban drainage systems

Importantly, this hazard modeling approach is valid to simulate flooding scenarios associated with extreme rain events that represent different climate change scenarios. Hence, it stands as a valuable tool for planification of measures, both structural and operational, to improve resilience against floods in future horizons.

6.1.4 Data requirements

The table below summarizes the data needs of the pluvial flooding hazard model:

Table 6. Data required (model inputs) for the pluvial flooding hazard model

Data requirements for the pluvial flooding hazard model		
Data group	Description	Source
Historic climate data	Historic datasets of pluvial data with the highest time resolution possible (mm / 1 to 5 min resolution)	EU/National/Regional meteorological agencies Meteorological databases (e.g. Copernicus)
	IDF curves of historic rain events	Results of Task 1.2
Future climate projections	Local downscaled precipitation projections of different climate change scenarios	Results Task 1.2
	Future IDF curves considering different climate change scenarios scenarios and time horizons	
Land use and terrain information	Digital Terrain Model with high resolution (e.g. 2x2m)	Regional/national geography agencies
	GIS information on urban buildings including building, dimensions, characteristics and land use	
Sewer system data	Complete sewer system network including all pipes, nodes and single infrastructures. This dataset has to include all dimensions, absolute altitude and operational characteristics of all pipes and elements of the network	Local sewer system operators or municipalities
	Sewer network rain gauge flow historic recordings datasets	

Data requirements for the pluvial flooding hazard model		
	Historic measurements/recordings of flooding events in the surface of the model domain	Local sewer system operators or municipalities. News agencies and citizen's recordings.
Hydrological parameters	Parameter values/functions to determine the rain-runoff conversion: hydrological losses due to infiltration in previous terrain, initial rain loss value, initial infiltration rate, residual infiltration rate, decay and recovery infiltration constants.	Literature and empirical data
Boundary conditions	Historic recordings of sea and river mean water height in the sewer system outlets.	EU/National/Regional meteorological and water management agencies

6.2 Storm surge flooding

6.2.1 Model setup, calibration and validation

Extensive literature and historic events highlight the fact that coastal urban areas and its infrastructures are heavily affected by sea-related hazards such as the mean sea level rise or extreme sea levels during storm surges. The latter are capable of causing serious damage to assets and threatening citizens integrity (Hallegatte et al., 2011, Androulidakis et al., 2015, Pycroft et al., 2016). Frequently, storm surges generate extreme sea levels (ESL) that can cause flooding of low-lying coastal areas (Hallegatte et al., 2011 and Qiang et al., 2021). The hazard posed by this phenomenon to the risk receptors can be assessed based on the simulated coast food associated with a storm of a given return period. The simulation of such events can be based either on static or dynamic models. Statistical storm surge models, often described as "bath-tub" models, determine flooded locations as those hydraulically connected to the coast and with a lower elevation in comparison to a ESL associated to a storm surge. This approach has low data and computational requirements but does not take into account important characteristics and processes of storm tide flooding such as wave propagation or the time variations of the flooding process. On the other hand, the complex dynamic models are capable of simulating the physical processes related to storm tide flooding involving the sea-land interactions. They offer more accurate results at the cost of extensive datasets and higher computational requirements (Ramirez et al., 2016).

In project ICARIA, the methodology suggested to quantify the flood depth in coastal areas is based on a simplistic hydrostatic approach that has been successfully used in other EU research projects such as Crisis-Adapt II (Russo et al., 2020b). The model is based on a Digital Terrain

Model (DTM) with the best possible resolution of the coastal area and an estimation of the ESL associated with different return periods.

The ESL parameter can be calculated with the following equations:

$$ESL = MSL + \eta_s + \eta_{W-SS}$$

Where MSL is the mean sea level, η_{tide} is the height of the tide, and η_{W-SS} is the extreme contribution from waves and storm surges that is estimated according to the equation:

$$\eta_{W-SS} = SSL + 0.2H_s$$

Where SSL is the storm surge level, H_s is the significant wave height, and 0.2 is a generic approximation of the wave setup (USACE 2002).

Following the hydrostatic approach of the model, the ESL value is “added” to the normal sea level. The comparison between the coastal DTM and the ESL scenario permits to estimate the area affected by the flooding and the potential water height that can be observed. This addition and comparison processes can be developed with most commercial geographical information system (GIS) commercial softwares.

6.2.2 Model results

The model outputs are coastal flooding maps showing the water depth and the area affected by storm surge related flooding of a given return period.



Figure 29. Examples of coastal flood hazard maps for pedestrians (on the left) and vehicles (on the right). Red = high, orange = medium and green = low. T=100 for Baseline (current) scenario (Russo et al., 2020b).

6.2.3 Data requirements

The table below summarizes the data needs of the storm surge flooding hazard model.

Table 7. Data required (model inputs) for the storm surge flooding hazard model

Data requirements for the storm surge flooding hazard model		
Data group	Description	Source
Historic climate data	Historic datasets of the sea level and wave height recordings with the best time resolution possible	EU/National/Regional meteorological agencies Meteorological databases
Future climate projections	Future projections of ESL events considering different change scenarios and time horizons	Results Task 1.2
Land use and terrain information	Recent bathymetry of coastal area with best possible resolution	Regional/national geography agencies
	Digital Terrain Model with high resolution of the coastal area (e.g. 2x2m) GIS information on urban buildings including building, dimensions, characteristics, kind of land use of the coastal area	

6.3 Fluvial flooding

To assess the impact of extreme precipitation events on rural areas with respect to flooding, hydrological and hydrodynamic models are used. Hydrological models are a valuable tool to understand how much water flows through a given territory, the consequences of different management options, as well as the potential risks of human settlements near water bodies.

A hydrological model requires data such as daily precipitation, temperature (daily average, minimum and maximum), wind and radiation as meteorological inputs. Furthermore, auxiliary input data such as soil maps providing different soil parameters is needed. This information is necessary to calculate the amount of water that can be stored in a given soil type as well as the runoff generated.

Even though the above described approach offers great potential, it lacks an understanding of the flood dynamics. The typical time scales and spatial resolutions of the models discussed above cannot provide information on the water dynamics. For modeling flash floods, or similarly tsunamis, more detailed hydrodynamic models are required. They demand highly precise input, with respect to the water sources as well as the DEM. Typically, in order to investigate such problems, 2D hydrodynamic models are used. Besides the high demands on the input side, they are also computationally expensive and require large computing power.

6.3.1 Model setup, calibration and validation

Within ICARIA we focus on compound events and the assessment of possible adaptation scenarios. Therefore, the HydroMT-SFINCS has been chosen. It is a physics-reduced hydrological model, runned by integrating the HydroMT framework with the Structure Functions In Catchments and Soils (SFINCS) approach, supplying a powerful tool to understand and assess river flood hazards. It has been tested for different use cases and also with respect to compound events (Eilander et al., 2023). The model employs physics-based principles to simulate key hydrological processes such as river discharge, precipitation and spatially-varying infiltration and bed roughness. By reducing computational complexity without sacrificing essential physical principles, HydroMT-SFINCS efficiently captures the interactions between land, water and atmosphere that influence river flooding.

In understanding river flood hazards, the model considers various factors, including topography, land use characteristics, and weather conditions. HydroMT-SFINCS excels in providing insights into the timing, magnitude, and spatial distribution of river floods. Its reduced physics approach enables faster simulations, allowing researchers to conduct extensive scenario analyses. By incorporating historical data and climate change projections, the model can be used to assess the evolving nature of river flood hazards over time. The model's versatility extends to its ability to assess the effectiveness of flood mitigation measures and adaptation strategies. It can be used to evaluate the impact of land-use changes, infrastructure modifications, or climate resilience measures on river flood risks.

Based on the input data HydroMT-SFINCS produces maximum flood depth maps that are used as input for the impact assessment models. For past events, the simulated flood depth map will be validated against observations to assess the model's ability to represent local characteristics. Based on the quantitative/qualitative analysis, future flood depth will be corrected or accepted as is.

In summary, HydroMT-SFINCS is a valuable tool for understanding river flood hazards by efficiently capturing essential hydrological processes. Its application extends to scenario planning, climate change impact assessments, and the development of strategies to enhance river flood resilience. The model's reduced physics approach strikes a balance between accuracy and computational efficiency, making it a practical asset for researchers and policymakers alike.

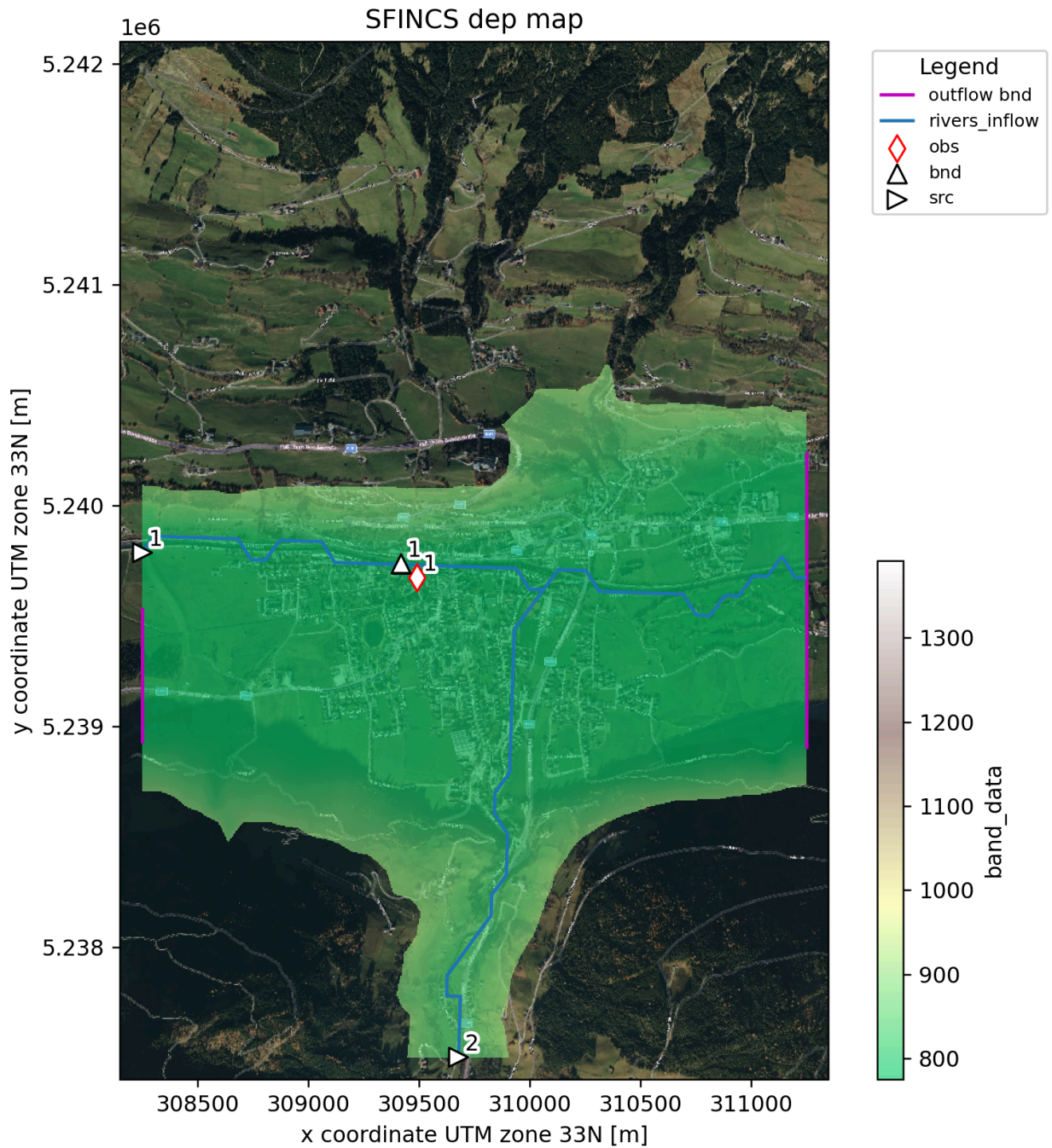


Figure 30. Example of Mittersill, an area within the Salzburg region highly affected by flooding, displaying the elevation within the modeling area, rivers, settlements and road network.

6.3.2 Data requirements

The table below summarizes the data needs of the fluvial flooding hazard model.

Table 8. Data required (model inputs) for the fluvial flooding hazard model

Data requirements for the fluvial flooding hazard model		
Data group	Description	Source
Historic climate data	Historic datasets of precipitation	EU/National/Regional meteorological agencies Meteorological databases
Future climate projections	Local downscaled precipitation projections of climate change scenarios	Results Task 1.2
	Future IDF curves considering different change scenarios and time horizons	
Land use and terrain information	River bathymetric and width information	Regional/national geography agencies; Copernicus
	Terrain model and land cover data (including building information in settlement areas)	
	Digital Elevation Model (1x1m); road network, infrastructure	

6.4 Heat wave in urban areas

6.4.1 Model setup, calibration and validation

In the context of climate change, the development and refinement of heat wave hazard models play a key-role in both understanding and mitigating the impacts of extreme temperature events. Such models aim to predict the spatial and temporal patterns of heat wave occurrence within a defined geographical domain, taking into account thresholds, duration, and recurrence intervals as main relevant factors. As widely described in the sectoral scientific literature, by integrating meteorological data, climate projections and land cover characteristics these models offer valuable insights into both the distribution of heat waves and their severity (Lindberg et al., 2016; Zuccaro & Leone, 2021). Consequently, they allow for estimating related impacts, giving the opportunity to policymakers, public health officials, and resilient planning experts to implement proactive strategies and measures in order to protect communities from possible negative effects of rising temperatures (EC, 2013).

The exacerbation of local hazard conditions is compounded by all those transformative processes related to urban growth, land use changes, and anthropic activities within urbanized areas (e.g., industry, transport, services, etc.). Indeed, the intensity and repercussions of heat waves induced by climate change are strongly influenced by the characteristics of the built environment, which presents a high level of complexity depending on the shape and layout of buildings, building typologies, configuration of open spaces, surface materials, and/or density

and distribution of vegetation (Leone & Raven, 2018). Therefore, coupling 2.5D GIS-based modeling tools and 3D parametric design models allows to identify main areas susceptible to the urban “heat island effect” during an extreme heat wave with a certain return period as well as accurately analyze the urban microclimate variation related to the built environment at different levels.

For heat wave extremes, the modeling tool that will be used in the ICARIA project is the HWLEM (Zuccaro & Leone, 2021), originally designed to evaluate not only the heat wave hazard but also the associated impacts on human health in terms of mortality increase and hospitalization costs. Developed within the H2020 CLARITY project (CLARITY, 2017), HWLEM hazard/impact assessment model takes into account i) short- to long-term climate change scenarios until 2100 and ii) the urban microclimate variability. In this sense, HWLEM integrates information that can be deduced from large-scale climate projections (city/district level) with variations at small-scale (block/building level), identifying specific relationships between the built environment features and the local effects of heat waves and slow-onset changes.

Temperature values are the starting point for evaluating local hazards conditions because relying exclusively on the analysis of historical data obtained from the observation of past events and projected into the future (i.e., downscaling of regional climate models) is insufficient to encompass the microclimatic variability related to the built environment. Indeed, urban morphology and land cover/use play a crucial role as they can significantly amplify or reduce the thermal stress experienced by individuals in urban contexts (Leone & Zuccaro, 2021). For this reason, the model represents a valuable support to properly identify and prioritize suitable and sustainable adaptation/mitigation measures that, by acting on both urban morphology and land cover, may not only be effective against heat wave hazard/impact but also bring social, economic and environmental co-benefits. In this context, the flexibility of the model offers the possibility of analyzing:

- the *current state scenario*, intended as the existing city configuration, prior to any adaptation/mitigation measure with respect to current and future climate;
- the *worst case (or “business-as-usual”) planning scenario*, intended as the city of the future where a limited consideration is given to climate change hazards/impacts;
- the *best case (or “best practice”) planning and design scenario*, intended as the city of the future where climate-resilient principles are widely applied through suitable adaptation/mitigation measures..

Within HWLEM, the variation of thermal stress in different city areas is simulated through:

- 1) **Mean Radiant Temperature (T_{mrt})**, one of the most important meteorological variables influencing human energy equilibrium and outdoor thermal comfort. It arises from the cumulative effect of longwave and shortwave radiant fluxes from the surrounding environment to which a human body is exposed (UTCI, <http://www.utci.org/index.php>;

Lindberg et al., 2016). This indicator is usually derived from the air temperature, surface temperature, urban morphology and land cover features (e.g., albedo, emissivity and transmissivity of surfaces, density and distribution of vegetation, sky view factor). The approach used to calculate T_{mrt} values does not consider wind speeds. However, as during heat waves low wind speeds are recorded, the simplification adopted in the model is acceptable (Gulyás et al., 2006, Chen et al., 2016, Oke et al., 2017).

- 2) **Universal Thermal Climate Index (UTCI)**, representative of perceived thermal stress that individuals experience in a certain area. It mainly depends on the T_{mrt} , relative humidity, air temperature, and wind speed that significantly affect the human being's physiological response to the surroundings. Thermal stress is divided into 10 UTCI range categories, from extreme heat stress (above +46°C) to extreme cold one (below -40°C). Between +9°C to +26°C there is no thermal stress. UTCI value also takes into account the clothing of individuals as a system of adaptation to external temperatures.

In order to estimate both the T_{mrt} and UTCI values, HWLEM usually takes into account three main variables:

- *Time period*, in which reference events occur. Such events can represent the current (i.e., 2011-2040) or future climate (i.e., 2041-2070, and 2071-2100);
- *Frequency* of reference events, which can be frequent (i.e., 1-year return period), occasional (5-year return period), or rare (20-year return period);
- *Greenhouse gas emissions*, which are expressed by the Representative Concentration Pathways (RCPs) (IPCC, 2014) and which the IPCC's Sixth Assessment Report (AR6) has integrated with the Shared Socioeconomic Pathways (SSPs) (IPCC, 2023).

Within HWLEM, the 2.5D analyses are carried out at the city/district level through GIS tools, while the 3D analyses are performed at the block/building scale using Algorithm Aided Design (AAD) tools (e.g., Rhinoceros + Grasshopper). If the first type of analyses provides urban heat hotspots, the second type assesses technical solutions integrating climate-resilient aspects with other green building and environmental design criteria and benchmarks.

The setup of the 2.5D/3D urban heat wave model is based on several consecutive steps and requires a minimum database containing information on climate, terrain morphology, land use, and vulnerability of the population involved (see Table 9). The whole modeling procedure unfolds as follow:

1. Data collection (see Table 9)
2. Define the weather conditions that characterize the event to be investigated (meteorologic data and climate projections)
3. Import the land use data and terrain information in GIS (2.5D) format to carry analyses at the urban/district scale

4. Transfer all data in Rhinoceros/Grasshopper (3D) format, in the event that analyzes at the block/building scale need to be conducted
5. Attribution of parameters to the land use data, also taking into account terrain information
6. Tmrt and UTCI evaluation

Utilizing local land use data, HWLEM allows deepening the spatial resolution of simulations, yielding outcomes on a 250 m grid (Figure 31, top right part). Each cell within the grid can be further analyzed in greater detail to identify areas characterized by critical hazard conditions related to the built environment (e.g., low-medium density areas with a prevalence of waterproof dark horizontal surfaces, lack of green areas, and trees).

A calibration of surface temperature and Tmrt values in heat wave conditions are generally carried out to support the assumptions done within HWLEM, based on elaborations from ENVI-MET (Simon & Bruse, 2020) and SOLWEIG (Lindberg & Grimmond, 2011) models (Figure 31, Figure 32 and Figure 33).

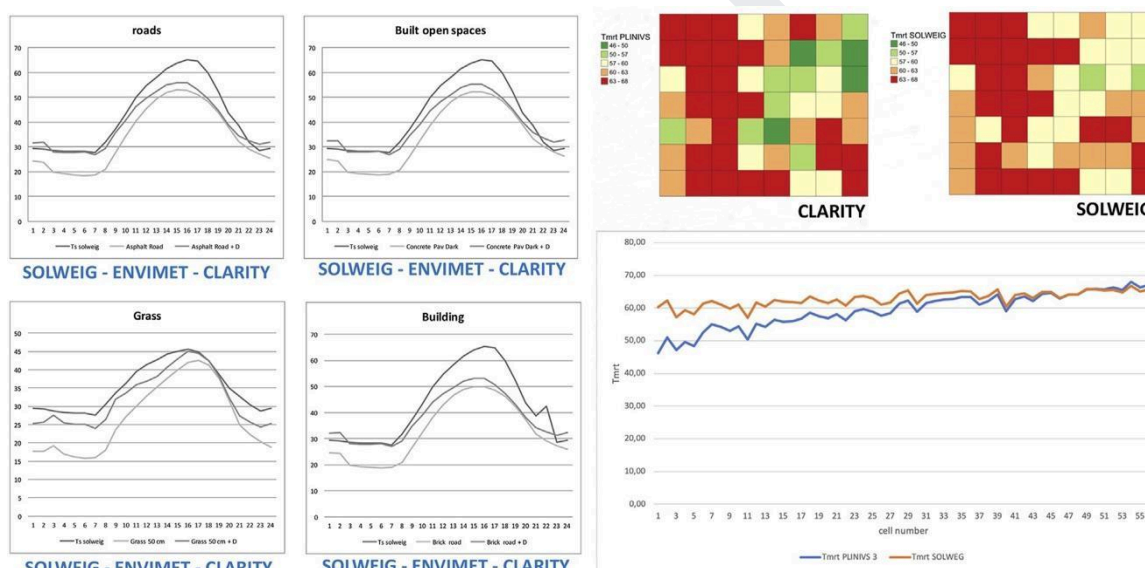


Figure 31. Comparison of surface temperature values between HWLEM and ENVI-MET model results (left) and Tmrt values between HWLEM and SOLWEIG model results (right).

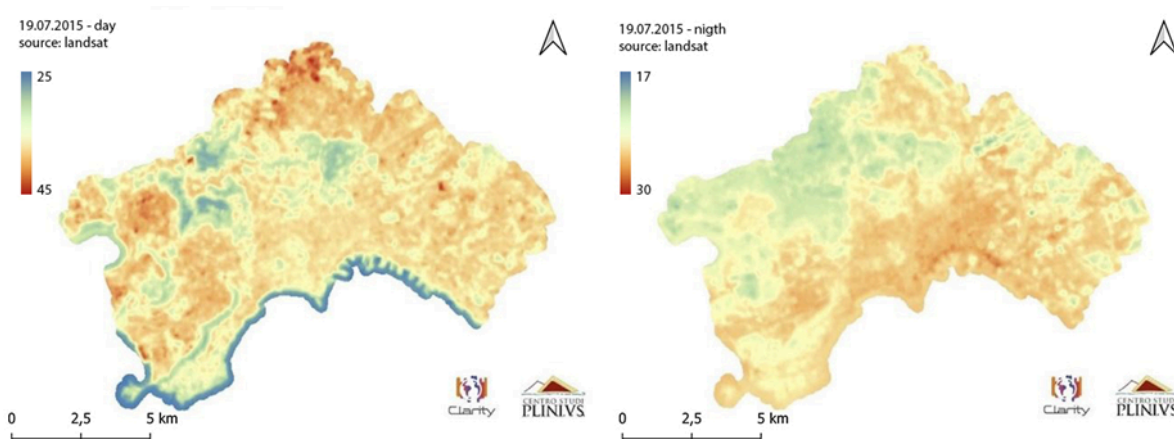


Figure 32. Calibration of surface temperature values within HWLEM: land surface temperature observed on July 19th, 2015 in the Municipality of Naples, corresponding to a 3-day heat wave with maximum temperatures of about 36-37°C (Landsat satellite data).

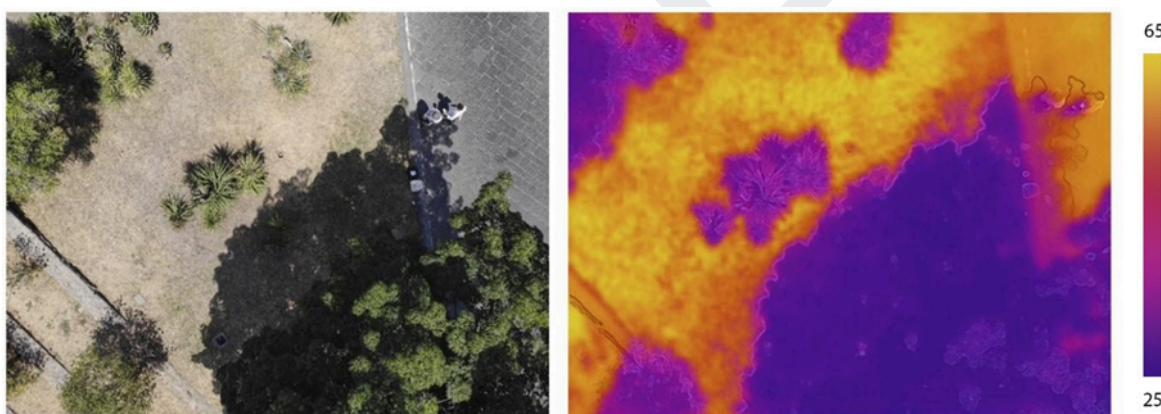


Figure 33. Calibration of surface temperature values within HWLEM: land surface temperature observed on July 30th, 2020 in the Municipality of Naples, corresponding to a 5-day heat wave with maximum temperatures of about 34-35°C (data collected during a drone campaign).

6.4.2 Model results

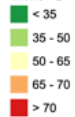
The primary outcomes of the HWLEM approach consist of 2.5D GIS and 3D AAD hazard maps which illustrate the extent of urban heat, represented by the T_{mrt} values, and the potential stress experienced by individuals in specific areas, represented by the UTCI values, at different scales (Figure 34, Figure 35 and Figure 36).

**Heat wave hazard
Mean Radiant Temperature**

Current state scenario

rcp 8.5
period: 2011-2040
hw occurrence: rare
Tair: 38° C

Tmrt °C



□ subdistricts

■ current state scenario land use

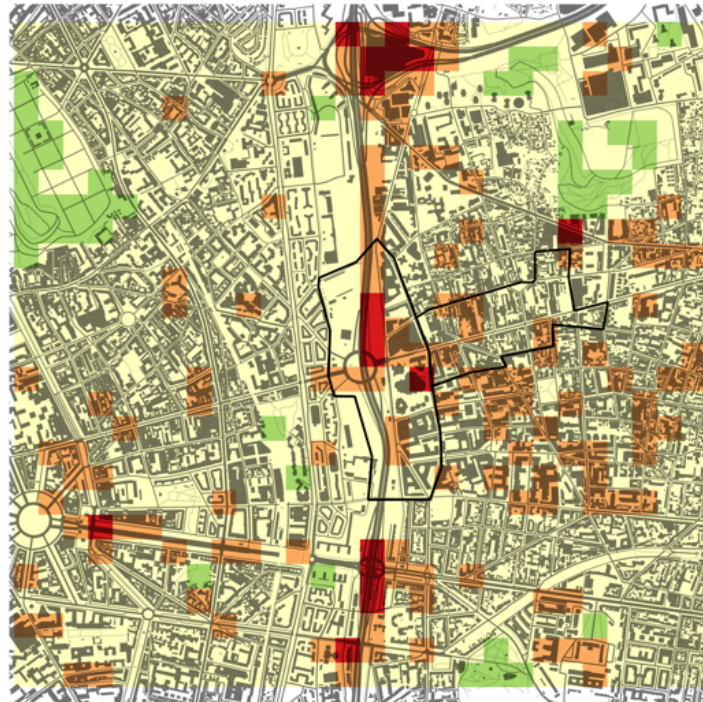
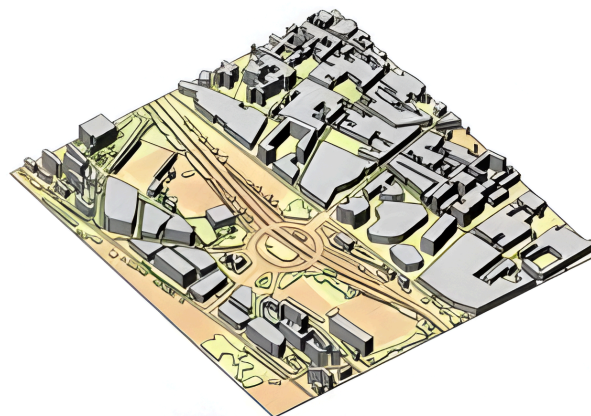


Figure 34. Example of the heat wave hazard simulation in the Paris metropolitan area . The simulation, developed with GIS tools, corresponds to a “rare” event characterized by a 38°C air temperature in the period 2011-2040, and RCP 8.5.

TMRT



Radiant Temperature
Aug 15 1:00 - Aug 15 24:00

Figure 35. Example of the heat wave hazard simulation in the Paris metropolitan area. The simulation, developed with the Rhinoceros/Grasshopper tools, corresponds to a “rare” event characterized by a 38°C air temperature in the period 2011-2040, and RCP 8.5.

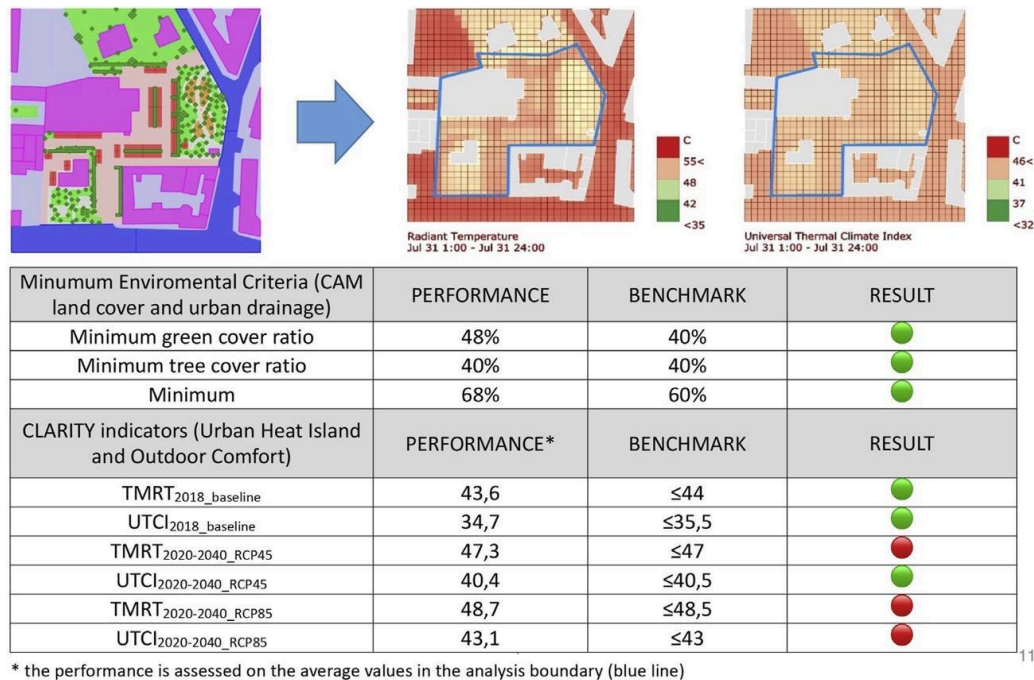


Figure 36. Example of application of the HWLEM model for performance evaluation of adaptation/mitigation measures applied to a neighborhood scale intervention.

A summary of the outputs provided by the model is reported below:

[City/District scale – 2.5D GIS]

- Heat Wave Hazard analysis
 - Land Surface Temperature (LST) [°C]
 - Mean Radiant Temperature (TMRT) [°C]
 - Universal Thermal Climate Index (UTCI) [°C]

[Block/Building scale – 3D AAD]

- Heat Wave Hazard analysis
 - Mean Radiant Temperature (TMRT) [°C]
 - Universal Thermal Climate Index (UTCI) [°C]

These results allows of defining several aspects related to a heat wave event:

- 1) Perform robust hazard and adaptation/mitigation assessments through relevant quantitative indicators, including those aligned with EU Taxonomy/Do Not Significant Harm principles.
- 2) Streamline the use of quantitative indicators to support a multiscale evaluation of planning and design solutions at both the city/district and block/building scales.

- 3) Incorporate urban climate design principles into urban planning and building/open space design.
- 4) Establish connections between the climate benefits (adaptation/adaptation) of proposed plans/projects and the social, economic, and environmental co-benefits of climate-resilient developments.

6.4.3 Data requirements

The table below summarizes the data needs of the heat wave hazard model.

Table 9. Data required (model inputs) for the heat wave hazard model.

Data required or the heat wave hazard model		
Data Group	Description	Source
Historic climate data	Historic datasets of heat climate data	EU/National/Regional meteorological agencies Meteorological databases
Future climate projections	Projections of local climate data downscaled according to climate change scenarios Future IDF curves considering different change scenarios and time horizons	Results Task 1.2
Land use and terrain information	Building information (dimensions, roof material) Trees information (dimensions, species, foliage colour) Digital Elevation Model and land cover data (crops/vegetation type, paving material)	National/Regional/Local geography agencies; Copernicus
Vulnerability information	Distribution (number) and composition (group of age) of the population Mortality rates, cost of health care, and productivity data	EU/national statistics agencies

6.5 Forest fire

6.5.1 Model setup, calibration and validation

The objective of forest fire hazard assessment is to reveal the most prone to wildfire areas of the region of interest under certain circumstances. The modeling approach for this specific hazard in the context of Project ICARIA is based on the combination of two separate models. The first one is the Canadian Forest Fire Weather Index System (FWI). It is used to assess fire danger conditions and fire occurrence across the area of interest. Nevertheless, forest fires result from complex interactions among a multitude of factors including weather, combustion, hydrology, and the biosphere. In this sense, high-resolution coupled atmosphere-wildfire behavior simulations are key for the prediction and risk assessment, and thus aid in wildfire preparedness and response. In order to account for these interactions, the Weather Research and Forecasting model (WRF-Fire) is to be used as a secondary tool. It is a physics module within the WRF model that allows users to model the growth of a wildfire in response to environmental conditions, terrain slope, fuel characteristics, atmospheric conditions and the dynamic feedbacks with the atmosphere. The following sections present both models in more detail.

a) *Canadian Fire Weather Index*

The Canadian Forest Fire Weather Index System consists of six components that account for the effects of fuel moisture and weather conditions on fire behavior. The first three components are fuel moisture codes, which are numeric ratings of the moisture content of the forest floor and other dead organic matter. Their values rise as the moisture content decreases. There is one fuel moisture code for each of three layers of fuel: litter and other fine fuels; loosely compacted organic layers of moderate depth; and deep, compact organic layers. The remaining three components are fire behavior indices, which represent the rate of fire spread, the fuel available for combustion, and the frontal fire intensity; these three values rise as the fire danger increases.

The diagram below, on the left, illustrates the components of the FWI System. The calculation of the components is based on consecutive daily observations of temperature, relative humidity, wind speed, and 24-hour precipitation. The six standard components provide numeric ratings of relative potential for wildfire.

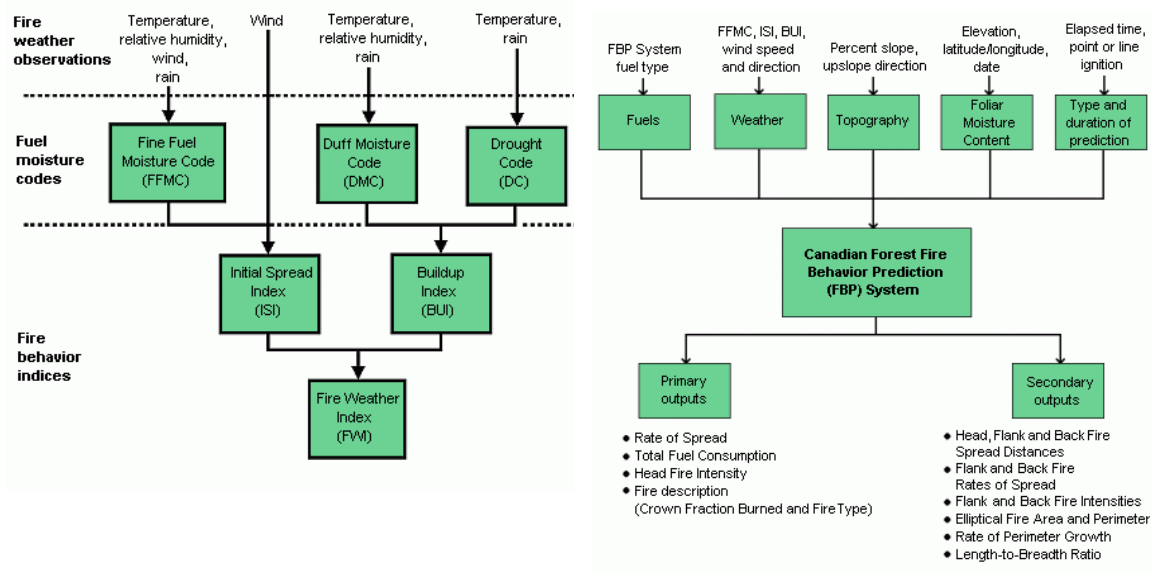


Figure 37. Structure components on the left and flow diagram of the FWI calculation process of the Canadian Forest Fire Behaviour Prediction System on the right.

b) Weather Research and Forecasting

The Forest Fire Behavior Prediction model, included in the WRF-FIRE, provides quantitative estimates of potential head fire spread rate, fuel consumption, and fire intensity, as well as fire descriptions, based on elliptical fire growth models. It provides estimates of fire area, perimeter, perimeter growth rate and the fire behavior at the head and its flanks.

WRF-Fire Software Layers and Dependencies

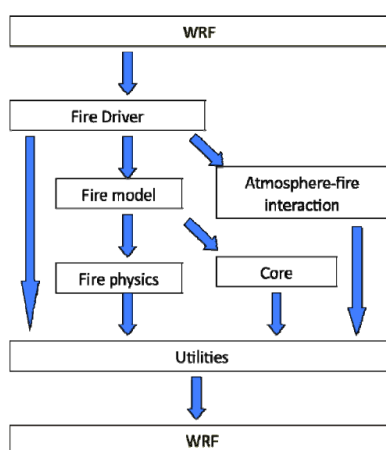


Figure 38. Structure and flow diagram of WRF-Fire.

The required inputs for the WRF-FIRE include the forest fuel type in the categories linked to the type of forest. The fuel types recognized by the system are those specified by the Canadian Forest Fire Behavior Prediction System and can be modified by various parameters, which are set by the user in the Fire Behavior Prediction extension prior to building the grids. These parameters include green up date, crown base height, and percent conifer. C1-C7 refers to Coniferous category, D1 to deciduous, S1-S3 to slash, O1 to open and finally M1-M4 to mixedwood category. These categories are summarized below:

Fuel Type description

- C1 - Spruce–Lichen Woodland
- C2 - Boreal Spruce
- C3 - Mature Jack or Lodgepole Pine
- C4 - Immature Jack or Lodgepole Pine
- C5 - Red and White Pine
- C6 - Conifer Plantation
- C7 - Ponderosa Pine–Douglas-Fir
- D1 - Leafless Aspen
- S1 - Jack or Lodgepole Pine Slash
- S2 - White Spruce–Balsam Slash
- S3 - Coastal Cedar–Hemlock–Douglas-Fir Slash
- O1 - Grass
- M1 - Boreal Mixedwood–Leafless
- M2 - Boreal Mixedwood–Green
- M3 - Dead Balsam Fir Mixedwood–Leafless
- M4 - Dead Balsam Fir Mixedwood–Green

Within WRF-FIRE a “fire” domain should be set up. The user also sets the number of ignitions, their time, location, and shape, and the fuel moisture content in the ignition area.

The description of the six standard components provide numeric ratings of relative potential for wildfire as summarized below:

- Fine Fuel Moisture Code, (FFMC), is a numeric rating of the moisture content of litter and other cured fine fuels.
- Drought Code, (DC), is a numeric rating of the average moisture content of deep, compact organic layers.
- Initial Spread Index, (ISI), is a numeric rating of the expected rate of fire spread.
- Buildup Index, (BUI), is a numeric rating of the total amount of fuel available for combustion.
- Fire Weather Index, (FWI), is a numeric rating of fire intensity. It is based on the ISI and the BUI, and is used as a general index of fire danger.
- Daily Severity Rating, (DSR), is a numeric rating of the difficulty of controlling fires. It is based on the FWI but it more accurately reflects the expected effort required for fire suppression.

6.5.2 Model results

Head Fire Intensity (HFI) is the predicted intensity, or energy output, of the fire at the front or head of the fire. It is measured in kilowatts per meter of fire front and is based on the Rate of Spread and the Total Fuel Consumption. Rate of Spread (ROS) is the predicted speed of the fire at the front or head of the fire (where the fire moves fastest), and takes into account both crowning and spotting. It is measured in meters per minute and is based on the Fuel Type, Initial Spread Index, Buildup Index, and several fuel-specific parameters such as phenological state.

The table below presents the classification of FWI and ISI values into fire danger classes appropriate for the European territory environments, as proposed by the European Forest Fire Information System (EFFIS). However, in this analysis, the approach of Percentile indices was used, which provides suitably varying FWI boundaries of classes based on the specific physical characteristics of the study area as proposed by Varela et al., 2018. For FWI inputs the model calibration and validation should be performed based on the weather parameters needed as inputs (Temperature, Rain, Wind).

Table 10. The classification of values for the FWI and its sub-component the ISI (Politi et al., 2023b).

FWI classes by EFFIS	FWI Percentiles by Varela et al. (2018)	ISI classes BY EFFIS
Very low (<5.2)		Very low <3.2
Low (5.2-11.2)	Low 25 th percentiles	Low 3.2-5
Moderate (11.2-21.3)	Moderate 50 th percentiles	Moderate 5-7.5
High (21.3-38)	High 75 th percentiles	High 7.5-13.4
Very high (38-50)		Very high 13.4-30
Extreme (>=50)	Extreme 90 th percentiles	Extreme >30

Examples of the produced model outputs are depicted in the following figures:

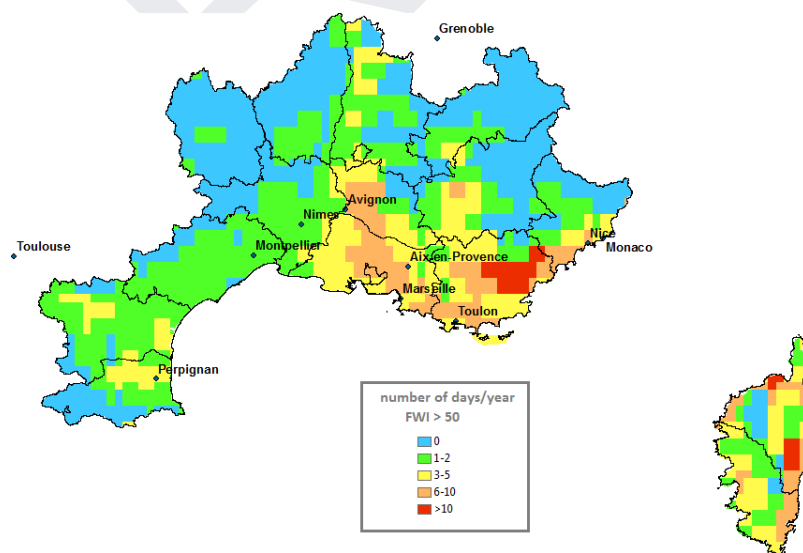


Figure 39. Example with the spatial distribution in the categories of yearly number of days with extreme fire weather (FWI > 50) in period: 2006–2015. (Varela et al., 2019, Sfetsos et al., 2021)

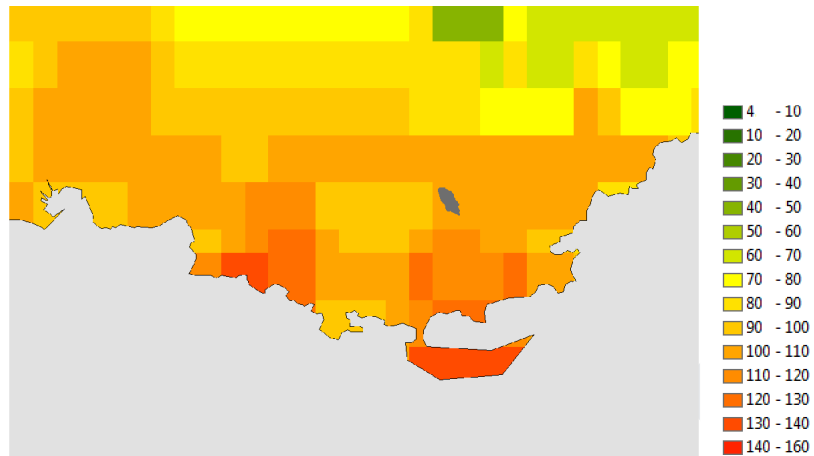


Figure 40. Fire spreading overlaid by extreme 95% value of FWI under RCP8.5 period: 2036–2045 (Sfetsos et al., 2021).

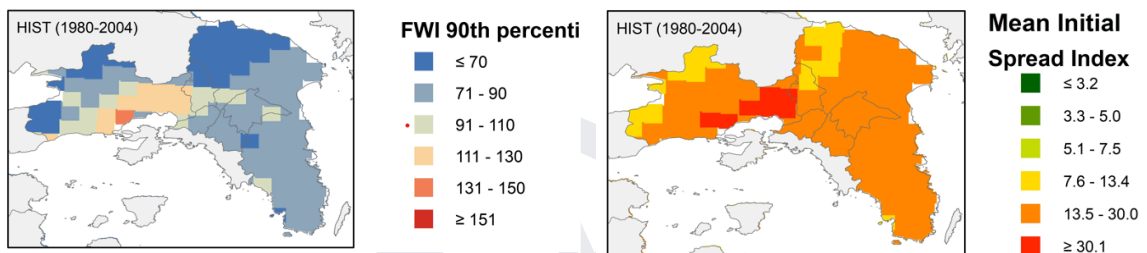


Figure 41. The extreme percentile of FWI (left) and the mean initial spread index (right) for the period 1980-2004 in the Attica region (Politi et al., 2023c).

For each year, FWI is calculated only for the fire season that has a duration from April to October (included) in the Mediterranean. Daily values of the FWI are calculated for each grid point, for consistent present day weather or future climate scenarios and fire season. The calculation of the values of the Canadian FWI can be performed using the package CFFDRS of R statistical computing software.

6.5.3 Data requirements

The data requirements for the forest fire hazard model presented are stated below.

Table 11. Data requirements (model inputs) for the forest fire hazard model.

Data required or the forest fire hazard model		
Data Group	Description	Source
Historic climate data	Historic downscaled datasets of daily observations of temperature, relative humidity, wind speed, and 24-hour precipitation	EU/National/Regional meteorological agencies Meteorological databases
Future climate projections	Future downscaled datasets of daily observations of temperature, relative humidity, wind speed, and 24-hour precipitation	Results Task 1.2
Land use and terrain information	Digital Terrain Model with high resolution	Regional/national geography agencies
	Land cover information and information of the vegetation type	

6.6 Drought

6.6.1 Model setup, calibration and validation

As it has been mentioned in previous sections, drought is a phenomenon that can be analyzed from many different points of view. In the case of ICARIA, the hazard posed by this extreme event to the regional case studies will be assessed from the point of view of hydrological drought (assessing the impact of rainfall deficits on the water resources availability based on parameters such as stream flow, reservoir and lake levels, and ground water table decline (National Weather Services 2023)). From this point of view, (hydrological) drought is understood as below-normal water levels in the main water storages of a region (considering lakes, streams, aquifers and reservoirs). Such abnormalities can be quantified based on generally accepted indicators (e.g. standardized runoff index, the surface water supply index, the groundwater resources index), or alternatively, comparing total volume of stored water in reservoirs with historic mean values (Forero-Ortiz et al., 2020).

In this sense, the hazard assessment methodology proposed is based on the approach presented in Forero-Ortiz et al., 2020, based on the Hydrologiska Byråns Vattenbalansavdelning (HBV) model. It is a well-known and widely used hydrological model that was developed by the Swedish Meteorological and Hydrological Institute in the 1970s (Bergström, 1990 and 1992). This tool is designed to simulate and analyze the components of the hydrological cycle within a watershed or catchment area. The HBV model is widely recognized for its simplicity, flexibility, and ability to

provide valuable insights into runoff generation, streamflow, and other hydrological processes. For project ICARIA, an updated version of the original HBV model, the HBV Light, is suggested to be used.

This version of the software provides a user-friendly interface to use a hydrologic semi-distributed model. It requires to divide the catchment into sub-catchments (or sub-watersheds) and to provide a time series of daily rainfall and air temperature for the whole simulation period. For each sub-catchment, the model simulates the behavior of water and the processes involved in the rainfall-runoff conversion process. HBV Light refers to these processes as “routines”, each one computing the behavior of water in specific parts of the catchment surface and sub-surface.

Another important input of the model is a daily time series of the evapotranspiration potential of each sub-catchment. In literature there are plenty of methodologies to estimate this parameter with different degrees of complexity. In this case, it is suggested to use the Thornthwaite formula (RESCCUE, 2018).

Schematically, the following figure represents the different routines built in the model. As a result, the model returns a time series (with daily resolution) of the water runoff exiting the catchment.

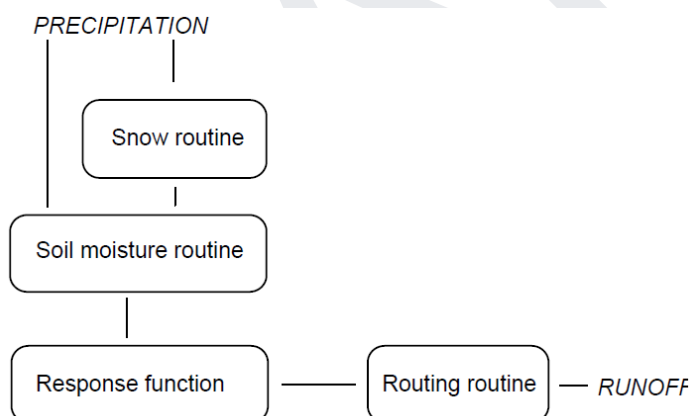


Figure 42. Schematic representation of the routines in HBV Light.

In the context of ICARIA, the aim of the drought model is to estimate the surface water resources availability for a region. In this sense, the focus is put on the water storage in reservoirs that accumulate water to be used in downstream regions. In order to correlate the HBV Light simulation results (runoff time series) with water storage in a reservoir (water volume), the hydrologic catchments simulated correspond with the catchment that discharges its runoff into the reservoir of interest. The picture below depicts the catchment, and its subdivisions, of “La Baells”, one of the main freshwater reservoirs of the AMB. It can be seen that all 9 sub-catchments end up discharging their runoff in it.

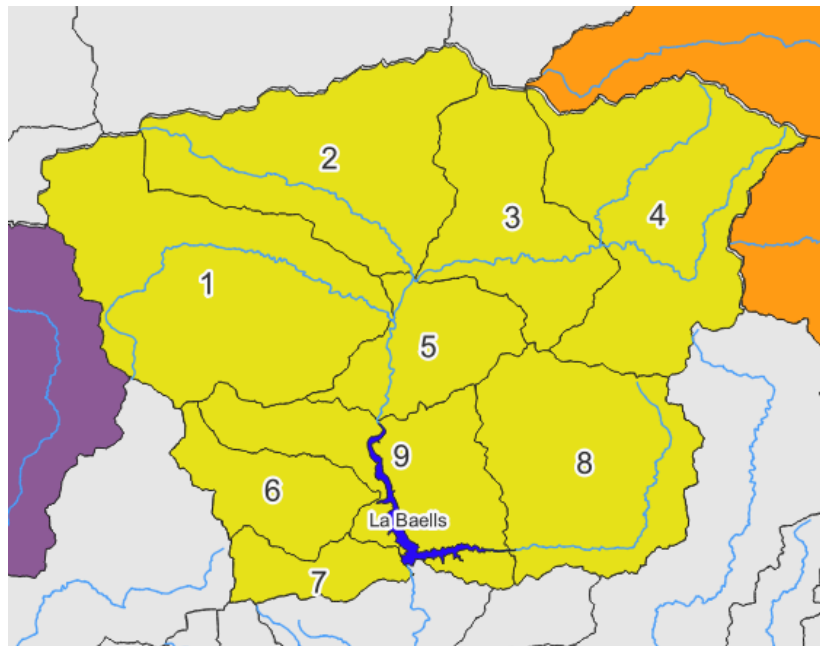


Figure 43. Representation of la Baells catchment and sub-catchment divisions

As mentioned, the output of the HBV Light simulations are surface runoff time series expressed in flow units (m³/d). Hence, in order to translate these results to actual water volume stored in a reservoir, a results post processing is required.

The volume of water stored in a reservoir can be understood as the following equation if direct evaporation from its surface is neglected.

$$V(t) = V(t - 1) + [Q_{in}(t) - Q_{out}(t)] * 1 \text{ day}$$

Where V (m³) corresponds to the stored volume at a given time, Q_{in} (m³/d) is the daily water discharge of the catchment into the reservoir and Q_{out} (m³/d) is the water loss of the reservoir due to exploitation. Q_{in} data is provided by the results of the HBV Light simulations. Q_{out} corresponds to the historic data of daily water discharge of the reservoir (usually registered by the reservoir operator). Such an approach is valid for historic periods where datasets of precipitation, temperature (in the meteorological stations in the catchment) and reservoir discharge data are available.

To forecast water availability for future scenarios, extended datasets of these three key parameters (T , P and Q_{out}) are needed. For the case of T and P , datasets can be provided by projections of future precipitation and temperature trends based on climate downscaling methodologies. In ICARIA, such data will be obtained from the results of Task 1.2.

For the case of reservoir exploitation (Q_{out}) forecasting data is not so straightforward. Project RESCCUE proposed an approach that gave satisfactory results. However, several assumptions need to be made. Firstly, the historic time series of reservoir water discharge is needed. Next, this

time series has to be analyzed to determine the average daily discharge volume of the reservoir for each month of the year from the beginning of the time series to the present. This analysis makes it possible to estimate an average value of daily discharge rate of the reservoir and extrapolate it to the future, generating the required time series of Q_{out} to support the forecast of water resources availability. The figure below shows a graphic conceptualization of this approach to assess water volume storage based on the HBV model results.

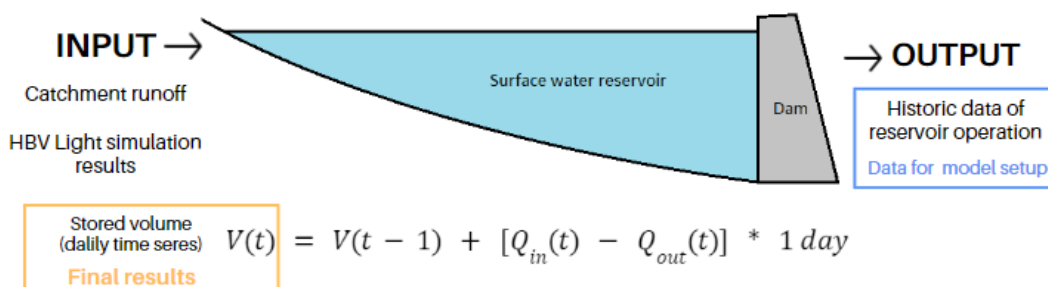


Figure 44. Graphic conceptualization of the approach to assess water volume storage in reservoirs based on the HBV model results.

6.6.2 Model results

The final result of this methodology is a time series of expected water storage in reservoirs that provide water to a specific region for different climate change scenarios up to different time horizons. This information can be used to estimate the frequency, duration and importance of hydrologic drought periods.

The figure below shows a graphical representation of the estimate of water availability in a reservoir in Spain up to year 2100 considering a climate scenario corresponding to RCP 4.5.

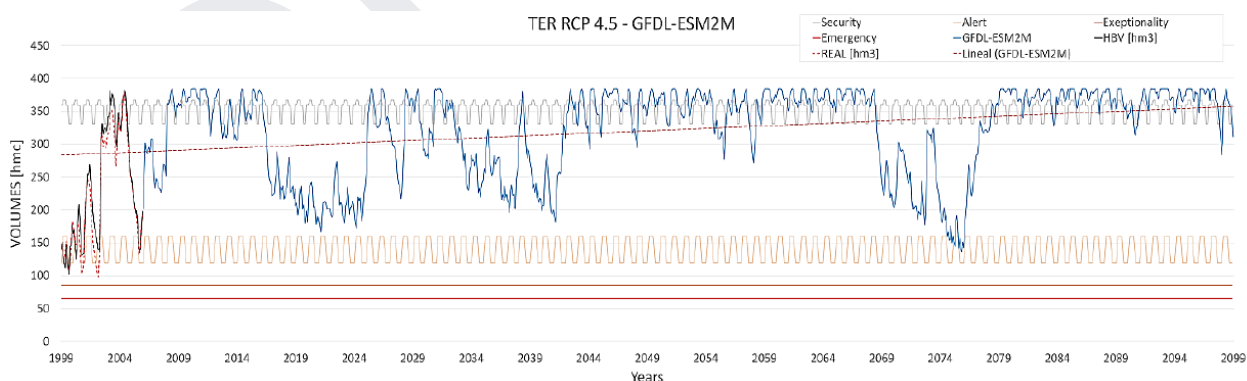


Figure 45. Graphical representation of the estimate of water availability in a reservoir up to year 2100 considering a climate scenario corresponding to RCP 4.5 (results corresponding to project RESCCUE (RESCCUE, 2019)).

6.6.3 Data requirements

The table below summarizes the data requirements of the drought hazard model presented.

Table 12. Data requirements (model inputs) for the drought hazard model.

Data requirements for the drought hazard model		
Data group	Description	Source
Historic climate data	Historic daily datasets of P and T of all (or as much as possible) meteorological stations located in the hydrological catchments of interest. For model setup and calibration, these datasets should extend from 1980 to 2022 approximately.	EU/National/Regional meteorological agencies Meteorological databases
	Daily dataset of evapotranspiration potential for each sub-catchment	Results of the Thornthwaite equation
Future climate projections	Future projections of precipitation and temperature in the catchments of the reservoir of interest.	Results Task 1.2
Terrain information	Digital terrain model (DTM) information to determine the extension of the whole catchment and determine its sub-catchments	Regional/national geography agencies
Other information	Location of the meteorological stations within the catchment of interest	Regional/national geography agencies
	Historic dataset of daily water discharge of the reservoir of interest	National/regional water management agencies

6.7 Extreme winds

In the context of assessing the climate resilience of critical assets, it is of paramount importance to assess the wind hazard at the highest possible temporal and spatial resolution, also considering the impact of climate change and future climate scenarios. Within ICARIA high resolution regional climate simulations are performed with WRF and COSMO-CLM regional climate models. Driven by 2 CMIP6-model input data, 2 to 5 km² simulations are performed until 2100 to determine wind gusts and wind speed at 10 m to assess extreme wind. Single extreme events will be simulated at a spatial resolution of 1 km² to better represent local characteristics, such as topography that highly influences wind speed.

There is clear added value of the higher resolution simulations focused on the assessment of extreme winds. According to Outten et al 2021, the high horizontal resolution of the RCMs allows for realistic fine scale structure to be seen in the extreme winds across Europe and over the surrounding oceans and seas. The same study, also, highlights the effects of individual mountain

valleys, drag from cities, and even storm tracks over the seas that are all visible, and all have a strong influence on the extreme winds on a local scale.

For the risk assessment of extreme winds, the excess above certain thresholds is proposed. For instance, the estimation of the number of days above 8 Beaufort (> 17 m/s) in the historical and future period, as well as the maximum wind gusts.

6.7.1 Model explanation

The models proposed are regional climate models. On the one hand the Weather Research and Forecast (WRF) Model and on the other hand the COSMO climate model (CCLM). Both models are numerical models that represent the climate processes and thereby are able to compute future climate conditions. Their main characteristics are explained in more detail below:

a) Weather Research and Forecast

WRF is a state-of-the-art mesoscale numerical weather prediction system designed for both atmospheric research and operational forecasting applications. It features two dynamical cores, a data assimilation system, and a software architecture supporting parallel computation and system extensibility. The model serves a wide range of meteorological applications across scales from tens of meters to thousands of kilometers. The effort to develop WRF began in the latter 1990s and was a collaborative partnership of the National Center for Atmospheric Research (NCAR), the National Oceanic and Atmospheric Administration, the U.S. Air Force, the Naval Research Laboratory, the University of Oklahoma, and the Federal Aviation Administration. The WRF model can be set up to work with different types of data either reanalysis e.g. ERA5 or ERA-INTERIM reanalysis or climate predictions from GCM.

Within ICARIA, the model should be initialized with ERA5 data for validation purposes and CMIP6 model simulation of MPI-ESM1-2-HR until 2100.

The WRF model configuration applied in this study includes a one-way nested domain, with a spatial resolution of 15 km × 15 km in the outermost domain (D01, 330× 330 grid cells), centered in the Mediterranean basin, and 5 km × 5 km D09 and D11. All domains have 54 vertical layers. The model domains share the same options of physics for radiation, microphysics, boundary layer scheme, and convection. More specifically, the MYNN. Regarding cloud microphysics, the Thompson microphysics and Grell-Freitas cumulus parameterization options can be used. Figure 46 depicts the main data inputs and workflow of the WRF model.

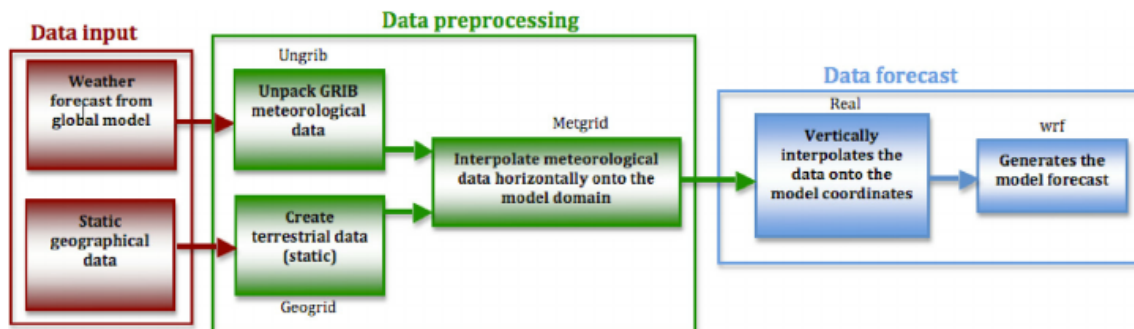


Figure 46. Workflow of the data processing to the WRF model.

The bullet points below describe the data pre-processes shown in Figure 46.

1. Geogrid – It defines the simulation domains and interpolates various terrestrial data sets to the model domains.
2. Ungrib – It reads GRIB (Gridded Binary) files, ‘degrib’ the data, and writes the data in a simple format.
3. Metgrid – It takes the output data from Ungrib and horizontally interpolates it to the simulation domains defined by geogrid. The vertical interpolation is performed by the WRF real program.

In what concerns the rest of the physics schemes, the radiation scheme has to be set to the CAM scheme; for both longwave and shortwave radiation. The updated Noah-MP LSM has to be employed as the land surface model (LSM), as it is widely adopted for climate studies. Finally, the IGBP Modified MODIS 20-category Land Use Categories has to be selected as the land use dataset.

b) COSMO-Model

The COSMO-Model is a nonhydrostatic limited-area atmospheric prediction model. It has been designed for both operational numerical weather prediction and various scientific applications on the meso- β and meso- γ scale. The COSMO-Model is based on the primitive thermo-hydrodynamical equations describing compressible flow in a moist atmosphere. The model equations are formulated in rotated geographical coordinates and a generalized terrain following height coordinate. A variety of physical processes are taken into account by parameterization schemes.

Within ICARIA, it is initialized using a different global climate model to better represent possible future states. The model used for the initial state and boundary conditions is the EC-Earth-Veg and the simulated domains are represented within Figure 47. The outer domain covers central and southern Europe to incorporate the case studies of Salzburg and South Aegean.



Figure 47. The case study areas are simulated at a 2kmx2km resolution until 2100.

6.7.2 Model calibration and validation

The validation of the WRF physics configuration and general model set-up has to be carried out by performing evaluation of simulated temperature, wind speed and precipitation fields against observational data. Climatological data has to be used for exhaustive quantitative validation as extensively described in Sfetsos et al., 2000, Politi et al., 2018, 2020 and 2021, Katopodis et al., 2019 and 2021 and Emmanouil et al., 2021. In this sense, the wind speed values at 10 m of the high resolution WRF climate simulation over can be compared with the available observational data using the following statistical measures: (i) the normalized standard deviation (ii) the mean Bias (iii) the mean absolute error and (v) the root mean square error.



Figure 48. Topography of the greek region along with the height of the stations used for calibrating the model in the SAR case study.

As an example of the results of the model presented, the figures below show the outputs of simulations representing a return period analysis of extremes over a 50-year period to determine the likelihood of exceeding the probability of design thresholds. Also they show the estimated likelihood of exceeding the wind threshold of 40 m/s, to define how the return of 50 years changes under the future scenarios.

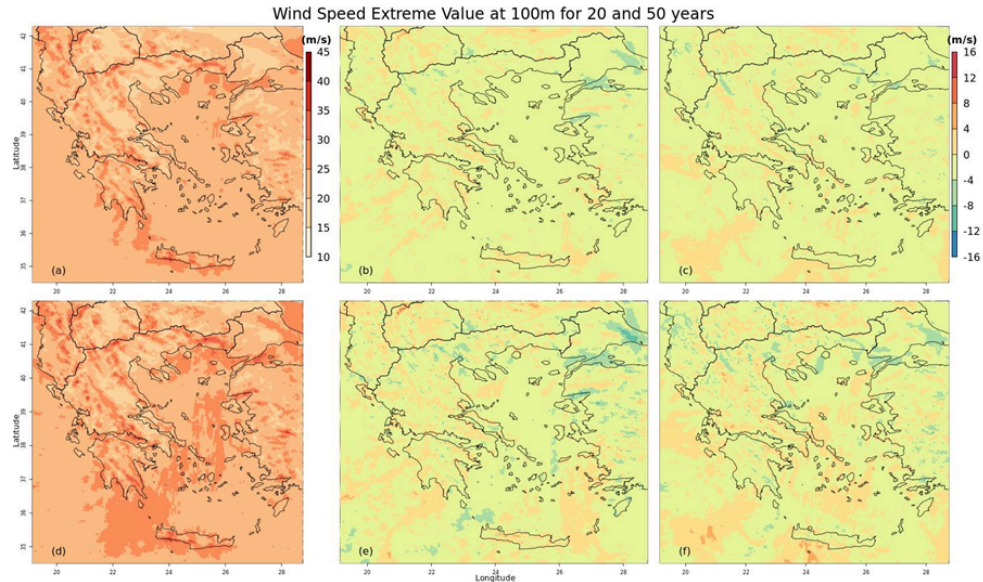


Figure 49. Extreme wind speeds values for 50-y return period for (a) historic data and (b) RCP 4.5 and (c) RCP 8.5.

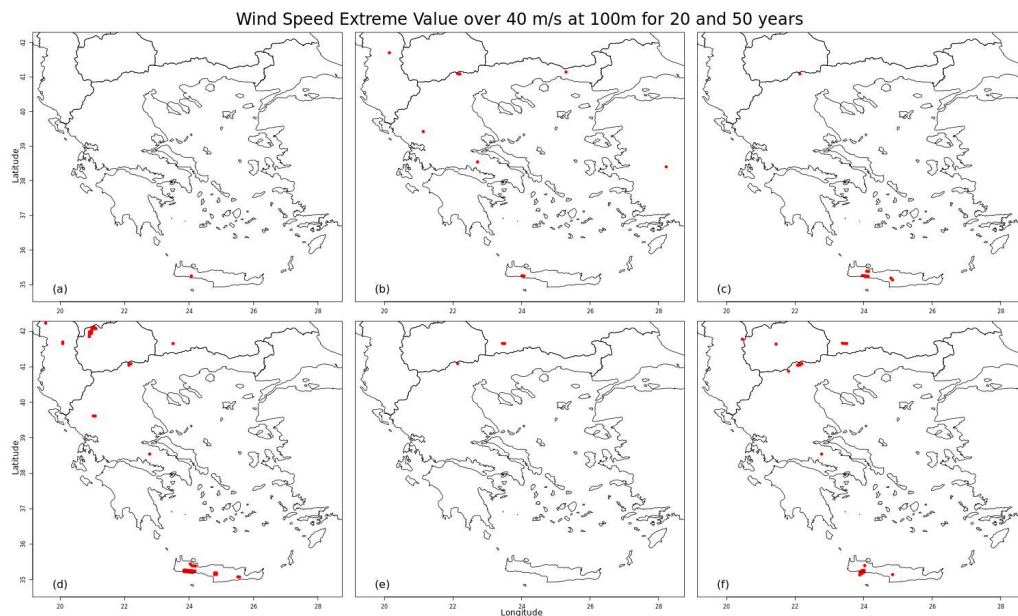


Figure 50. Mean wind extreme value over 40 m/s at 100 m for (a) historical and (b) RCP 4.5 and (c) RCP 8.5 for 50 years return period analysis.

Depending on the selected parameterization and schemes more than 100 variable fields (2D and 3D) are generated (in "netcdf" format) following the domain size setup by the users. Model outputs and corresponding metadata can be easily accessed via programming languages such as Python, R, etc., or graphic user interfaces. The selected output variable, more relevant to the wind case, are the following ones:

WRF Model output variables:

- Time (minutes / hours)
- XLAT (Latitude, south is negative)
- XLONG(Longitude, west is negative)
- U("x-wind component" / "m s⁻¹")
- V("y-wind component" / "m s⁻¹")
- W("z-wind component" / "m s⁻¹")
- P("perturbation pressure" / "Pa")
- PB("Base state Pressure" / "Pa")
- PSFC("Surface pressure" / "Pa")
- U10("U at 10 M" / "m s⁻¹")
- V10("V at 10 M" / "m s⁻¹")
- UST("U* IN SIMILARITY THEORY" / "m s⁻¹")

6.7.3 Data requirements

The table below summarizes the data needs of the extreme wind hazard model

Table 13. Data required (model inputs) for the extreme wind hazard model

Data requirements for the extreme wind hazard model		
Data group	Description	Source
Static input data	For the WRF: Land use, albedo, leaf area index, topography	EU/National/Regional meteorological agencies Meteorological databases
	For the COSMO-CLM: Land use, albedo, leaf area index, topography	Results of the Thornthwaite equation

7 Conclusions

Scientific research in multiple fields and disciplines has proven that the current context of climate change is contributing to the occurrence of more frequent and severe extreme weather events. Among those, concern is rising in relation to multi-hazard events. This concept refers to scenarios where two or more hazards occur in the same region and/or time period where the resulting impact can be greater than the sum of the individual impacts. Hence, the integration of the multi-hazard events risk assessment perspective is essential to improve the resilience of services and critical infrastructures against extreme weather events.

ICARIA aims at developing a comprehensive asset level modeling framework to achieve a better understanding about climate related impacts produced by multi-hazard events on critical assets to identify suitable, sustainable and cost-effective adaptation solutions.

As a first step in this endeavor Deliverable 2.1 has a triple objective: (1) identify the main climatic hazards that currently affect the three case study regions and assess how will this situation evolve in the future climate change context, (2) analyze multi-hazard events to identify the mechanisms of interaction between the individual hazards of interest and (3) identify historic extreme events (both single and multi-hazard) that have affected the case studies.

Based on a bibliographic review and a workshop involving relevant stakeholders of each case study region, the main climatic hazards of interest for the project ICARIA have been identified: Floods (Pluvial and Fluvial), Storm Surge, Drought, Heatwave, Forest Fire and Extreme winds.

Regarding the assessment and identification of physical interactions between single hazards during multi-hazard events, the following cases have been analyzed:

- Coincident storm surges and extreme rain events can lead to increased flash floods in coastal urban areas due to a reduction of the drainage systems capacity caused by the intrusion of seawater as a result of the mean sea level rise.
- Drought conditions can enhance the possibility of occurrence of forest fire due to the reduction of water content in the vegetation, increasing its likelihood of ignition as well as the fuel availability.
- Combined precipitation deficits and warm periods (heat wave) cause reduced surface runoff that lead to hydrological drought conditions. However, the land–atmosphere feedbacks between heat waves and periods with reduced rainfall are not yet fully understood and remain as an open debate.
- Heatwaves have a triggering effect on forest fires as prolonged high temperatures, associated with simultaneous dry conditions, contribute to reducing soil and vegetation humidity leading to a more likely ignition.
- Extreme winds have the capacity to increase the impact of forest fires due to the fact

that they can contribute to a faster spread and an increased intensity of the fire.

- Heatwave, drought and forest fire stand as a worst case scenario where the combined effect of drought and heat generate forest fire prone conditions.

As for the historic extreme events, for each case study a non-exhaustive list has been developed to illustrate the potential impacts of such events. It should be noted that, given the relative recent interest of the risk reduction community on multi-hazard events it has been hard to identify historic events of that kind as very often they are not identified as such.

The last chapter of this report provides a review of hazard assessment methodologies for single hazard events based on the work developed in previous EU research projects. For each case, a description of the model setup, calibration and validation is provided together with a detailed list of data requirements and the main output of the models.

In the context of ICARIA, Deliverable 2.1 stands as the reference methodological document to support later steps of the project related to multi-hazard risk assessment, such as the evaluation of joint probabilities of occurrence of combined and compound events (Task 2.2) and the development of innovative coupled multi-hazards modeling tools (Task 2.3).

DRAFT

References

Ajuntament de Barcelona. (2018). *Pla Clima*. Available at: https://www.barcelona.cat/barcelona-pel-clima/sites/default/files/documents/pla_clima_cat_maij_ok.pdf

Ajuntament de Barcelona. (2019). *Pla Director Integral de Sanejament de la ciutat de Barcelona (PDISBA)*. Available at: <https://bcnroc.ajuntament.barcelona.cat/jspui/handle/11703/119275>

Ali, E., Cramer, W., Carnicer, J., Georgopoulou, E., Hilmi, N. J. M., Le Cozannet, G., & Lionello, P. (2022). Cross-Chapter Paper 4: Mediterranean Region. In: *Climate Change 2022: Impacts, Adaptation and Vulnerability. Contribution of Working Group II to the Sixth Assessment Report of the Intergovernmental Panel on Climate Change*: (H.-O. Pörtner, DC Roberts, M. Tignor, ES Poloczanska, K. Mintenbeck, A. Alegría, M. Craig, S. Langsdorf, S. Lösschke, V. Möller, A. Okem, B. Rama (eds.)). IPCC, Cambridge, *United Kingdom and New York, NY, USA*.

AMB. (2016). *Pla Clima i Energia 2030*. Available at: <https://www.amb.cat/es/web/medi-ambient/actualitat/publicacions/detall/-/publicacio/plan-clima-y-energia-2030/7155151/11818>

AMB. (2023). *L'àrea metropolitana Àrea Metropolitana de Barcelona*. Available at: www.amb.cat/s/home.html.

Andrews, P.L., Loftsgaarden, D.O., Bradshaw, L.S. (2003). Evaluation of fire danger rating indexes using logistic regression and percentile analysis. *International Journal of Wildland Fire*, 12, 213–226.

Androulidakis, Y. S., Kombiadou, K. D., Makris, C. V., Baltikas, V. N., Krestenitis, Y. N. (2015). Storm surges in the Mediterranean Sea: Variability and trends under future climatic conditions. *Dynamics of Atmospheres and Oceans*, 71, 56-82.

Aubrecht, C., Almeida, M., Polese, M., Reva, V., Steinnocher, K., & Zuccaro, G. (2013). Temporal aspects in the development of a cascading-event crisis scenario: a pilot demonstration of the CRISMA project. In: EGU (2013). *Geophysical Research Abstracts* vol. 15, EGU General Assembly 2013, Vienna, Austria, 7-12 April 2013.

Bergström, S. (1990). Parametervärden för HBV-modellen i Sverige, Erfarenheter från modelkalibreringar under perioden 1975-1989 (Parameter values for the HBV model in Sweden, in Swedish), *SMHI Hydrologi*, No.28, Norrköping, 35 pp.

Bergström, S. (1992). The HBV model - its structure and applications. *SMHI RH* No 4. Norrköping. 35 pp.

Bevacqua, E., Maraun, D., Vousdoukas, M. I., Voukouvalas, E., Vrac, M., Mentaschi, L., & Widmann, M. (2019). Higher probability of compound flooding from precipitation and storm surge in Europe under anthropogenic climate change. *Science Advances*, 5(9).

Blanchi, R., Leonard, J., Haynes, K., Opie, K., James, M., & de Oliveira, F. D. (2014). Environmental circumstances surrounding bushfire fatalities in Australia 1901–2011. *Environmental Science & Policy*, 37, 192-203.

Bradstock, R. A., Hammill, K. A., Collins, L., & Price, O. (2010). Effects of weather, fuel and terrain on fire severity in topographically diverse landscapes of south-eastern Australia. *Landscape Ecology*, 25, 607-619.

Bulti, D. T., & Abebe, B. G. (2020). A review of flood modeling methods for urban pluvial flood application. *Modeling earth systems and environment*, 6, 1293-1302.

Bundesministerium. (2021). *Zweiter Fortschrittsbericht zur österreichischen Strategie*. Available at: https://www.bmk.gv.at/themen/klima_umwelt/klimaschutz/anpassungsstrategie/publikationen/oe_strategie.html.

CDP. (2021). *2021 Haiti Earthquake and Tropical Storm Grace*. Available at: <https://disasterphilanthropy.org/disasters/2021-haiti-earthquake-and-tropical-storm-grace/>

Chen, L., Yu, B., Yang, F., and Mayer, H. (2016). Intra-urban Differences of Mean Radiant Temperature in Different Urban Settings in Shanghai and Implications for Heat Stress under Heat Waves: a GIS-Based Approach. *Energy and Buildings* 130, 829–842.

Cid, A., Menéndez, M., Castanedo, S., Abascal, A. J., Méndez, F. J., & Medina, R. (2016). Long-term changes in the frequency, intensity and duration of extreme storm surge events in southern Europe. *Climate Dynamics*, 46, 1503-1516.

CLARITY. (2017). *Project CLARIT: Integrated Climate Adaptation Service Tools for Improving Resilience Measure Efficiency*. Available at: <https://clarity-h2020.eu/>

Copernicus (2023). *2023: A year of intense global wildfire activity*. Available at: <https://atmosphere.copernicus.eu/2023-year-intense-global-wildfire-activity>

Cramer, W., Guiot, J., Fader, M., Garrabou, J., Gattuso, J. P., Iglesias, A., ... & Xoplaki, E. (2018). Climate change and interconnected risks to sustainable development in the Mediterranean. *Nature Climate Change*, 8(11), 972-980.

CRISMA. (2012). *Project CRISMA: Modeling crisis management for improved action and preparedness*. Available at: <https://cordis.europa.eu/project/id/284552>

Cruz, M. G., Sullivan, A. L., Gould, J. S., Sims, N. C., Bannister, A. J., Hollis, J. J., & Hurley, R. J. (2012). Anatomy of a catastrophic wildfire: the Black Saturday Kilmore East fire in Victoria, Australia. *Forest Ecology and Management*, 284, 269-285.

Cruz, M. G., & Alexander, M. E. (2019). The 10% wind speed rule of thumb for estimating a wildfire's forward rate of spread in forests and shrublands. *Annals of Forest Science*, 76(2), 1-11.

- Cruz, M. G., Alexander, M. E., Fernandes, P. M., Kilinc, M., & Sil, Â. (2020). Evaluating the 10% wind speed rule of thumb for estimating a wildfire's forward rate of spread against an extensive independent set of observations. *Environmental Modelling & Software*, 133, 104818.
- De Pippo, T., Donadio, C., Pennetta, M., Petrosino, C., Terlizzi, F., & Valente, A. (2008). Coastal hazard assessment and mapping in Northern Campania, Italy. *Geomorphology*, 97(3-4), 451-466.
- De Ruiter, M. C., Couasnon, A., Van den Homberg, M. J. C., Daniell, J. E., Gill, J. C., & Ward, P. J. (2020). Why we can no longer ignore consecutive disasters, *Earth's Future*, 8, e2019EF001425.
- Domingo, N. D. S., Paludan, B., Madsen, H., Hanses, F., & Mark, O. (2010). Climate Change and Storm Surges: Assessing Impacts on Your Coastal City Through Mike Flood Modeling. *DHI Group*.
- Dong, L., Mitra, C., Greer, S., & Burt, E. (2018). The dynamical linkage of atmospheric blocking to drought, heatwave and urban heat island in southeastern US: A multi-scale case study. *Atmosphere*, 9(1), 33
- Ebel, B. A. (2012). Wildfire impacts on soil–water retention in the Colorado Front Range, United States. *Water Resources Research*, 48(12).
- Edwards, D.C. and T.B. McKee. (1997). Characteristics of 20th Century Drought in the United States at Multiple Time Scales. Climatology Report Number 97-2. *Colorado State University*, Fort Collins.
- Eilander, D., Couasnon, A., Leijnse, T., Ikeuchi, H., Yamazaki, D., Muis, S., Dullaart, J., Haag, A., Winsemius, H. C., and Ward, P. J. (2023). A globally applicable framework for compound flood hazard modeling, *Nat. Hazards Earth Syst. Sci.*, 23, 823–846.
- Emmanouil, G., Vlachogiannis, D., & Sfetsos, A. (2021). Exploring the ability of the WRF-ARW atmospheric model to simulate different meteorological conditions in Greece. *Atmospheric Research*, 247, 105226.
- EC. (2013). Non-paper Guidelines for Project Managers: Making Vulnerable Investments Climate Resilient. Brussels. European Commission. Available at: <https://climate-adapt.eea.europa.eu>
- EXPLORIS. (2002). Project EXPLORIS: *Explosive eruption risk and decision support for eu populations threatened by volcanoes*. Available at: <https://cordis.europa.eu/project/id/EVR1-CT-2002-40026/it>
- Forero-Ortiz, E., Martínez-Gomariz, E., & Monjo, R. (2020). Climate Change Implications for Water Availability: A Case Study of Barcelona City. *Sustainability*, 12(5), 1779.
- Garcia-Aristizabal, A., Almeida, M., Aubrecht, C., Polese, M., Mário, L., Viegas, & D., Zuccaro, G. (2014). Assessment and Management of Cascading Effects Triggering Forest Fires. In: *Advances in Forest Fire Research*, 1073-1085.
- Gill, J. C., Hussain, E., & Malamud, B. D. (2021). Workshop Report: Multi-Hazard Risk Scenarios for Tomorrow's Cities.

Gulyás, Á., Unger, J., and Matzarakis, A. (2006). Assessment of the Microclimatic and Human Comfort Conditions in a Complex Urban Environment: Modelling and Measurements. *Building Environ.* 41 (12), 1713–1722.

Hallegatte, S., Ranger, N., Mestre, O., Dumas, P., Corfee-Morlot, J., Herweijer, C., & Wood, R. M. (2011). Assessing climate change impacts, sea level rise and storm surge risk in port cities: a case study on Copenhagen. *Climatic change*, 104, 113-137.

Harris, R., Furlan, E., Pham, H. V., Torresan, S., Mysiak, J., & Critto, A. (2022). A Bayesian network approach for multi-sectoral flood damage assessment and multi-scenario analysis. *Climate Risk Management*, 35, 100410.

Hao, Z., Hao, F., Xia, Y., Feng, S., Sun, C., Zhang, X., ... & Meng, Y. (2022). Compound droughts and hot extremes: Characteristics, drivers, changes, and impacts. *Earth-Science Reviews*, 235, 104241.

Henonin, J., Russo, B., Mark, O., & Gourbesville, P. (2013). Real-time urban flood forecasting and modelling—a state of the art. *Journal of Hydroinformatics*, 15(3), 717-736.

Hoerling, M., Eischeid, J., Perlwitz, J., Quan, X., Zhang, T., & Pegion, P. (2012). On the increased frequency of Mediterranean drought. *Journal of climate*, 25(6), 2146-2161.

ICARIA. (2023a). Deliverable 1.1 - ICARIA Holistic Modeling Framework. Project ICARIA, grant agreement number 101093806

ICARIA. (2023b). Deliverable 5.4 - Stakeholder Engagement Plan. Project ICARIA, grant agreement number 101093806

IPCC. (2014). in *Climate Change 2014: Synthesis Report*. Contribution of Working Groups I, II and III to the Fifth Assessment Report of the Intergovernmental Panel on Climate Change, Core Writing Team. Editor R. K. L. A. Pachauri Meyer. Cambridge University Press, Cambridge, United Kingdom and New York, NY, USA,

IPCC. (2022). *Climate Change 2022: Impacts, Adaptation and Vulnerability*. Contribution of Working Group II to the Sixth Assessment Report of the Intergovernmental Panel on Climate Change [Core Writing Team: Pörtner, H.O., Roberts, D.C., Tignor, M., Poloczanska, E.S., Mintenbeck, K., Alegría, A., Craig, M., Langsdorf, S., Lösschke, S., Möller, V., Okem, A., Rama, B. (eds.)]. Cambridge University Press, Cambridge, United Kingdom and New York, NY, USA, 3056 pp.

IPCC. (2023). *Climate Change 2023: Synthesis Report*. Contribution of Working Groups I, II and III to the Sixth Assessment Report of the Intergovernmental Panel on Climate Change [Core Writing Team: Lee, H., & J. Romero (eds.)]. IPCC, Geneva, Swiss, 184 pp.

Jacob, D., Petersen, J., Eggert, B., Alias, A., Christensen, O. B., Bouwer, L. M., ... & Yiou, P. (2014). EURO-CORDEX: new high-resolution climate change projections for European impact research. *Regional environmental change*, 14, 563-578.

Kappes, M. S., Keiler, M., von Elverfeldt, K., & Glade, T. (2012). Challenges of analyzing multi-hazard risk: a review. *Natural hazards*, 64, 1925-1958.

Katopodis, T., Vlachogiannis, D., Politi, N., Gounaris, N., Karozis, S., & Sfetsos, A. (2019). Assessment of climate change impacts on wind resource characteristics and wind energy potential in Greece. *Journal of Renewable and Sustainable Energy*, 11(6).

Katopodis, T., Markantonis, I., Vlachogiannis, D., Politi, N., & Sfetsos, A. (2021). Assessing climate change impacts on wind characteristics in Greece through high resolution regional climate modelling. *Renewable Energy*, 179, 427-444.

Land Salzburg. (2017). *Strategie zur Anpassung an den Klimawandel in Salzburg im Rahmen der Klimaund Energiestrategie SALZBURG 2050*. Available at: https://www.salzburg.gv.at/umweltnaturwasser_/Documents/Strategie%20zur%20Anpassung%20an%20den%20Klimawandel%20in%20Salzburg_WEB-V24-05-18.pdf

Land Salzburg. (2022). *Strategie zur Anpassung an den Klimawandel in Salzburg*. Available at: https://www.salzburg.gv.at/umweltnaturwasser_/Documents/Fortschrittsbericht_Klimawandelanpassungsstrategie_2022_Ver%C3%B6ffentlichung.pdf

Laster Grip, I., Haghigatafshar, S., & Aspegren, H. (2021). A methodology for the assessment of compound sea level and rainfall impact on urban drainage networks in a coastal city under climate change. *City and Environment Interactions*, 12.

Lead, C. (2020). Climate and environmental change in the mediterranean basin—current situation and risks for the future. Union for the Mediterranean, Plan Bleu; UNEP/MAP: Marseille, France.

Leone, M. F., & Raven, J. (2018). Metodi progettuali multiscalarari e mitigazione adattiva per la resilienza climatica delle città. *Techne*, 15, 299-310.

Leone, M.F., & Zuccaro, G. (2021). Climate-resilient urban transformation pathways as a multi-disciplinary challenge: the case of Naples. *TECHNE - Journal of Technology for Architecture and Environment*, 2, 159-164.

Lindberg, F., and Grimmond, C. S. B. (2011). The Influence of Vegetation and Building Morphology on Shadow Patterns and Mean Radiant Temperatures in Urban Areas: Model Development and Evaluation. *Theor. Appl. climatology* 105 (3-4), 311–323.

Lindberg, F., Onomura, S., and Grimmond, C. S. B. (2016). Influence of Ground Surface Characteristics on the Mean Radiant Temperature in Urban Areas. *Int. J. Biometeorol.* 60 (9), 1439–1452.

Lionello, P., & Scarascia, L. (2018). The relation between climate change in the Mediterranean region and global warming. *Regional Environmental Change*, 18, 1481-1493.

Littell, J. S., Peterson, D. L., Riley, K. L., Liu, Y., & Luce, C. H. (2016). A review of the relationships between drought and forest fire in the United States. *Global Change Biology*, 22(7), 2353–2369.

- Llasat, M. C., Llasat-Botija, M., Prat, M. A., Porcu, F., Price, C., Mugnai, A., ... & Nicolaides, K. (2010). High-impact floods and flash floods in Mediterranean countries: the FLASH preliminary database. *Advances in Geosciences*, 23, 47-55.
- Llasat, M. C., Marcos, R., Turco, M., Gilabert, J., & Llasat-Botija, M. (2016). Trends in flash flood events versus convective precipitation in the Mediterranean region: The case of Catalonia. *Journal of Hydrology*, 541, 24-37.
- Lin-Ye, J., García-León, M., Gràcia, V., Ortego, M. I., Lionello, P., Conte, D., ... & Sánchez-Arcilla, A. (2020). Modeling of future extreme storm surges at the NW mediterranean coast (Spain). *Water*, 12(2), 472.
- Lorenzo, N., Díaz-Poso, A., & Royé, D. (2021). Heatwave intensity on the Iberian Peninsula: Future climate projections. *Atmospheric Research*, 258, 105655.
- Mark, O., Henonin, J., St. Domingo, N. (2014) Deliverable 2.2 Report and papers with guidelines on calibration of urban flood models. Project CORFU.
- Martzikos, N. T., Prinos, P. E., Memos, C. D., & Tsoukala, V. K. (2021). Statistical analysis of Mediterranean coastal storms. *Oceanology*, 63(1), 133-148.
- McKee, T.B., N.J. Doesken and J. Kleist. (1993). The relationship of drought frequency and duration to time scale. In: Proceedings of the Eighth Conference on Applied Climatology, Anaheim, California, 17–22 January 1993. Boston, *American Meteorological Society*, 179–184.
- Ming, X., Liang, Q., Dawson, R., Xia, X., & Hou, J. (2022). A quantitative multi-hazard risk assessment framework for compound flooding considering hazard inter-dependencies and interactions. *Journal of Hydrology*, 607, 127477
- Miralles, D. G., Gentine, P., Seneviratne, S. I., & Teuling, A. J. (2019). Land–atmospheric feedbacks during droughts and heatwaves: state of the science and current challenges. *Annals of the New York Academy of Sciences*, 1436(1), 19-35.
- Monjo, R., Gaitán, E., Pórtoles, J., Ribalaygua, J., & Torres, L. (2016). Changes in extreme precipitation over Spain using statistical downscaling of CMIP5 projections. *International Journal of Climatology*, 36(2), 757-769.
- Molina, M. O., Sánchez, E., & Gutiérrez, C. (2020). Future heat waves over the Mediterranean from an Euro-CORDEX regional climate model ensemble. *Scientific reports*, 10(1), 8801.
- MYRIAD. (2022). Deliverable 1.2 - Handbook of Multihazard, Multi-Risk Definitions and Concepts. Project MYRIAD, grant agreement number 10100327.
- National Weather Services. (2023). *Drought types*. National Oceanic and Atmospheric Administration. Available at:
<https://www.weather.gov/safety/drought-types#:~:text=Meteorological%20Drought%20is%20based%20on,and%20ground%20water%20table%20decline>

Oke, T. R., Mills, G., Christen, A., and Voogt, J. A. (2017). *Urban Climates*. New York/London: Cambridge University Press.

Osman, M., Zaitchik, B. F., & Winstead, N. S. (2022). Cascading drought–heat dynamics during the 2021 Southwest United States heatwave. *Geophysical Research Letters*, 49(12), e2022GL099265.

Outten, S., & Sobolowski, S. (2021). Extreme wind projections over Europe from the Euro-CORDEX regional climate models. *Weather and Climate Extremes*, 33, 100363.

Owen, L. E., Catto, J. L., Stephenson, D. B., & Dunstone, N. J. (2021). Compound precipitation and wind extremes over Europe and their relationship to extratropical cyclones. *Weather and Climate Extremes*, 33, 100342.

Pina, R. D., Ochoa-Rodriguez, S., Simões, N. E., Mijic, A., Marques, A. S., & Maksimović, Č. (2016). Semi-vs. fully-distributed urban stormwater models: model set up and comparison with two real case studies. *Water*, 8(2), 58.

Politi, N., Nastos, P. T., Sfetsos, A., Vlachogiannis, D., & Dalezios, N. R. (2018). Evaluation of the AWR-WRF model configuration at high resolution over the domain of Greece. *Atmospheric Research*, 208, 229-245.

Politi, N., Sfetsos, A., Vlachogiannis, D., Nastos, P. T., & Karozis, S. (2020). A sensitivity study of high-resolution climate simulations for Greece. *Climate*, 8(3), 44.

Politi, N., Vlachogiannis, D., Sfetsos, A., & Nastos, P. T. (2021). High-resolution dynamical downscaling of ERA-Interim temperature and precipitation using WRF model for Greece. *Climate Dynamics*, 57(3-4), 799-825.

Politi, N., Vlachogiannis, D., Sfetsos, A., Nastos, P. T., & Dalezios, N. R. (2022). High Resolution Future Projections of Drought Characteristics in Greece Based on SPI and SPEI Indices. *Atmosphere*, 13(9), 1468.

Politi, N., Vlachogiannis, D., Sfetsos, A., & Nastos, P. T. (2023a). High resolution projections for extreme temperatures and precipitation over Greece. *Climate Dynamics*, 61(1-2), 633-667.

Politi, N., Vlachogiannis, D., Sfetsos, A., Gounaris, N., & Varela, V. (2023b). Investigation of Fire Weather Danger under a Changing Climate at High Resolution in Greece. *Sustainability*, 15(3), 2498.

Politi, N., Vlachogiannis, D., Sfetsos, A., & Gounaris, N. (2023c). Fire Weather Assessment of Future Changes in Fire Weather Conditions in the Attica Region. *Environmental Sciences Proceedings*, 26(1), 186.

Pycroft, J., Abrell, J., & Ciscar, J. C. (2016). The global impacts of extreme sea-level rise: a comprehensive economic assessment. *Environmental and Resource Economics*, 64, 225-253.

- Qiang, Y., He, J., Xiao, T., Lu, W., Li, J., & Zhang, L. (2021). Coastal town flooding upon compound rainfall-wave overtopping-storm surge during extreme tropical cyclones in Hong Kong. *Journal of Hydrology: Regional Studies*, 37, 100890.
- Ramirez, J. A., Lichter, M., Coulthard, T. J., & Skinner, C. (2016). Hyper-resolution mapping of regional storm surge and tide flooding: comparison of static and dynamic models. *Natural Hazards*, 82, 571-590.
- RESCCUE. (2018). Deliverable 2.2 - Multi-hazards assessment related to water cycle extreme events for current scenario. Project RESCCUE, grant agreement number 700174
- RESCCUE. (2019). Deliverable 2.3 - Multi-Hazards Assessment Related To Water Cycle Extreme Events For Future Scenarios (Business As Usual). Project RESCCUE, grant agreement number 700174
- Richardson, D., Black, A. S., Irving, D., Matear, R. J., Monselesan, D. P., Risbey, J. S., ... & Tozer, C. R. (2022). Global increase in wildfire potential from compound fire weather and drought. *NPJ climate and atmospheric science*, 5(1), 23.
- Ridder, N. N., Pitman, A. J., Westra, S., Ukkola, A., Do, H. X., Bador, M., ... & Zscheischler, J. (2020). Global hotspots for the occurrence of compound events. *Nature communications*, 11(1), 5956.
- Ridder, N. N., Ukkola, A. M., Pitman, A. J., & Perkins-Kirkpatrick, S. E. (2022). Increased occurrence of high impact compound events under climate change. *NPJ Climate and Atmospheric Science*, 5(1), 3.
- Riley KL, Abatzoglou JT, Grenfell IC, Klene A, Heinsch FA (2013) The relationship of large fire occurrence with drought and fire danger indices in the western USA, 1984– 2008: the role of temporal scale. *International Journal of Wildland Fire*, 22, 894–909.
- Ruffault, J., Curt, T., Moron, V., Trigo, R. M., Mouillot, F., Koutsias, N., ... & Belhadj-Khedher, C. (2020). Increased likelihood of heat-induced large wildfires in the Mediterranean Basin. *Scientific reports*, 10(1), 13790.
- Russo, A., Gouveia, C. M., Dutra, E., Soares, P. M. M., & Trigo, R. M. (2019). The synergy between drought and extremely hot summers in the Mediterranean. *Environmental Research Letters*, 14(1), 014011.
- Russo, B., Suñer, D., Velasco, M., & Djordjević, S. (2012). Flood hazard assessment in the Raval District of Barcelona using a 1D/2D coupled model. In *Proceedings of 9th International Conference on Urban Drainage Modelling*.
- Russo, B., Gómez, M., & Macchione, F. (2013). Pedestrian hazard criteria for flooded urban areas. *Natural hazards*, 69, 251-265.

- Russo, B., Sunyer, D., Velasco, M., & Djordjević, S. (2015). Analysis of extreme flooding events through a calibrated 1D/2D coupled model: the case of Barcelona (Spain). *Journal of Hydroinformatics*, 17(3), 473-491.
- Russo, B., Velasco, M., Locatelli, L., Sunyer, D., Yubero, D., Monjo, R., ... & Gómez, A. G. (2020a). Assessment of urban flood resilience in Barcelona for current and future scenarios. The RESCCUE project. *Sustainability*, 12(14), 5638.
- Russo, B., Velasco, M., Locatelli, L., Paindelli, A., Bojic, O., Scapinelli, D., Torres, I., De Juan, M., Skouroupathi, M., Nisiforou, O., Diogo, P., Monjo, R., & Juncosa, L. (2020b). Description of tools for modelling climate related impacts - Project Crisi-Adapt II.
- Russo, B., Valentín, M. G., & Tellez-Álvarez, J. (2021). The relevance of grated inlets within surface drainage systems in the field of urban flood resilience. A review of several experimental and numerical simulation approaches. *Sustainability*, 13(13), 7189.
- Russo B., Paindelli A., Locatelli L., Yubero D. (2022). Use of social media crowdsourcing data for pluvial flood modeling validation to assess future climate-related impacts. The Crisi-Adapt Project. *Proceeding 39th Edition of International Association for Hydro-Environment Engineering and Research (39th IAHR)*. Granada, España.
- Russo, B., de la Cruz Coronas, À., Leone, M., Evans, B., Brito, R. S., Havlik, D., ... & Sfetsos, A. (2023). Improving Climate Resilience of Critical Assets: The ICARIA Project. *Sustainability*, 15(19), 14090.
- Russo, S., Sillmann, J., & Fischer, E. M. (2015). Top ten European heatwaves since 1950 and their occurrence in the coming decades. *Environmental Research Letters*, 10(12), 124003.
- Sanuy, M., Rigo, T., Jiménez, J. A., & Llasat, M. C. (2021). Classifying compound coastal storm and heavy rainfall events in the north-western Spanish Mediterranean. *Hydrology and Earth System Sciences*, 25(6), 3759–3781.
- Schmitt, T. G., Thomas, M., & Ettrich, N. (2004). Analysis and modeling of flooding in urban drainage systems. *Journal of hydrology*, 299(3-4), 300-311.
- Scott, J.H., Burgan, R.E. (2005). Standard fire behavior fuel models: a comprehensive set for use with Rothermel's surface fire spread model. Gen. Tech. Rep. RMRS-GTR153. U.S. Department of Agriculture, Forest Service, Rocky Mountain Research Station, Fort Collins, CO.
- Sebald, J., Senf, C., Heiser, M., Scheidl, C., Pflugmacher, D., & Seidl, R. (2019). The effects of forest cover and disturbance on torrential hazards: large-scale evidence from the Eastern Alps. *Environmental Research Letters*, 14(11), 114032.
- Sheffield, J., Wood, E. F., & Roderick, M. L. (2012). Little change in global drought over the past 60 years. *Nature*, 491(7424), 435-438.
- Simon, H., & Bruse, M. (2020). Modelling of microclimates. *Eco-Design Buildings Infrastructure: Dev. Period 2016–2020*, 4, 318-334.

- Sfetsos, A. (2000). A comparison of various forecasting techniques applied to mean hourly wind speed time series. *Renewable energy*, 21(1), 23-35.
- Sfetsos, A., Giroud, F., Clemencau, A., Varela, V., Freissinet, C., LeCroart, J., ... & Hahmann, S. (2021). Assessing the effects of forest fires on interconnected critical infrastructures under climate change. Evidence from South France. *Infrastructures*, 6(2), 16.
- Squire, D. T., Richardson, D., Risbey, J. S., Black, A. S., Kitsios, V., Matear, R. J., ... & Tozer, C. R. (2021). Likelihood of unprecedented drought and fire weather during Australia's 2019 megafires. *NPJ Climate and Atmospheric Science*, 4(1), 64.
- Stangl M., Formayer H., Hiebl J., Pistotnik G., Orlik A., Kalcher M., Michl C. (2022). Klimastatusbericht Österreich 2021, Graz
- Sutanto, S. J., Vitolo, C., Di Napoli, C., D'Andrea, M., & Van Lanen, H. A. (2020). Heatwaves, droughts, and fires: Exploring compound and cascading dry hazards at the pan-European scale. *Environment international*, 134, 105276.
- Tilloy, A., Malamud, B. D., Winter, H., & Joly-Laugel, A. (2019). A review of quantification methodologies for multi-hazard interrelationships. *Earth-Science Reviews*, 196, 102881.
- Tramblay, Y., Koutroulis, A., Samaniego, L., Vicente-Serrano, S. M., Volaire, F., Boone, A., ... & Polcher, J. (2020). Challenges for drought assessment in the Mediterranean region under future climate scenarios. *Earth-Science Reviews*, 210, 103348.
- Tsoutsos, M. C. (2023). Cascading Effects of Major Natural Hazards in Greece. In Proceedings (Vol. 87, No. 1, p. 27). MDPI.
- Tzanes, G., Zafeiraki, E., Papapostolou, C., Zafirakis, D., Konstantinos, M., Kavadias, K., ... & Kaldellis, J. K. (2019). Assessing the status of electricity generation in the non-interconnected islands of the Aegean Sea region. *Energy Procedia*, 159, 424-429.
- UNDRR. (2015). *Prevention Web*. United Nations Disaster Risk Reduction. Available at: <https://www.preventionweb.net/understanding-disaster-risk/component-risk/disaster-risk>
- UNDRR. (2020). *The Human Cost of Disasters: An Overview of the Last 20 Years (2000–2019)*. Geneva, Switzerland.
- UNISDR. (2012). *UN System task team in the POST-2015 UN development agenda*. Available at: https://www.un.org/en/development/desa/policy/untaskteam_undf/thinkpieces/3_disaster_risk_resilience.pdf
- USACE. (2002). *Coastal Engineering Manual, U.S. Army Corps of Engineers*, Washington, DC.
- Xanthopoulos, G., & Athanasiou, M. (2019). A tale of two fires and a seaside tragedy. *Wildfire*, 28(2), 18-21.

- Varela, V., Sfetsos, A., Vlachogiannis, D., & Gounaris, N. (2018). Fire Weather Index (FWI) classification for fire danger assessment applied in Greece. *Tethys*, 15, 31-40.
- Varela, V., Vlachogiannis, D., Sfetsos, A., Karozis, S., Politi, N., & Giroud, F. (2019). Projection of forest fire danger due to climate change in the French Mediterranean region. *Sustainability*, 11(16), 4284.
- Vicente-Serrano, S.M., S. Beguería and J.I. López-Moreno. (2010). A multi-scalar drought index sensitive to global warming: the Standardized Precipitation Evapotranspiration Index. *Journal of Climate*, 23(7): 1696-1718..
- Vousdoukas, M. I., Voukouvalas, E., Annunziato, A., Giardino, A., & Feyen, L. (2016). Projections of extreme storm surge levels along Europe. *Climate Dynamics*, 47, 3171-3190.
- Ward, P. J., de Ruiter, M. C., Mård, J., Schröter, K., Van Loon, A., Veldkamp, T., ... & Wens, M. (2020). The need to integrate flood and drought disaster risk reduction strategies. *Water Security*, 11, 100070.
- White, R. H., Anderson, S., Booth, J. F., Braich, G., Draeger, C., Fei, C., ... & West, G. (2023). The unprecedented Pacific Northwest heatwave of June 2021. *Nature Communications*, 14(1), 727.
- Svoboda, M., Hayes, M., & Wood, D. (2012). Standardized precipitation index: user guide.
- Zarikos, I., Politi, N., Gounaris, N., Karozis, S., Vlachogiannis, D., & Sfetsos, A. (2023). Quantifying the Long-Term Performance of Rainwater Harvesting in Cyclades, Greece. *Water*, 15(17), 3038.
- Zong, X., Yin, Y., Yin, M., Hou, W., Deng, H., & Cui, T. (2023). Occurrence and hotspots of multivariate and temporally compounding events in China from 1961 to 2020. *NPJ Climate and Atmospheric Science*, 6(1), 168.
- Zscheischler, J., Naveau, P., Martius, O., Engelke, S., & Raible, C. C. (2021). Evaluating the dependence structure of compound precipitation and wind speed extremes. *Earth system dynamics*, 12(1), 1-16.
- Zuccaro, G., Cacace, F., Spence, R.J.S., Baxter, P.J. (2008). Impact of explosive eruption scenarios at Vesuvius, *Journal of Volcanology and Geothermal Research*, 178 (3), 416-453.
- Zuccaro, G., & De Gregorio, D. (2013). Time and space dependency in impact damage evaluation of a sub-Plinian eruption at mount Vesuvius, *Natural Hazards*, 68, 1399-1423.
- Zuccaro, G., De Gregorio, D., & Leone, M. F. (2018). Theoretical model for cascading effects analyses. *International journal of disaster risk reduction*, 30, 199-215.
- Zuccaro, G. & Leone, M.F. (2021). Climate Service to Support Disaster Risk Reduction and Climate Change Adaptation in Urban Areas: the CLARITY project and the Napoli Case Study. *Frontiers in Environmental Sciences*, 9, 693319.

DRAFT

Annex A: Data Management Statement

Table A.1. Data used in preparation of ICARIA Deliverable 2.1

Dataset name	Format	Size	Owner and re-use conditions	Potential utility within and outside ICARIA	Unique ID
-	-	-	-	-	-

Table A.2. Data produced in preparation of ICARIA Deliverable 2.1

Dataset name	Format	Size	Owner and re-use conditions	Potential utility within and outside ICARIA	Unique ID
-	-	-	-	-	-

More info: www.icaria-project.eu



This project has received funding from the European Union's Horizon Europe research and innovation programme under grant agreement No. 101093806. The publication reflects only the authors' views and the European Union is not liable for any use that may be made of the information contained therein.